UNDERSTANDING

ACTIVE NOISE CANCELLATION

Colin H. Hansen

Understanding Active Noise Cancellation

Understanding Active Noise Cancellation

Colin H Hansen

London and New York

First published 2001 by Spon Press
11 New Fetter Lane, London EC4P 4EE

Simultaneously published in the USA and Canada
by Spon Press
29 West 35th Street, New York, NY 10001

Spon Press is an imprint of the Taylor & Francis Group

This edition published in the Taylor & Francis e-Library, 2003.

This book was prepared from camera-ready copy supplied by the author.

British Library Cataloguing in Publication Data
A catalogue record for this book is available from the British Library

Library of Congress Cataloging in Publication Data
A catalog record for this book has been requested.

ISBN 0-203-46733-7 Master e-book ISBN

ISBN 0-203-77557-0 (Adobe eReader Format)
ISBN 0-415-23377-1 (pbk)
0-415-23191-4 (hbk)

TABLE OF CONTENTS

PREFACE

This book is derived from material used at short courses given by the author on active noise control and was written after several requests were received for a simple text on the subject that could be understood easily by graduate and undergraduate science and engineering students as well as researchers interested in the topic. There are many other people who wish to read a brief text on active noise control so that they can gain enough understanding and knowledge to evaluate potential applications without necessarily having to become an expert practitioner. It is the intention of the text to provide the reader with an overview of the discipline of active noise control, with detail provided where necessary to enable those interested readers to gain a deeper understanding. A basic familiarity with noise control (see, for example, Bies and Hansen, 1996) is necessary to be able to understand most of this book.

The material in the book is intended as a precursor to more complex books available on the subject and may also be expected to provide sufficient background for the reader to understand more advanced discussions at conferences and in other books. Practical applications are emphasized and control algorithms and structures are discussed to the extent necessary to enable the reader to implement them.

The book begins with a brief introduction to active noise control followed by a sketchy overview of its history from the first patent to the present time. Possible future directions are also discussed. In the second chapter, physical mechanisms that result in noise reduction are explained in simple terms. This is followed by a description of the basic structure of feedforward and feedback control systems (both adaptive and non-adaptive) and the process of control system optimisation.

In chapter 3, various parts of the electronic control system and control algorithms are discussed in sufficient detail to allow a full understanding of the principles involved and how such controllers may be implemented in practice. Various practical implementation issues are also discussed. In chapter 4, suitable active control sound source types and their practical implementation are discussed. In chapter 5, error sensing strategies, error sensors and reference sensors, and practical issues associated with their implementation are discussed. In chapter 6, applications of the technology are discussed as are a number of commonly mentioned potential applications which are impractical. In chapter 7, current and future research directions are discussed and information on relevant web sites is provided.

It is hoped that this book will provide the background necessary for the reader to understand the principles underlying active noise control, to apply the principles to the evaluation of potential applications and to use, with a good understanding, commercially available hardware and software to implement active noise control for the identified applications.

ACKNOWLEDGEMENTS

I would like to express my deep gratitude to my many graduate students and colleagues who provided much of the background material on which this book is based. In particular, I would like to thank Dr Ben Cazzolato, Dr Carl Howard, Dr Colin Kestell, Dr Xun Li, Dr Xiaojun Qiu and Dr Scott Snyder I would also like to thank my family for their continuing tolerance throughout the preparation of the manuscript.

This book is dedicated to Susan, to Kristy, to Laura and to my parents, Betty and Ludwig, without whose support this book would not have been possible.

CHAPTER ONE

A LITTLE HISTORY

1.1 INTRODUCTION

Active noise cancellation, also known as "anti-noise" and "active noise control" involves the electro-acoustic generation (usually with loudspeakers) of a sound field to cancel an unwanted existing sound field. The preferred term to describe the phenomenon is "active noise control", because in many cases it is arguable that cancellation is the true mechanism causing the unwanted noise to diminish.

Is active noise control ever likely to find widespread application in industry and consumer goods, or is it forever destined to be a laboratory tool and a rich source of research activity for underpaid academics? Hopefully, this question will be one of many that will be answered as the tale in this book unfolds. For now, suffice it to say that there are many systems installed in industry to reduce low frequency fan noise emanating from air exhaust ducts and quite a few propeller aircraft are already benefiting from the technology. In addition, mining equipment and truck manufacturers are in the process of applying the technology to their vehicles to reduce noise in the driver's cabin and radiated exhaust noise.

A typical single-channel active noise cancellation system consists of:

- a microphone reference sensor to sample the disturbance to be cancelled,
- an electronic control system to process the reference signal and generate the control signal,
- a loudspeaker driven by the control signal to generate the cancelling disturbance and
- an error microphone to provide the controller with information so that it can adjust itself to minimise the resulting sound field.

The active noise cancellation system just described is known as an "adaptive" system as it can adapt itself to changing characteristics of the noise to be cancelled and changing environmental conditions that affect the acoustic field. Non-adaptive systems are not very useful in practice (except in active noise cancelling headsets and ear muffs) and are only discussed briefly in this book.

In the discussions that follow, single-channel systems (one loudspeaker control source and one microphone error sensor) are used as a basis for describing the underlying principles. However, many active noise cancellation systems that are implemented in practice are multi-channel systems, consisting of a number of microphones and loudspeakers to generate the required cancelling sound field. Extension of the single-channel system to a multi-channel system is relatively complex because of the interaction between all of the microphones and loudspeakers. Means for implementing multi-channel systems and the associated electronic control system will be discussed briefly here for completeness.

Who has benefited most from all the effort and hundreds of millions of dollars that have so far been spent on developing active noise control technology? Perhaps the profession that has so far benefited most from the invention of active noise control is the legal profession, which has been involved in a number of patent infringement law suits as well as the preparation of numerous patent applications. The number of patent applications has been increasing exponentially for the past 15 years and far exceeds the number of commercial applications of the technology. Nevertheless the many hundreds of patents granted indicate that many individuals and companies see the day eventually coming when active noise control systems will be widespread in industry and consumer goods.

Why is active noise cancellation of any interest to industry? It is because it offers a possible lower cost alternative to passive noise control for the control of low frequency noise that has traditionally been difficult and expensive and in many cases not feasible to control, because of the long acoustic wavelengths involved. If only passive control techniques are considered, these long wavelengths make it necessary to use large mufflers and heavy enclosures for noise control, and very soft isolation systems and/or extensive structural damping treatment for vibration control.

Many of the techniques described in this book for active noise cancellation apply equally well to active vibration cancellation. In many cases the two types of disturbance are very closely related, as structures often radiate unwanted sound as a result of their vibration.

The purpose of this book is to provide the reader with some insight into how active noise cancellation systems work. It is written so that most of it can be understood by a technically competent lay reader who has some understanding of noise control; however, there are some parts where the treatment goes a bit deeper (including a few mathematical equations) and these parts are intended for a reader with a science or engineering degree. However, readers without the background education necessary to understand these parts can skip them and still obtain a basic understanding of how active noise cancellation works and for what applications it is suitable.

1.2 EARLY HISTORY

Although the first observation of sound cancellation (using two Bell telephones) was noted by Thompson in 1878, it was not until 1930 that the French engineer, H.Coanda (1930) documented and then patented the idea of sound cancellation by destructive interference. He described an electro-acoustic system (microphone, amplifier and loudspeaker) to generate a signal of opposite phase to the unwanted noise. A few years later a German physicist, P.Lueg (1933) described and patented the idea of using active sound cancellation as an alternative to passive control for low frequency sound in a duct. His idea was to use a transducer (control source) to introduce a secondary (control) disturbance into the duct to cancel the existing (primary) disturbance, thus resulting in an attenuation of the original sound as illustrated in Figure 1.1. The cancelling disturbance was to be derived electronically based upon a

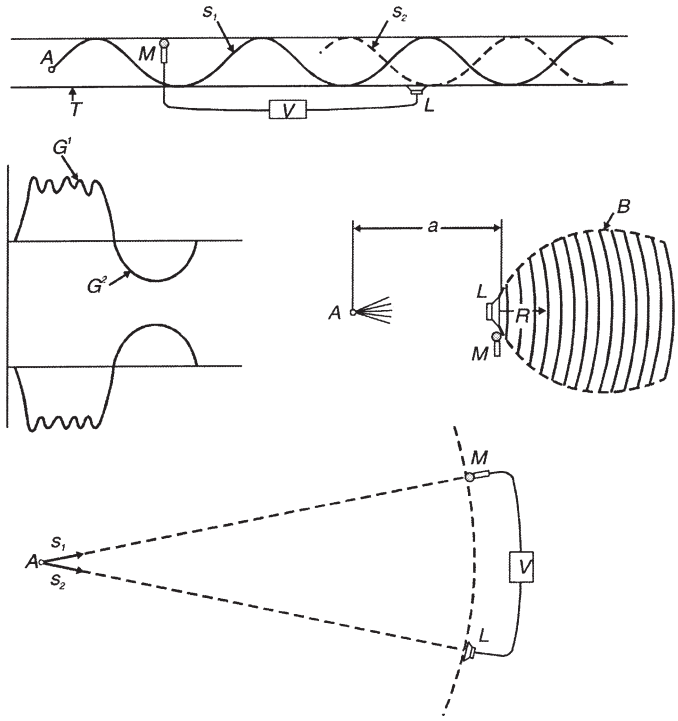

Figure 1.1 Figures derived from Lueg's patent (after P.Lueg, 1937)

measurement of the primary disturbance. However, neither Coanda nor Lueg ever demonstrated a successful system and the technology lapsed into oblivion for two decades. One of the problems with Lueg's system was that there was no allowance for the controller to adapt to system changes that would occur as a result of such things as minor temperature changes.

In the 1950s the idea was rekindled by a man named Olson (1953, 1956) who investigated possibilities for active sound cancellation in rooms, in ducts and in headsets and earmuffs using feedback control. One of Olson's patents is illustrated in Figure 1.2. Unfortunately Olson's system provided very limited attenuation over a very limited frequency range and suffered from instability due to high frequency noise for which the phase delays through the system exceeded 180°. Again, limitations in the available electronic control hardware as well as limitations in control theory prevented this technology from being commercially realised.

Around about the same time as Olson was experimenting in his laboratory, W. Conover (1956) of General Electric demonstrated an active noise cancellation system for transformer noise (see Figure 1.3). Unfortunately the controller had to be adjusted manually and only reduced the sound over a very narrow angle subtended from the loudspeaker to the measurement microphone. Of course, this system was completely impractical because it had to be continually adjusted manually due to changes in

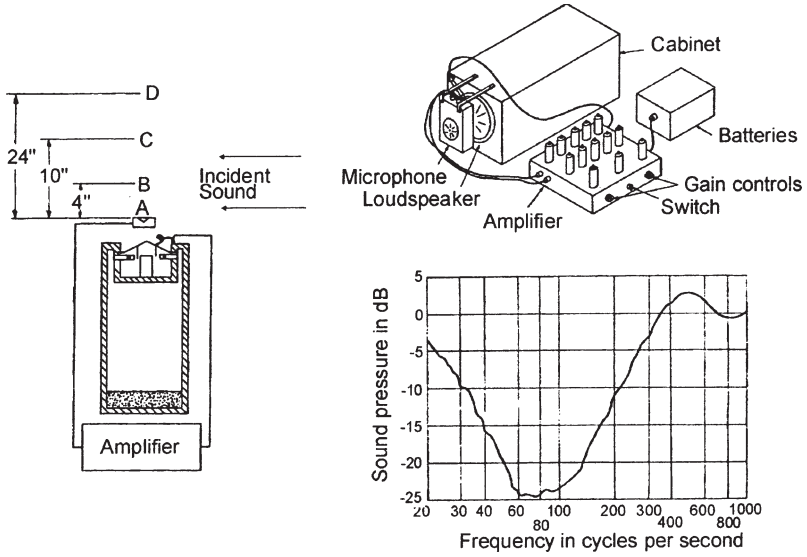

Figure 1.2 Olson's electronic sound absorber (reprinted with permission from, H.Olson, "Electronic sound absorber", *Journal of the Acoustical Society of America,* **25**, 1130–1136, 1953. Copyright, Acoustical Society of America, 1953).

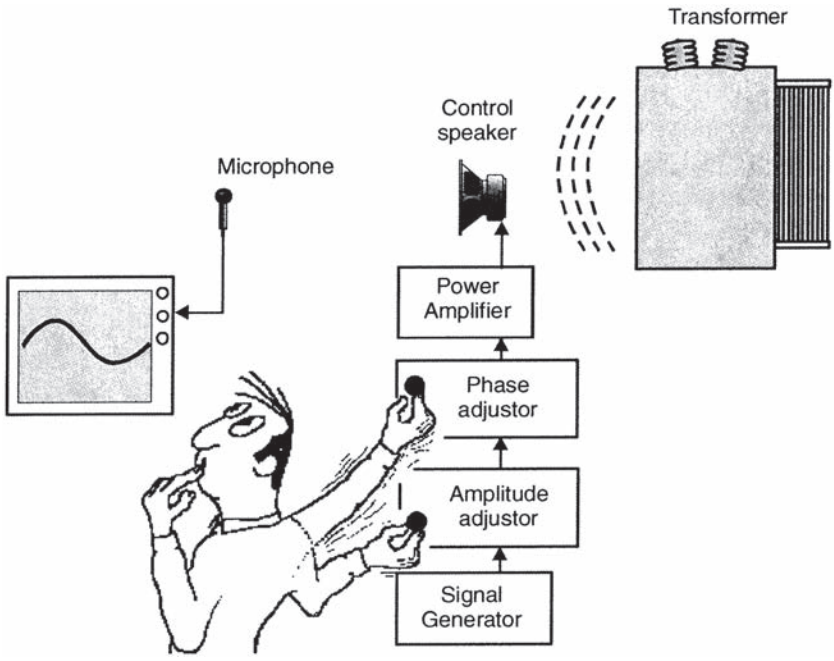

Figure 1.3 Conover's active noise control system for transformer noise

environmental conditions affecting the sound field. It was also of limited benefit even when adjusted to its optimum performance due to the very localised area of reduced sound. Although there are now commercially available active noise control systems for electric power transformer noise control, a large number of loudspeakers and microphones (as well as vibration actuators on the transformer tank) are needed. Even then the achievement of a significant amount of global noise reduction is difficult (even though 15–20 dB is possible at the specific error microphone locations).

In the early 1980s, a number of researchers extended Olson's work to produce feedback systems that were more robust (Eghtesadi et al., 1983; Hong et al, 1987). At the same time, Chaplin (1980) and Chaplin and Smith (1983) reported a waveform synthesis technique to cancel periodic noise and Warnaka et al. (1981, 1984), Ross (1981) and Burgess (1981) developed a duct cancellation system based on adaptive filter theory.

1.3 LATER HISTORY

Since the original idea was conceived in those very early days, the active control of sound as a technology has been characterised by transition: transition from a dream to practical implementation and from a laboratory experiment to mass production. This transition has taken a long time, partly because of the time it took to develop sufficiently powerful signal processing electronics, partly because of a lack of understanding of the physical principles involved and partly because of the multi-disciplinary nature of the technology, which combines a wide range of technical disciplines including Control, Signal Processing, Electronics, Acoustics and Vibration. Being a collection of pieces, in which the strength of the chain is only as strong as its weakest link, it is little wonder that the technology has been characterised by advances that have come in a series of spurts rather than in a continuous flow. It was not until the early 1990s that regular implementations of active noise cancellation outside of the laboratory were reported (Ericksson, 1990, 1991) and Wise et al. (1992). Since that time numerous practical implementations have been reported, including systems for reducing helicopter and aircraft cabin noise.

The resurgence of interest in the technology is reflected in the exponentially increasing number of research publications on active control: the number of technical papers published on the topic since Coanda's and Lueg's work in the 1930s has increased from approximately 240 before 1970 to 850 in the 1970s to 2,
200 in the 1980s, and to over 4,000 in the 1990s.

1.4 CURRENT COMMERCIAL APPLICATIONS

Although there are many companies and universities currently undertaking research and development of active noise control applications, only a few applications have actually reached the commercialisation stage. Those applications include:

- low frequency tonal noise from mid-size propeller aircraft (many systems currently installed);
- headsets and ear muffs that actively reduce low frequency noise at the ear (many thousands of units manufactured monthly);
- helicopter cabin noise (by actively controlling the transmission of rotor and gearbox vibration through the support structure);
- industrial air handling systems and large office building air conditioning systems (hundreds of installed systems, mainly in the USA);
- diesel engine exhausts on stationary equipment and buses (only a few systems installed); and
- automobile engine vibration isolation (currently restricted to one or two models of vehicle in Japan).

1.5 THE FUTURE

Potential applications of active noise cancellation that we could potentially see on a daily basis in the future are numerous and may include:

- Consumer goods such as refrigerators, washing machines, air conditioners, lawn mowers, personal computers, range hoods, chain saws and vacuum cleaners;
- Cars—engine noise (both using loudspeakers in the passenger compartment and active vibration isolation of the engine) and road noise;
- Trucks and mining equipment—exhaust noise and cabin noise;
- Air handling systems in industry are likely to become more common candidates for active control—applied to ductwork carrying the noise;
- Public phone booths;
- Aircraft and helicopter cabin noise control will become more widespread and will include aerodynamic noise as well as propeller noise;
- Naval ships and pleasure boats; and
- Diesel locomotives.

Many of the applications mentioned above have seen successful laboratory demonstrations, but that seems to be where they stall.

The main reason that active noise control systems have yet to be commonly found in consumer products is their cost. A complete system includes a DSP and associated electronics as well as loudspeakers and microphones. The cost of these components is acceptable to the aircraft industry but not currently to the automotive or consumer goods industry. Especially in the automotive industry, successful implementations have been developed (for low frequency engine and road noise, including active engine vibration isolation), but have not found widespread use because of their cost. Perhaps the key to more widespread application will be the integration of active noise control systems with existing hardware. For example the electronic signal processing for an automotive system could be done with the engine management computer (provided it was made sufficiently powerful) and use could be made of

the stereo system loudspeakers and amplifiers as active noise cancellation generators (without affecting the quality of the music).

Even if cost requirements of complete systems can be brought in line with what the market is prepared to pay, we must never lose sight of the fact that there are physical limitations which make the application of the technology impractical in many instances. Examples of impractical applications are discussed in Chapter 6.

Perhaps the main reason for the lack of industrial application examples (as opposed to mass produced consumer goods) is the seemingly excessive cost of such installations, which may easily exceed the actual hardware cost by one or two orders of magnitude. The high cost of the labour component is associated with the high level of engineering expertise and high level of understanding of the principles of active noise control that are required if the installation is to be successful. As active noise control expertise includes acoustics, signal processing, automatic control and electronics, the number of true experts throughout the world who are capable of developing and successfully installing active noise control systems is very limited. This also serves to limit the spread and commercialisation of the technology. Adding to the cost of the labour component is the unique nature of most problems to which active noise control is applied, thus tending to preclude the use of a generic system that can be installed by non-expert technicians. In many cases, the unique nature of the problems involved requires a large injection of development funds just to get to the laboratory demonstration stage.

Unfortunately, an inexpensive, clever, commercial control system, which includes a selection of source and sensor transducers to satisfy most problems, and software to guide users in the correct choice and location of such transducers, does not yet exist. The word "clever" used above to describe the commercial control system, which does not yet exist, needs some explanation. If a controller is to be useful to a wide range of people, the effort involved in setting it up must be very small. This means that the controller must itself be controlled by a high level expert system or neural network that automatically sets input and output gains to maximise system dynamic range, convergence coefficients to optimise convergence speed and stability trade-offs, control filter type and weight numbers to optimise noise reduction, as well as leakage coefficients and system ID algorithms, filter types and configurations to maximise controller performance and stability. In addition, the controller should also be able to perform as an adaptive feedforward or adaptive feedback controller, be extendable to a large number of channels simply by adding together identical modules, and provide advice on the suitability of feedforward control compared to feedback control based on the quality of the available reference signal. Finally the controller/user interface during set-up (which should really be a question/answer session) should be Windows based for maximum flexibility. The ability to connect a modem to the controller to allow remote access and interrogation of current performance and the state of transducers and other system components is also an important labour saving device.

Recently, low cost active noise control hardware and software has become commercially available. As a result, the implementation complexity has been reduced somewhat, putting it in the reach of people with an understanding and knowledge of

acoustics and/or vibration, but only a superficial knowledge of signal processing, control and electronics. However, much remains to be done to make the implementation of active noise control sufficiently simple that it can be installed by the same technicians that install passive noise control hardware.

In addition to the development of more user friendly control systems to implement applications that are already proven such as low frequency tonal noise control in a range of situations outdoors and indoors and low frequency random noise control in ducts, current research is directed at extending the applications even further. It is expected that more effort will be focussed on feedback control systems for random noise, especially for passengers in aircraft. Effort will also be directed at extending the frequency range to higher limits, particularly for the control of gearbox and engine noise in Naval vessels and aircraft. With this type of control, it will be necessary to implement the active cancellation as close to the source as possible, probably using vibration actuators to control the vibration that is subsequently transmitted through a structure and radiated as noise.

Unfortunately, the past history and credibility of active noise control as a viable alternative control measure has been tainted with a minority of commercial companies making premature public claims regarding its application, which were far in excess of what was realistic (or what they could deliver). This has resulted in the technology being viewed with suspicion by key manufacturers of particular mass market products that have potential to benefit from the judicious application of active noise control technology. The field has also been tainted by the unscrupulous patenting by some companies of technology that had been published by other unrelated researchers in journal papers or consulting reports years before the filing of the subject patents. This unscrupulous patenting is often followed up with equally unscrupulous threats of indefensible legal action against users of the technology. Unfortunately, this activity is still continuing in some cases, and it is very likely that many of the current 800 to 1000 patents relevant to active noise or vibration control can be shown to be invalid.

CHAPTER TWO

FOUNDATIONS OF ACTIVE CONTROL

2.1 PHYSICAL MECHANISMS

To appreciate the physical problems that limit the application of active noise control, it will be useful to first discuss the physical mechanisms that are responsible for the noise reduction achieved by an "anti-noise" source. In applications of active noise control, the cancelling signal is generated electronically and introduced into the system using transducers such as loudspeakers that convert the electronic signal to sound. In many cases, the physical mechanism responsible for the reduction of the unwanted noise is a little more subtle than mere cancellation. In cases where cancellation is the only control mechanism, the noise level may be reduced at some locations, but will be increased at others so that the total energy of the unwanted noise and the cancelling sound is conserved. This type of control is known as "local cancellation". Examples of applications employing this mechanism are active headsets, (where the noise is cancelled at the entrance to the ear canal but increased at other locations) and noise cancelling headrests in aircraft and other transportation vehicles.

Other possible physical mechanisms responsible for the successful application of active noise control include a change in the acoustic radiation impedance of the unwanted noise source as a result of introducing the "anti-noise" sources, absorption of sound by the "anti-noise" sources or, in the case of a confined space such as a duct, reflection of sound by the "anti-noise" sources.

The suppression of the primary source sound radiation by a change in its radiation impedance may be understood on the basis of the following considerations. If it were possible to make the entire cancelling sound field (or almost all of it) 180° out of phase with the original (primary) field, then the sound radiated by the primary source would be effectively "cancelled" leaving one to wonder where all the energy had gone. The answer is that in this case, the control mechanism is not really cancellation; the sound field generated by the control (or cancelling) sound sources has effectively "unloaded" the primary source, changing the acoustic radiation impedance that it "sees" so that it radiates much less sound (even though the motion of the physical source, such as a vibrating surface, may remain unchanged). In this case, the control sources act to suppress the sound power radiated by the primary source. To achieve effective suppression of the primary source output by presenting a purely reactive impedance to it, the control sources must be sufficiently large and located such that they are capable of presenting the required impedance to the primary source. In one dimensional wave guides, such as air conditioning ducts, these constraints are relatively easy to satisfy and the distance between the control and primary sources is not too important. However, in 3-D space, the control source, in

general, will need to be close to the primary source to affect its radiation impedance significantly. It will also need to be of similar size with a similar volume velocity output (or source strength).

An example of a change in radiation impedance is the active control of a periodic plane wave propagating in a duct and originating from a source somewhere in the duct. The active control source generates a sound field that changes the radiation impedance "seen" by the original sound source, thus reducing its sound output. An electrical analogy to this situation is a power point in a wall, which may be considered to be a source of electrical energy. If a light is plugged into it, the power point will supply the power for which the light is designed, which may be 60 W. On the other hand, if a radiator is plugged into the power point, 1500 W may be produced (depending, of course, on the rating of the radiator). Thus, the power produced by the power point is dependent on the load impedance that it "sees". A similar argument holds for the radiation impedance of an acoustic source, where the radiation impedance can be altered by the introduction of another sound source.

Another example, this time a free field example, is that of two loudspeakers placed in close proximity to one another. If the first loudspeaker is excited with tonal sound, then it is possible to tune the amplitude and phase of the excitation to the second loudspeaker so that the pressure directly in front of the first loudspeaker is cancelled. Conversely, the first loudspeaker will then cancel the pressure in front of the second and there will then be no net flow of energy, just a sloshing back and forth of fluid between the two loudspeakers, due to the change in radiation impedance "seen" by both of the speakers. The result is that no sound pressure is radiated to the far field, but rather a local sound field just exists between the two speakers. Of course, the preceding scenario assumes that the second loudspeaker sound field can completely cancel the first and vice versa. In practice, small differences in speaker construction as well as harmonic distortion of the excitation signal prevent this and the result is usually a reduced noise level, but not complete silence! The best possible result obtainable with the source suppression mechanism for a source radiating into free space is when the control source amplitude is adjusted for zero sound pressure immediately in front of it. This results in some suppression of the primary source power output and no control source power output.

Returning to the duct example, if the propagating sound is random or transient in nature, then it seems clear that the control mechanism is NOT a change in radiation impedance of the original source by the "anti-noise" sources. This is because the noise to be cancelled is not periodic; thus the required sound field at the location of the undesired sound source to produce a change in radiation impedance will not be predictable in advance. In this case, the "anti-noise" source either absorbs energy or reflects it back from whence it came where it is eventually dissipated. When the "anti-noise" loudspeaker absorbs sound, it will still need electrical power to drive it to the correct displacement for energy absorption, as the acoustical energy it absorbs is insufficient to overcome the source mechanical impedance and move the cone significantly. This is because the acoustical efficiency of loudspeakers and other artificial sound sources is so poor. Thus, in practice, the electrical power requirement to drive a loudspeaker control source is not noticeably different when the speaker is

absorbing sound energy than when it is radiating it. Except for plane wave propagation in ducts, the absorption mechanism is undesirable as generally in the process of absorbing power, the control source changes the radiation impedance of the primary source in such a way that the primary source radiates more power.

An interesting side issue is that at frequencies that correspond to acoustic resonances in the medium filling a duct, the active control mechanism involving changing the source radiation impedance can still be effective for a random noise source because the reverberation associated with the resonance effectively makes the random noise appear to be quasi-periodic at this frequency.

2.2 BASIC STRUCTURE OF ACTIVE NOISE CONTROL SYSTEMS

Modern active sound control systems consist of one or more control sources used to introduce a secondary (or controlling) disturbance into the structural/acoustic system. This disturbance suppresses the unwanted noise originating from one or more primary sources. The (control) signals that drive the control actuators are generated by an electronic controller, which uses as inputs, measurements of the residual field (remaining after introduction of the control disturbance) and in the case of feedforward adaptive systems, a measure of the incoming primary disturbance.

Active noise control systems are ideally suited for use in the low frequency range, below approximately 500 Hz. Although higher frequency active control systems have been built, a number of technical difficulties, both structural/acoustic (for example, more complex vibration and radiated sound fields) and electronic (where higher sampling rates are required) limit their efficiency, so they are restricted to very special applications. Also, at higher frequencies, passive systems generally become more cost effective. A "complete" active noise control system would usually consist of active control for low frequencies and passive control for higher frequencies.

An important property of many modern active sound control systems (particularly feedforward systems) is that they are self-tuning (adaptive) so that they can adapt to small changes in the system being controlled. These changes are a result of such things as a changing acoustic environment and transducer wear. Changes only need to be small to cause a non-adaptive feedforward control system to become ineffective. Non-adaptive controllers are generally confined to the feedback type in cases where slight changes in the environmental conditions will not be reflected in significant degradation in controller performance. One example of an effective non-adaptive feedback control application is in active ear protection and headsets where analog feedback control systems have been used successfully for some time. An interesting aside is that an adaptive feedforward controller is effectively a closed loop implementation of a non-adaptive feedforward controller.

As integrated microprocessors dedicated to signal processing become cheaper and faster (the speed having doubled every 18 months for the last 10 years), potential active control applications increase in number. However, it should not be assumed that more processing power will extend the applications endlessly. There are some supposedly potential applications (for example, control of traffic noise in living

rooms), which will remain impractical, no matter how much processing power is available, because the limitations are a result of the structural/acoustic characteristics of the problem. Although more powerful signal processing electronics help to alleviate the electronic problems associated with extending the application of active control to higher frequencies and to more complex multi-channel problems, the structural/acoustic limitations mentioned remain. For the example cited above, to provide significant (or any) attenuation of the unwanted disturbance, a vast array of sensors and actuators would be required: it would be cheaper and more convenient to build a thicker wall!

Two major types of active noise control system will be considered; adaptive filtering (either feedforward or feedback) and waveform synthesis (a type of feedforward control that is suited only to periodic noise). In addition, both time domain and frequency domain versions of the feedforward adaptive filtering form and the time domain version of the feedback form of controller will be discussed.

It is useful to begin with an overview of single channel adaptive feedforward and feedback control. Non-adaptive feedforward systems are generally impractical for most industrial applications, because of the time-variability in the physical system being controlled, and thus will not be considered further here. However, non-adaptive feedback systems are often used for ear-muffs and sometimes for the control of noise propagating in ducts. Waveform synthesis will be discussed later in Section 2.2.3.

The simplest example to consider for the illustration of the principles of feedforward and feedback control is the active control of plane wave sound propagation in a duct.

An adaptive feedforward active noise control system (the most common type) consists of a reference sensor, a control source, an error sensor, a control algorithm and an electronic controller, as illustrated in Figure 2.1 (a). The controller usually consists of an adaptive digital filter, and an adaptive algorithm that sets the weights in the adaptive digital filter. These components are discussed in detail in Chapter 3. The electronic controller part in Figure 2.1 (a) is the only component that is different for a time domain compared to a frequency domain system and this is discussed in detail in Chapter 3.

A feedback system is illustrated in Figure 2.1(b). For an adaptive system, the electronic controller is an adaptive filter and algorithm, whereas for a non-adaptive system, the electronic controller consists of a fixed low pass filter and an amplifier.

2.2.1 Adaptive Feedforward Control

Referring to Figure 2.1 (a) (feedforward control), a reference sensor (usually a microphone) samples the incoming signal, which is filtered by the electronic controller to produce the output signal to drive the control source (loudspeaker in this case). The controller effectiveness is measured by the error sensor, which provides a signal for the control algorithm to use in adjusting the controller output so that the sound pressure at the error microphone is minimised. The signal processing time of the controller must be less than the time for the acoustic signal to propagate from the

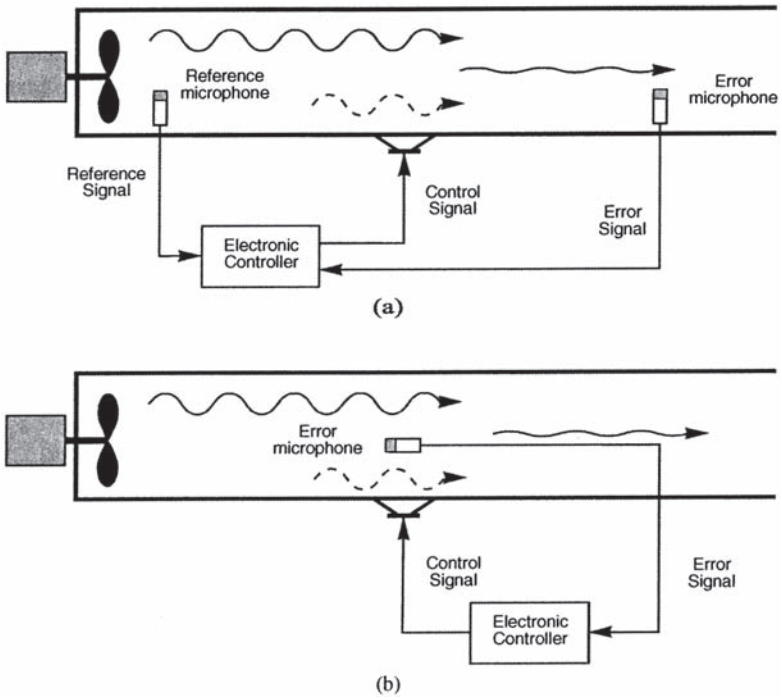

Figure 2.1 Basic active noise control systems.
(a) Feedforward system
(b) Feedback system

reference sensor to the control source for broadband noise control, but for tonal noise control, the maximum permitted processing time can be much larger (as the signal is repetitive), but it is limited by the rate at which the amplitude and frequency of the tones change.

The cancellation path is the electro-acoustic path from the loudspeaker input to the error microphone output. The transfer function of this path must be taken into account in most controller algorithms and thus it must be measured for every installed system. Indeed, it is essential in most practical commercial systems that some means is implemented in the controller to measure this transfer function regularly while the controller is operating as it can change quite quickly in some cases. This will be discussed in more detail in Chapter 3.

Because of their inherent stability, feedforward controllers are generally preferred over feedback controllers when a reference signal, which is correlated with the error signal, is available. One exception is the active ear muff case, for which it has been found that an adaptive feedback controller seems to cope better than an adaptive feedforward controller to head movement of the wearer (Bao and Pan, 1996). However, most active hearing protection is made using non-adaptive feedback systems. This arrangement minimises cost and maximises performance. One disadvantage of feedforward controllers that is not shared by feedback controllers is

the often encountered problem of feedback of the control source output to the reference sensor via an acoustic path. Unless this is compensated for in the controller adaptation algorithm and control filter, instability is likely to result. Appropriate algorithms and filters are discussed in Chapter 3. One way of avoiding the problem is to use a non-acoustic reference sensor such as a tachometer on the machine causing the noise, as shown in Figure 2.2

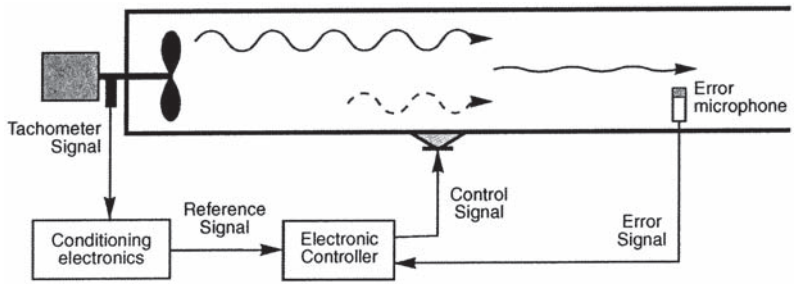

Figure 2.2 Basic active noise control system with tachometer reference signal.

A tachometer reference signal is only useful if it is desired to only control the harmonics or sub-harmonics of the machine rotational frequency. All other noise detected by the error sensor will be uncorrelated with the reference signal and thus will not affect the control system output (unless a specially developed non-linear filter and algorithm is used—see Chapter 3).

For a feedforward system used to control more than one sound source, a reference signal is required for each source, but all reference signals need to be summed together to form one signal for use by the controller.

The simple duct systems shown in the figures involve just one "anti-noise" source and one error sensor. More complex systems (such as those designed to control 3-dimensional sound fields) may require many sources and sensors. In this case the control algorithm becomes much more complex, as it must take into account the interactions between all sources and error sensors and provide the optimal cancelling signal to each control source. Such a system is referred to as a multi-channel system.

The objective of the control system is clear; it must minimise the signal detected by the error sensor. However, to derive the appropriate control source signal to achieve this objective, the change in the disturbance during propagation from the reference microphone to the control source must be accounted for, as must the change in the control signal as it progresses through filters, amplifiers, and speakers. The characteristics of these changes will alter significantly over time, with changing environmental conditions (such as temperature) and transducer wear. Therefore to be useful in practice, a feedforward control system must be adaptive (self-tuning); continually tuning itself to provide the optimal result. Thus, in practice, a feedforward controller must be implemented using digital electronics. To facilitate self-tuning, the signal from the error microphone is used together with an adaptive algorithm to continually update the characteristics of the control filter (shown as "digital filter" in Figure 2.3). Note that analog to digital (A/D) converters, anti-aliasing filters, digital

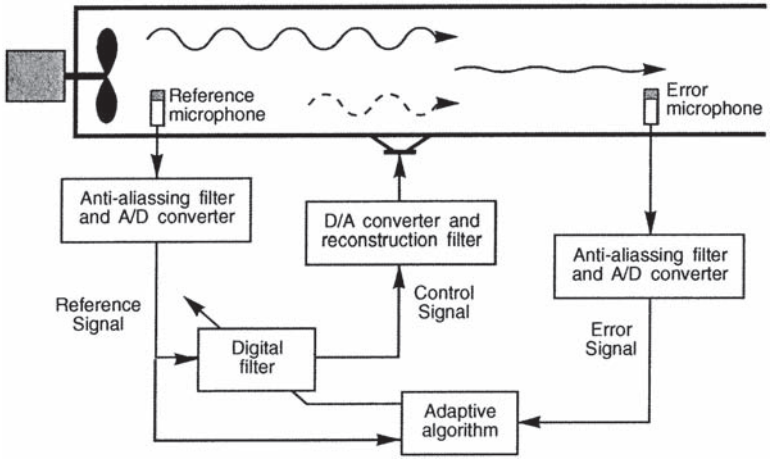

Figure 2.3 Feedforward active controller with adaptive algorithm.

to analog (D/A) converters and reconstruction filters are needed for practical operation of the system. Reconstruction filters are just low pass filters that "smooth out" the edges of the digital signal, thus preventing the passage of the high frequency components that are not desired in the control signal. With the adaptive algorithm, the filter weights are updated in a time frame of the order of the digital sampling rate, and much better results are obtained than if the filter is updated off-line. However, in practical implementations, an update rate of similar order to the cancellation path delay seems to work as well for a much smaller load on the digital signal processor. This aspect is discussed in more detail in Chapter 3. Various aspects that need to be taken into account in the filter weight update algorithm, such as the electroacoustic transfer functions of the loudspeaker and error microphone are also discussed in detail in Chapter 3.

Simply providing the basic system components shown in Figure 2.3 will not necessarily ensure that a successful active noise control installation will be achieved; that is, there is no guarantee of either local or global noise reduction. The achievement of noise reduction depends upon the design of, and harmony of operation between, two major subsystems; the "physical" system, and the electronic control system. The physical system encompasses the required transducers; the "control sources" for inducing the secondary disturbance, and the "error sensors" that monitor the performance of the active control system by providing some measure of the residual noise and/or vibration field. Thus, the physical system provides the structural/acoustic interface for the active control systems, and the electronic control system drives the physical system in such a way that the unwanted primary source noise and/or vibration field is attenuated.

The quality of the design of these two major subsystems is the critical factor in determining the ability of the active control system to produce the desired results. The design of the physical system, comprising the arrangement of control sources and error sensors, limits the maximum noise control that can be achieved by an ideal

active controller. The control electronics limit the ability of the active control system to reach this maximum achievable result. Thus, no active control system can function efficiently with an inefficient physical or electronic subsystem.

The design requirements for the electronic and physical subsystems are very different from, although not completely independent of, one another. Similarly, the design of these subsystems varies from application to application, in that the appropriate control strategy is dependent upon the control objective, whether it be vibration control, radiated sound power control, sound transmission control or some other objective. For example, the physical control system for an aircraft is not the same as the physical control system for an air handling duct or the system for vibration isolation of an electron microscope. However, the underlying principals of efficient design for each subsystem are the same.

Whether the sound field to be controlled is one dimensional or three dimensional makes a large difference to the complexity of the required controller and the extent of the noise reduction that may be achieved. In both 1- and 3-dimensional systems, the noise reduction achieved will be dependent on the physical arrangement of control sources and error sensors. Moving the locations of the control sources and sensors affects both system controllability (the achievable level of noise reduction) and stability (the rate at which the controller adapts to system changes while remaining stable). For feedforward systems, the physical system arrangement can be optimised independently of the controller, but for feedback systems, the physical system arrangement is an important part of the controller design.

Also of importance is the size of the source to be controlled compared to an acoustic wavelength at the lowest frequency to be controlled. Clearly, one small control source will NOT be effective in achieving GLOBAL control of a primary source that is many wavelengths in dimension because of the inability of the control source to significantly change the primary source radiation impedance.

To be able to decide on the best control system, it is necessary to know the characteristics of the noise to be controlled. Is the noise transient or continuous? Is it periodic (tonal) or random? It is always much easier to control periodic noise; practical control of random or transient noise is restricted to applications where the sound field is confined, such as in a duct.

2.2.2 Feedback Control

Feedback control systems differ from feedforward systems in the manner in which the control signal is derived. Whereas feedforward systems rely on some predictive measure of the incoming disturbance to generate an appropriate “cancelling” disturbance, feedback systems aim to attenuate the residual effects of the disturbance after it has passed. Feedback systems are thus better at reducing the transient response of systems, while feedforward systems are better at reducing the steady state response. In structures and acoustic spaces, feedback controllers effectively add modal damping, and in the duct system shown in Figure 2.1(b) the feedback controller also reflects incoming waves by modifying the duct wall impedance at the control loudspeaker.

Unlike feedforward systems for which the physical system and controller can be optimised separately, feedback systems must be designed by considering the physical system and controller as a single coupled system.

A feedback controller derives a control signal by processing an error signal, not by processing a reference signal as is done by a feedforward controller. For a feedback controller, the error signal is processed to derive a suitable control signal for the control source such that the error signal is minimised, whereas in feedforward systems, the error signal is used to help the controller to optimise its performance in terms of minimising the error signal, and it is the reference signal that is processed to generate the control signal.

In active noise control systems, the characteristics of the feedback control system are chosen so as to return the system (as measured at an error sensor) to its unperturbed state as quickly as possible. This type of controller is ideal in cases where it is not possible to sample the incoming disturbance sufficiently early for a feedforward controller to generate the required cancelling signal. However, the performance of a feedback controller is not as good as a feedforward controller and it is difficult to prevent it oscillating or going unstable when subjected to high frequency noise. Adaptive feedback systems have the additional limitation that they require the incoming signal to be characterised by a reasonably high auto-correlation coefficient (Bao and Pan, 1996).

A feedback controller must be designed to provide negative feedback (to reduce the amplitude of the undesired noise) rather than positive feedback, over the frequency range of interest. Feedback controller design usually relies on standard methods described in many text books on the subject. The bandwidth over which control will be effective (negative feedback) is fundamentally limited by the delay in the path between the controller output to the loudspeaker and the controller input from the error sensor. The bandwidth of effective control is directly proportional to the reciprocal of the delay. The phase shift associated with this delay always changes the system from a negative feedback system to a positive feedback system at high frequencies. This is the main disadvantage of feedback controllers.

When the phase shift (or delay) through the control system (including the path from the control source to the error sensor) exceeds 180°, and the overall gain exceeds unity, the system will become unstable, producing positive feedback instead of negative feedback, resulting in ever increasing noise levels that are only limited by the output capacity of the loudspeaker and its amplifier. This can cause serious acoustic noise problems in the presence of high frequency noise or if the physical system being controlled changes too much from the design condition (for non-adaptive feedback control) or too rapidly between states (for adaptive feedback control). An example may be the unstable oscillation (or screeching) in an active headset with analog control as the head set is adjusted on the head of the wearer or if the wearer enters an environment characterised mainly by impulsive or high frequency noise.

The instability problems of feedback controllers are usually minimised by keeping the controller gain within reasonable bounds, (which has the effect of limiting the controller noise reduction performance) and using low pass filters to attenuate incoming high frequency signals that cannot be controlled. Unfortunately if the

amplitude "roll-off" characteristic of the high pass filter is too steep, the phase at lower frequencies is affected adversely and this further limits the useful bandwidth of the controller.

To minimise acoustic delays and thus maximise feedback control system performance and stability, the physical locations of the control source and error sensor should be as close together as possible. The disadvantage of placing the error sensor close to the control source is that because of near field effects, the sound pressure at large distances from the error microphone may not be significantly reduced. This is not a problem, of course for active ear muffs because of the close proximity of the ear drum to the error sensor. The delays in the signal processing circuitry should also be as small as possible, usually resulting in the requirement for analog rather than digital circuitry for non-adaptive systems.

For feedback systems, the delay between the control source and error sensor can only be reduced to a certain limit. This is because of the near field effects that exist close to a loudspeaker, so that placing the microphone too close will reduce the far field performance of the controller, as it will be possible to achieve cancellation only at a very local area near the microphone, due to the non-uniformity of the near field. One consequence of the acoustic delay is that feedback controllers can only cancel periodic noise by a large amount. Following from this, one may conclude that for random noise, the feedback controller will perform better for noise that has a high auto-correlation coefficient for delays equal to and less than the delay through the controller and cancellation path. Non-adaptive feedback control is also effective in controlling transient noise to a certain extent, as it adds damping to an acoustic system.

Examples of the practical use of a feedback controller include active ear muffs (or active head sets), active vehicle suspension systems and active control of structural vibration.

Adaptive feedback control can really only be implemented with a digital filter and as a result it exhibits considerable processing delays. Such a system is thus suitable only for periodic noise. This type of controller is only preferred over feedforward control if it is impossible to obtain a reference signal of any type (and this is relatively uncommon) and a fixed, non-adaptive feedback controller is unsuitable.

2.2.3 Waveform Synthesis

Waveform synthesis uses a similar configuration to that shown in Figure 2.2. In this case, the pulses from the tachometer signal are used directly by the electronic controller to generate the cancelling signal. Each pulse from the tachometer is converted to a corresponding output amplitude by the electronic controller. The controller must be programmed with the number of pulses that will be provided for one complete cycle at the fundamental frequency to be controlled. In that way the controller can assign appropriate output amplitudes corresponding to each pulse, and then update the values after each cycle based on the error signal value. The error signal is sampled synchronously once for each pulse received by the controller. A gear wheel is usually needed to provide the required number of pulses per revolution

from the tachometer. The number of pulses required per waveform period increases as the required noise reduction increases or the number of harmonics to be controlled increases. This is because the accuracy of the output waveform shape is dependent on the number of pulses (and correspondingly the number of steps) per period (see Figure 2.4).

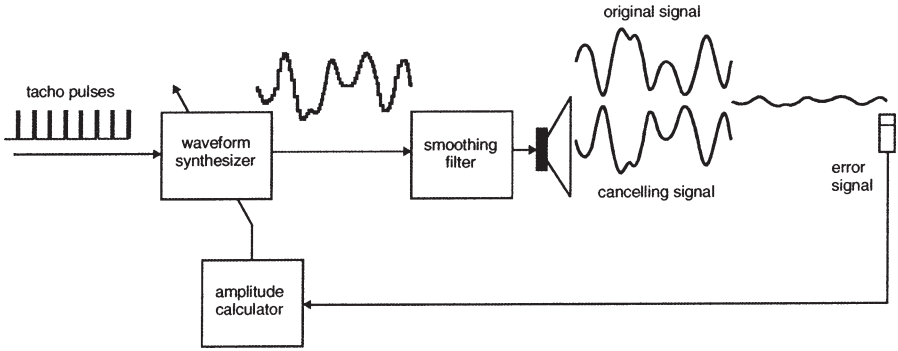

Figure 2.4 Arrangement of waveform synthesis controller.

The waveform synthesis system can attenuate noise at the fundamental frequency of the waveform and all its harmonics, but nothing in between. More details about this approach can be found in the discussion in Chapter 3.

2.3 CONTROL SYSTEM OPTIMIZATION

In general, the performance of an active noise control system is governed by a number of related factors that must be addressed in the appropriate order during the design procedure. Referring to Figure 2.5, it can be seen that the absolute maximum levels of (global) attenuation that are possible with a particular active noise control system are determined first by the placement of the control sources. This means that no matter how well the error sensors have been placed or how good are the electronics, an active control system will not function properly if the control source placement is not satisfactory. Even for the simple single channel case involving the control of plane waves in a duct, there are preferred locations for the control source that will give better results (in terms of power needed to drive the loudspeakers as well as noise reduction) than other locations.

After the control source placement has been optimised, the maximum performance achievable with the active control system will be determined by the locations of the error sensors, which must be such that they can effectively sense all parts of both the primary and control signals. For example, if the target of the control system is the reduction of noise levels in a reverberant space, the error sensors must be capable of adequately sensing all acoustic modes driven by the primary and control sources. Similarly, if the aim is to reduce the noise inside automobiles, the error sensors must be capable of sensing all acoustic modes excited in the vehicle cabin.

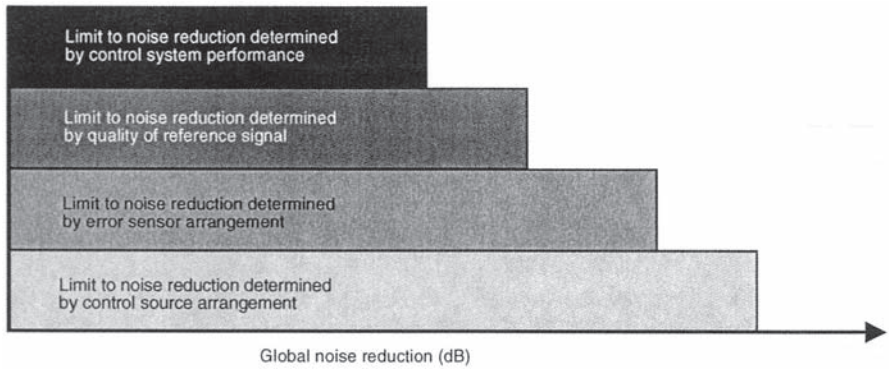

Figure 2.5 Performance hierarchy of an active noise control system.

After both control source and error sensor placements have been optimised, the maximum achievable performance of a feedforward control system will be limited by the quality of the reference signal. The control signal can only act to cancel that part of the error signal that is correlated (or coherent) with the reference signal. Thus, if the reference signal contains components that are not in the error signal, the dynamic range of the controller will be effectively reduced, with correspondingly poorer noise reduction results. On the other hand, if the error signal contains components that are not present in the reference signal, then the noise reduction measured by the error sensor will be proportionally reduced.

The final performance limiting factor for a feedforward control system is the performance of the electronic control system, which in turn is related to its calculation accuracy and dynamic range as well as the algorithms it uses. The dynamic range is determined by the number of bits characterising the A/D converters as well as the adjustment of the input amplifiers to ensure that the maximum possible signal level corresponds to the maximum digital output. Usually 16-bit A/D converters are adequate. The calculation accuracy depends on whether the processor is fixed point (16 bit) or floating point (32 bit). The floating point processor is much easier to use and set up than the fixed point processor due to its greater calculation accuracy making it more forgiving of the selection of parameters that impact on the calculation process. Thus, the floating point processor is recommended for use in all but low cost mass market implementations. Note that DSPs are used rather than ordinary microprocessors because most of the operations done by the adaptive algorithm are multiplication and addition.

Each of the performance limiting factors illustrated in Figure 2.5 and mentioned above (except for controller performance) will now be discussed in detail. The discussion of the influence of controller performance is left to Chapter 3.

The sources needed to generate the anti-noise field (control sources) must be capable of producing noise levels similar to those produced by the unwanted noise source. The control sources must also be able to survive in the particular industrial environment in which they are used. Typical control sources include loudspeakers, horn drivers or vibration actuators (piezoelectric patches, piezoelectric stacks, magnetostrictive

actuators, electrodynamic shakers, electromagnetic actuators, inertial shakers, hydraulic shakers and pneumatic shakers). The vibration actuators are used sometimes to control the vibration of surfaces that are radiating the unwanted sound.

2.3.1 Control Source Output Power and Placement

Achieving optimal control source placement is a complex process. To obtain global attenuation, the basic requirement is that the control source arrangement must be able to duplicate the unwanted sound field with some fidelity. For single control source systems, such as the control of plane waves in a duct, the optimal control source location is where the required displacement amplitude (of the control loudspeaker) is a minimum. This location can be determined theoretically or experimentally by trial and error. If the control source is not placed at the optimal location, the same amount of noise reduction may be possible in some cases, but the control loudspeaker will have to be driven much harder and in practice, there are likely to be locations where it simply cannot be driven hard enough (due to loudspeaker power limitations) to achieve the expected noise reduction.

For applications where many control sources are necessary, the optimal locations can be determined by a numerical procedure involving finite element (or boundary element) analysis and genetic algorithm optimisation. Finite element analysis is used to calculate the system modal characteristics, which are then used to calculate the sound field generated by the primary and control sources. For simple systems, (e.g., a simply supported panel radiating noise) the theoretical modelling may be based on an exact analysis using classical mechanics rather than finite element analysis. For each possible control source configuration, the control source strengths required to minimise the sum of the squared sound pressures at all possible sensing locations are calculated using quadratic optimisation (Hansen and Snyder, 1997, Chapter 8). For enclosed sound fields, total potential energy, rather than the sum of squared sound pressures at a number of locations may be used as the quantity to be minimised (cost function). For sound radiated by a source outdoors, the cost function may be total radiated sound power. The minimum value of the cost function is calculated for each control source configuration tested. The best control source configuration can then be determined by trial and error or a more sophisticated search procedure such as a genetic algorithm may be used as described by Simpson and Hansen (1996) and Hansen et al. (1996, 2000).

It should be noted that the modelling does not have to be purely analytical or numerical. Experimental data, namely transfer function measurements, between an array of possible sensing locations and the primary and possible control source locations, can be used to model active noise control performance. First the primary sound field (with no controlled field operating) is measured at the locations where it is desired to minimise the sound field. The number of locations can be much greater than the number of error sensors that are planned to be used. Next, transfer functions are measured (in the frequency domain, using a spectrum analyser) between all possible control source locations and the locations where the primary sound field

was measured. For a particular control source configuration, the optimum control source strengths that minimise the sum of the squared sound pressures at the specified sensing locations can then be calculated using commercial multiple regression packages as described in the literature (Snyder and Hansen, 1991c).

Note that the optimisation procedures outlined in the preceding paragraphs strictly apply only to a single frequency. Each frequency of interest will be characterised by a different optimum set of control source locations. If only one or a few tones are to be controlled (or if the frequency ranges to be controlled are narrow band in nature), the optimum locations may be calculated for each tonal frequency (or centre frequency of a particular narrow band) and a compromise determined to obtain the best overall noise reduction. However, if the noise to be controlled is broadband in nature, it is impractical to concentrate on optimising control source locations using the procedures just outlined unless one part of the spectrum is more important than all the other parts. Alternatively, it may be possible to divide the frequency range of interest into a number of narrow bands and determine optimum source locations for each band. The actual control source locations that are used may then be a compromise between the various optimal locations corresponding to the centre frequencies of each band and more control sources than originally expected may have to be used as well. What is likely to happen in practice is that some parts of the frequency spectrum will be controlled to a greater extent than other parts of the spectrum for a particular control source configuration.

One way of coping with broadband noise is to use more control sources than theoretically necessary for a single frequency source. An example is controlling sound propagating in a duct. If a single control source is used, there will be certain frequencies at which it cannot generate sufficient output to achieve significant control. In this case, it would be beneficial to have a second control source separated from the first axially along the duct by a distance corresponding to a third of a wavelength at the highest frequency of interest.

There are a few general rules that apply to control source placement. First, it is generally more difficult to obtain significant levels of global sound attenuation in free space than in an enclosed space. To duplicate the unwanted acoustic radiation pattern in free space generally requires the control sources (usually loudspeakers) to be placed in close proximity to the source of the unwanted noise. As an example, if the source of unwanted noise is a simple monopole and the control source is a second monopole, then to achieve a reduction of 10 dB in radiated power, the two sources must be no greater than one tenth of an acoustic wavelength, λ, apart, a constraint that is more easily satisfied at low frequencies. This constraint is clearly illustrated in Figure 2.6, which shows the attenuation as a function of distance, r, between the two sources (Nelson et al., 1987b).

If the excitation frequency is 100 Hz, and the primary source size is small compared to a wavelength of sound (less than $\lambda/5$), and if the control source is within approximately 30 cm of the source of the unwanted noise, 10 dB of global sound attenuation is the maximum that can be obtained. However, if the excitation frequency is 500 Hz, the control source must be within a few centimetres of the unwanted noise to achieve the same attenuation. Global sound attenuation refers to a reduction in the

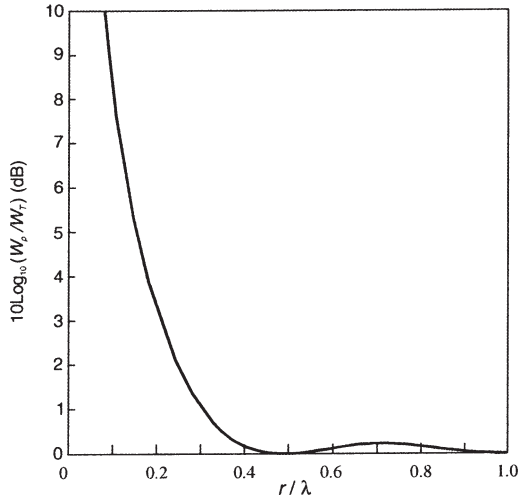

Figure 2.6 Maximum possible attenuation in sound power for a single monopole source by another monopole source as a function of separation distance.

total sound power radiated by the combined primary and control sources compared to that radiated by the primary source alone. On the other hand, it is possible to obtain "local attenuation" using a control source remote from the primary source. In this case, the sound levels at other locations are likely to increase with a resulting overall increase in the radiated sound power, as a result of the reduction in a localised area.

If the source of unwanted noise is greater in size than about one fifth of a wavelength, it will be necessary to use more than one independent control source to obtain appreciable global sound attenuation, and the larger the physical size of the unwanted noise source, the greater will be the number of control sources required. It is also important to note that unless the noise being generated is tonal, it is often difficult to obtain a reference signal, representing the impending unwanted disturbance, in sufficient time to generate the required control signal. This is not so much of a problem for periodic noise (such as electrical transformer hum) because in most cases, it may be assumed that the reference signal does not vary much from one cycle to the next.

In summary, we may conclude that to obtain a substantial amount of noise reduction, the control source signal must be coherent with the primary source output (that is, no extraneous noise may exist in either signal), the separation between the two sources must be small and the control source must be of similar size to the primary source and capable of generating a similar volume velocity at the frequencies to be controlled. Of course, if the primary and control sources are in a duct, rather than in free space, the source separation and size constraints do not apply.

The effect of control source location on the maximum achievable sound power reduction in a duct is illustrated in Figure 2.7 for a constant pressure primary source (e.g. a fan for which the acoustic pressure generated is independent of the acoustic

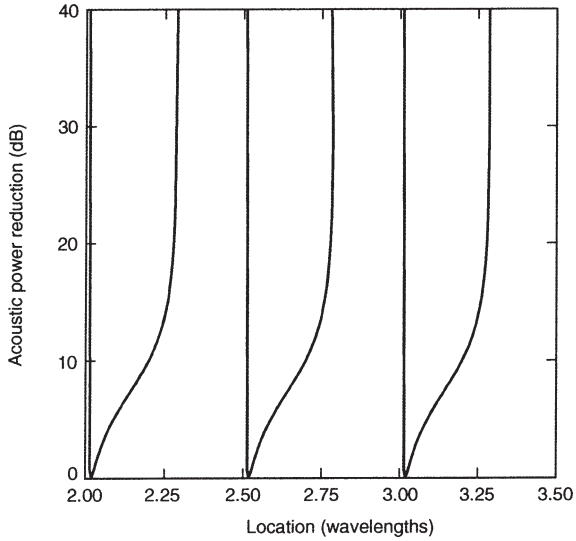

Figure 2.7 Total acoustic power reduction as a function of primary/control source separation for a constant pressure, non-rigid primary source (Hansen and Snyder, 1997).

load impedance that it sees) and a non-infinite impedance in the plane of the primary source. For an infinite impedance in the plane of the primary source, an infinite amount of control is achievable regardless of source location.

Note that the downstream duct impedance has no effect on the optimum control source location. It is also interesting to note that the best location for the control sound source in a duct turns out to be at one of the pressure maxima, so the best location may be determined by measurement of the sound pressure in the duct if the primary source termination impedance cannot be determined.

Figure 2.8 is interesting in that it shows how much volume velocity is required from the control source in relation to the primary source to achieve optimal control. It is clear that source location has a large influence on how hard it must be driven to achieve optimal control.

As previously explained, control source optimisation procedures usually only optimise at a single frequency. There are many industrial applications where this is inadequate and even in cases where a single frequency tone only is to be controlled, the frequency or wavelength is likely to shift with process changes or temperature changes. In these cases, it may be prudent to explore optimum control source locations at a number of frequencies and temperatures in the range to be controlled. The conclusion may then be that a number of control sources may be required to maximise the noise reduction in cases for which, theoretically, only one source should be sufficient.

An example is the control of a tonal noise in an industrial exhaust stack. The wavelength of the noise typically may change by about 20% due to process temperature changes and fan speed changes. Although a single control source is all

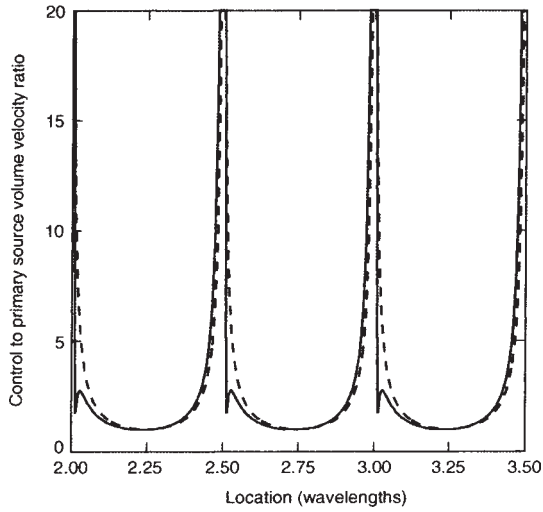

Figure 2.8 Relative control source volume velocity as a function of primary/control source separation for optimal control and constant pressure primary source (Hansen and Snyder, 1997).
———— non-rigid termination at primary source
- - - - - - - - - - - rigid termination at primary source

that is required to control a single frequency noise in a duct in which no higher order modes are cut-on, there are source locations that would require excessive source output. These locations vary as the wavelength varies and to cover all possibilities, it may be necessary to use up to three control sources spaced axially along the duct at intervals of one sixth of a wavelength at the highest frequency of interest.

Sometimes, one is interested in obtaining just local cancellation, rather than global control; for example, around the driver's head in the cabin of mobile mining equipment. The size of the "zone of quiet" achievable is a function of error sensor type and arrangement as well as the number and arrangement of control sources. Thus, the local cancellation case will be discussed in the next section.

2.3.2 Influence of Error Sensor Placement

As the control source configuration generally affects the optimum error sensor placement, it is important that the error sensor configuration only be optimised after the desired control source configuration has been determined.

With a theoretical or numerical analysis or with measured data that allows both the primary sound field and optimally controlled sound field to be calculated (or measured in the case of the primary field), it is possible to calculate the optimum error sensor locations. The optimally controlled sound field may be one that minimises the sum of the squared sound pressures at specified locations or it may be the sound power radiated by a source or the total potential energy in an enclosed space or in a

sub-volume of an enclosed space. The optimum error sensor locations are the locations of greatest difference in acoustic pressure levels between the primary and controlled sound fields.

Care must be taken to locate acoustic pressure error sensors in the far field of the control or primary sources (if possible), otherwise good control may not be achieved at large distances from the sources. At very low frequencies and for large sound sources, the near field can extend a long way from the primary and control sources. In this case, the result of using far field error sensors is a large delay in the control system cancellation path, which reduces controller stability and tracking speed. In these cases, better overall control system performance may be obtained by placing the error sensors in the near field of the control sources (for example in the control of the hum generated by large substation power transformers).

Better overall system performance is usually obtained if the error sensors are not placed symmetrically around the sources. However, the sensitivity of the control result to error sensor placement reduces as the primary and control source separation distance is reduced. Note that if sound intensity sensors are used, it is not necessary that they be placed in the far field of the control and primary sources. However, to date, poor results have been obtained using sound intensity sensors rather than simple sound pressure sensors, so the added complexity is not only not justified, it produces a poorer noise reduction performance, even when compared with that obtained with near field pressure sensors.

In many cases the optimum error sensor locations (as well as optimum control source locations) are frequency dependent, which means that more sensors must be used if a reasonable frequency bandwidth is to be covered. Also in some cases it may be adequate to use bandpass filtering, so that the error signal is only present at frequencies where its location is close to optimal. In the case of noise radiating structures, it is possible to replace microphone error sensors with PVDF film bonded to the noise radiating structure as the error sensors.

PVDF film, which is piezoelectric, may be cut to shapes, which result in them only sensing the structural vibration that is contributing to the radiated sound. This work is the subject of current research (see Cazzolato and Hansen, 1998, 1999).

For the case of local cancellation using a single error microphone, the size of the "zone of silence" in which a greater than 10dB sound reduction is obtained, is approximately one tenth of a wavelength. However, if the sound field is in an enclosed space and an energy density probe is used that detects the total energy in the acoustic field, the size of the "zone of silence" extends to one half of a wavelength, although the maximum attenuation obtained is a little less. Note that the total energy is made up of the sum of the kinetic energy (proportional to the square of the acoustic particle velocity) and the potential energy (proportional to the square of the acoustic pressure).

The preceding discussion applies mainly to feedforward control systems. Feedback systems have additional stability constraints, which usually require that the error sensor and control source be located close together. Also, for random noise, it is essential that the noise autocorrelation coefficient, corresponding to the delay through the controller, is greater than about 0.9 if the performance is to be at all useful.

2.3.3 Influence of Reference Signal Delay and Quality

Note that feedback systems do not have a reference sensor, so the following discussion applies only to feedforward systems. The reference signal influence on feedforward control system performance is twofold. First the delay for the unwanted noise signal to travel between the reference sensor location and control source location must be greater than the electronic delay through the control system or the controller performance for random noise control will be degraded. For example, a measurement of random noise at an upstream point in an air handling duct may be used to predict the noise at some downstream point in 3 milliseconds time (if the two points are separated by approximately one meter); however, the measurement cannot be used to predict the noise at the downstream point in, say, 10 or 20 milliseconds time. Periodic signals, which are slowly varying, need not satisfy this causality condition because it may be assumed that the characteristics of one period are sufficiently similar to those of the periods preceding it. Causality is even more important for feedback controllers because they have no reference signal. Instead, they rely on the autocorrelation of the noise to be controlled to be high for delays greater than the delay through the control system.

The total delay through the controller includes the delays associated with the A/D interface (significant delay), the signal processing (usually small) and the electroacoustic conversions associated with reference sensors (small) and control sources or loudspeakers (often large). The delays through each of these components may be characterised in terms of group delay, which is a measure of the time it takes for a given signal to propagate through a component. It is quite likely for the path between the reference signal input and control signal output to have a group delay of between 3 and 10 milli-seconds. The delay can easily be much larger for low frequency signals, as components designed to operate at low frequencies (anti-aliasing and reconstruction filters which cut off at low frequencies, and control sources that have maximum output levels at low frequencies) typically have group delays that are longer than similar components designed to operate at higher frequencies. Note that a group delay of 10 milli-seconds corresponds to the need for approximately 3.4 metres of space (at room temperature) between the reference sensor and control source in a duct full of air.

Regarding reference signal quality, the following characteristics are important:

- coherence between the reference and error signals;
- feedback of the control signal to the reference signal; and the
- relative magnitude and character of the main frequency components that make up the reference signal.

First, in terms of coherence (which can be measured with most audio spectrum analysers), the maximum possible fractional reduction in the power spectrum of the system error signal is defined by:

$$\frac{S_{ee}(\omega)opt}{S_{ee}(\omega)unc} = 1-\gamma^2(\omega), \tag{2.1}$$

where $S_{ee}(\omega)$ is the power spectrum of the error signal, *opt* and *unc* denote optimally controlled and uncontrolled signals, and γ^2 is the coherence coefficient between the error signal and reference signal. Clearly, the coherence coefficient must be close to one for significant attenuation to be possible as a result of active noise control. For example, using the above equation, the required minimum value of γ^2 to achieve a 20 dB noise reduction is 0.990.

Acoustic feedback can occur in a feedforward active noise control system if a microphone is used to provide the system reference signal and some of the noise generated by the control source reaches the microphone. If the acoustic feedback is small relative to the primary noise signal at the reference microphone location, then one is just restricted in the choice of control filter types that may be used (see Chapter 3). If the feedback signal is relatively large (the exact size is system dependent), then the control system may become unstable, regardless of whether an FIR or an IIR filter is used. Thus, it is important to find alternative reference sensors when possible, so that the feedback of the control signal to the reference signal is minimised. When only periodic noise generated by rotating equipment is to be controlled, a popular alternative for a reference sensor is a tachometer. Other possibilities for random noise include a microphone located near the noise source or an accelerometer mounted on a structure attached to the noise source. When microphones are used as reference sensors the influence of the control sources on the reference signal may be minimised by using directional microphone or control source arrangements.

For active noise control systems that operate in the time domain, the controller acts on the time varying reference signal, rather than explicitly on its frequency components. The control system operates so as to remove that part of the reference signal that is correlated with the error signal. This means that the control system will attempt to remove the dominant frequency component of the reference signal, which is also present in the error signal, even if this is not the desired result. For example, if the target of an active noise control implementation is a 30 Hz signal, and a 20 Hz signal (which need not be controlled in this particular application) is also present in both the reference and error signals, then the controller will attempt to minimise both the 20 Hz and 30 Hz components. If the amplitude of the 20 Hz component of the reference and error signals is 10 dB above that of the 30 Hz component, then the controller will attempt to attenuate the 20 Hz component by 10 dB before it explicitly attenuates the 30 Hz component. The control system can be viewed as having a "flattening" affect on the spectrum, where the frequency components in the error signal that are also present in the reference signal will be "pushed" down to approximately equal amplitudes. The control system can also be viewed as being able to subtract a limited amount of "energy" from the reference signal; the attenuation per frequency component is reduced as the number of frequency components requiring attenuation is increased. For example, assuming that the control system can attenuate both the 20 Hz and 30 Hz signal components, and if the amplitude of the 20 Hz component of the signals is 10 dB above the 30 Hz component, then the 20 Hz component may be attenuated 15 dB, while the 30 Hz component is attenuated 5 dB (the final spectrum is "flattened"). If the 20 Hz component is removed, the 30 Hz component may be attenuated 15 dB. However, if the controller cannot attenuate

the 20 Hz component, perhaps because the transducers were designed to operate at 30 Hz and cannot provide adequate output levels for attenuation at 20 Hz, and the 20 Hz component of the signals is dominant, the control system will go unstable as it tries to achieve the impossible task of attenuating the dominant signal component. To optimise the controller performance, the relative amplitudes of the frequency components in the reference signal should be the same as the relative amounts of attenuation required for each frequency component. That is, if 25 dB of control is required at frequency f_1 and 10 dB is required at f_2, then the amplitude of the reference signal power spectrum at f_1 should be 15 dB higher than the amplitude at f_2. In many cases this requires some filtering of the reference signal prior to it being used by the controller. This phenomenon can be explained by reference to the filter update equations discussed in Chapter 3 and the explanation will be discussed there.

CHAPTER THREE

THE ELECTRONIC CONTROL SYSTEM

3.1 INTRODUCTION

A number of alternative types of electronic control system will be described in detail here. First an overview of the different types will be given, then control filter types will be discussed followed by a discussion of the algorithms used for optimising them. Programming an electronic control system is a complex task and optimal performance requires that most of the programming be done in assembler code. Fortunately, with the advent of reasonably priced commercial controllers, it is probably not necessary for most users to know how to program them. Nevertheless even tuning a commercial active noise control system is an acquired art that takes quite a bit of practice to master.

Figures 2.2 and 2.3 show where the electronic controller fits into an adaptive feedforward active noise control system. In practically all feedforward implementations, the controller is digital. In some feedback systems that are non-adaptive, analog electronics are still used due to the minimal delays associated with them. The feedforward electronic controller is made up of three major components with two inputs and one output as shown in Figure 3.1.

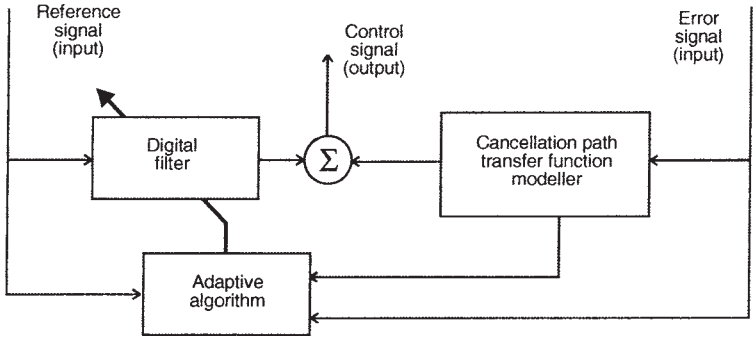

Figure 3.1 Basic components of the electronic part of a single-channel feedforward active noise control system.

Multi-channel controllers are similar in architecture to single channel controllers as shown in Figure 3.2; the major difference is in the adaptation algorithm. Adaptation algorithms for multichannel controllers are discussed in detail by Hansen and Snyder (1997) and Kuo and Morgan (1996) and will only be briefly mentioned here. In Figures 3.1 and 3.2, the input and output signals (reference, error, and control) are

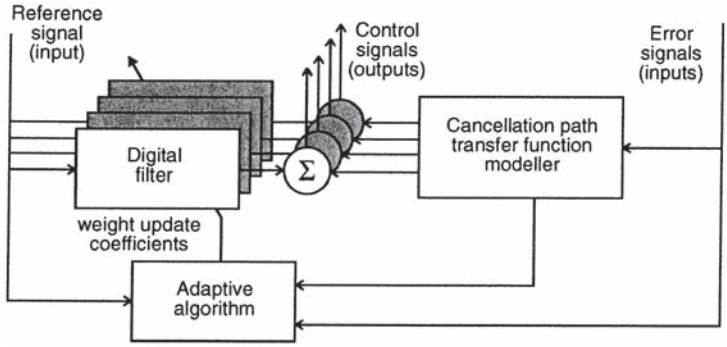

Figure 3.2 Basic components of the electronic part of a multi-channel feedforward active noise control system.

assumed to be digital (the analog to digital and digital to analog converters are not shown). The three major components of the controller shown in Figures 3.1 and 3.2 are: a digital filter, an adaptive algorithm, and a cancellation path impulse response modeller. Each of these will be discussed in detail in the sections to follow.

Adaptive feedback controllers differ from the structure shown in Figures 3.1 and 3.2 in that there is no external reference signal for a feedback system. Instead a pseudo-reference signal is synthesized from the error signal as will be seen later. Non-adaptive feedback controllers are usually based on analog electronics and consist solely of a filter and an amplifier as the electronic controller in Figure 2.1 (b). For the waveform synthesis implementation, the cancellation path transfer function modeller is not needed and the digital filter is replaced with a waveform synthesizer.

3.2 DIGITAL FILTERS (ADAPTIVE CONTROL FILTERS)

The digital filter component of the feedforward or adaptive feedback controller (sometimes referred to as a control filter) is responsible for generating a control signal output from the reference signal input. The control signal is fed to a control source (such as a speaker) that generates the cancelling sound. The control filter takes discrete samples of current and past reference inputs (and possibly filter outputs), multiplies them by a set of coefficients or weights, and adds the results to produce an output sample. The values of the filter weights determine how the reference signal is modified by the control filter to produce the required control output. To drive the loudspeaker, consecutive output samples are converted to an analog signal using a reconstruction filter.

The control filter may take a number of forms, the most common of which is the finite impulse response (FIR) filter. An FIR filter may be represented as in Figure 3.3, where z^{-1} represents a delay of one (input) sample and wi represents filter weight i.

The structure in Figure 3.3 is sometimes referred to as a transversal filter, or a tapped delay line. The number of "stages" in the filter (the number of present and past input samples used in the output derivation) is usually referred to as the number of

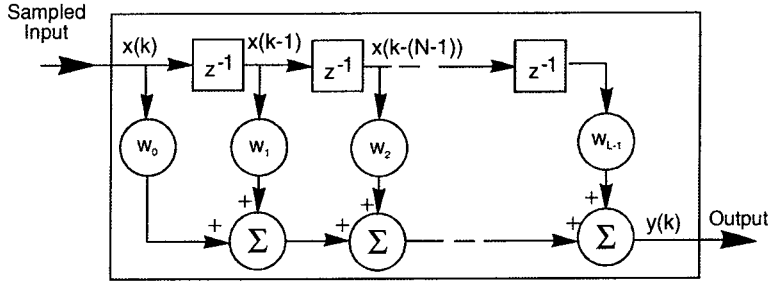

Figure 3.3 FIR filter architecture.

filter "taps". When subject to a unit step input, the filter output will eventually decay to zero, thus its name, finite impulse response filter. FIR filters are ideally suited to tonal noise problems, where the reference signal is one or perhaps a few sinusoids (probably the most common reference signal in active noise and vibration control work), and where the control signal does not in any way corrupt the reference signal.

In some cases, especially when there are resonances in the system to be controlled or if there is acoustic feedback from the control source to the reference sensor, leading to corruption of the reference signal, the FIR filter is not the best choice and the infinite impulse response (IIR) filter is often chosen for its ability to directly model the poles in the system resulting from the above mentioned effects. Such a filter has the architecture illustrated in Figure 3.4 and may be considered as being made up of two FIR filters.

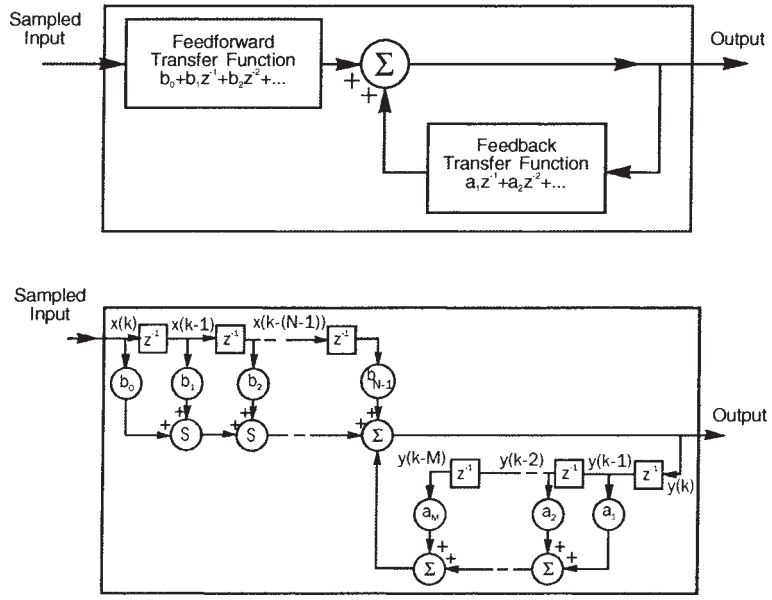

Figure 3.4 IIR filter architecture.

The output value of the IIR filter is equal to the weighted sum of present and past inputs and is defined by:

$$y(k)=b_0x(k)+b_1x(k\text{-}1)+ \cdots +b_nx(k\text{-}n) +a_1y(k\text{-}1)+a_2y(k\text{-}2)+ \cdots +a_my(k\text{-}m) \quad (3.1)$$

The equation for an FIR filter is obtained by setting all of the "a" coefficients to zero in the above equation.

The main advantage of the IIR filter (in addition to its ability to accurately model the acoustic feedback path and system resonances) is that it can model complex systems with much fewer weight coefficients than required by an FIR filter, thus reducing computational load. This advantage comes at the cost of inherent instability, slower convergence and the possibility of convergence to a local minimum in the error surface instead of a global minimum. This is in contrast to the existence of only one minimum for an FIR filter when a gradient descent algorithm is used (see Section 3.4.1). The lack of inherent stability in the IIR filter is a result of the presence of the feedback section of the filter: if the (feedback) loop gain becomes too great the system becomes unstable, as opposed to the case of the FIR filter for which the gain can become extremely large without causing instability. When an IIR filter is subjected to a unit step input, the feedback section ensures that its output will never decay to zero; thus its name, infinite impulse response filter.

IIR filters are preferred over FIR filters where the noise to be controlled is broadband in nature especially if the system to be controlled has resonances in the control frequency range or where the phase speed is not independent of frequency (such as higher order modes propagating in air handling ducts). IIR filters are also preferred over FIR filters in feedforward control systems where there is feedback from the control source to the reference microphone resulting in contamination of the reference signal. This problem often occurs in air handling ducts, where the reference signal is provided by a microphone in the duct. Although the problem can be reduced by using directional sound source and microphone arrangements, it can never be eliminated entirely when a microphone is used to provide a reference signal. System resonances and acoustic feedback from the control source to the reference microphone result in poles in the transfer function of the optimum control filter. These poles can be modelled easily with an IIR filter, as its transfer function is characterised by a denominator as well as a numerator, but as an FIR filter transfer function has no denominator, it takes a very long FIR filter to even approximately model the poles.

In some cases, particularly when there are non-linear acoustic control sources or non-linear systems to be controlled, neither of the IIR or FIR filter architectures are suitable. One possibility that addresses the non-linear problem is to use a non-linear filter such as illustrated in Figure 3.5 where x is the input signal, W_i, are the filter weight coefficients and x^4 and x^5 are the input signal raised to the 4th and 5th powers respectively. A second type of non-linear filter is a neural network, which is illustrated in Figure 3.6. An important characteristic of non-linear filters is that they can generate signals at frequencies that do not exist in the reference signal and thus they are ideal for controlling systems for which the control actuators suffer from significant harmonic distortion.

Each of the filter types just discussed requires a different algorithm for adjusting its weights to achieve a control signal that will minimise the error signal.

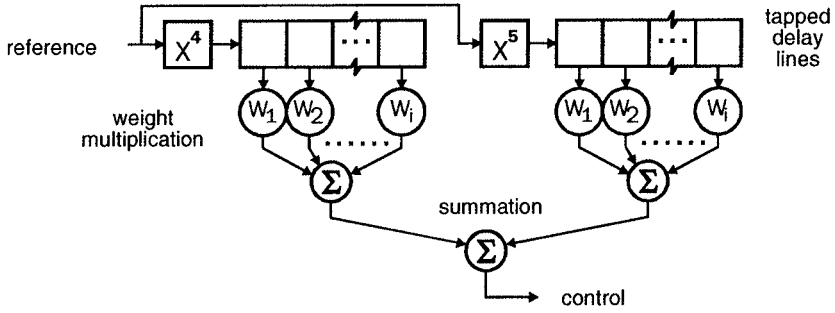

Figure 3.5 Non-linear polynomial (P4P5) filter for control of non-linear systems.

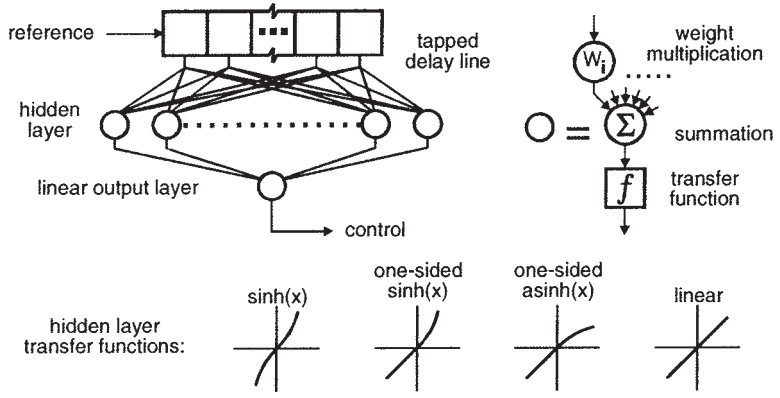

Figure 3.6 Non-linear neural network filter for control of non-linear systems.

In summary, there are three parameters that affect the performance of a digital filter in an active noise cancelling system: the type of filter, the filter weight values and the number of weights. For a single tone, in theory, only 2 weights are needed with an FIR filter to generate the required cancellation signal. In practice, a very large difference in the two weight values may occur, especially if the sampling rate is more than 20 times the frequency of the sine wave. This can result in less noise reduction being achieved, as there are inaccuracies associated with subtracting large numbers to calculate a small difference. It has been found that an FIR filter with between 4 and 20 weights is usually adequate. For multiple tones, 4 to 20 weights per tone should be used, with the actual number required being dependent on how different the sample rate is from 10 times the frequency to be controlled. The greater the difference, the greater the number of filter weights necessary for optimum performance. For random noise, several hundred filter weights are necessary and often an IIR filter gives better results (with less weights in the feedback path than in the feedforward path) for a fixed allowed number of weights. If acoustic resonances exist in the physical system, then 4 to 10 weights per resonance in the feedforward and in each of the feedback parts of an IIR filter are likely to be required for good control.

3.3 ADAPTATION ALGORITHMS FOR ADAPTIVE FILTERS

The adaptation algorithm component of the controller is responsible for tuning the digital filter weights so that the resulting control signal minimises the error signal received by the controller. Another adaptive algorithm is responsible for obtaining a model of the cancellation path impulse response (time domain equivalent to the frequency domain transfer function) as discussed in Section 3.3.2. To be able to accomplish the tuning task, the adaptive algorithm requires three inputs: the error signal(s) corresponding to the sound level where the sound is to be minimised; the reference signal; and the electroacoustic impulse response(s) between the electrical input to the control source and electrical output from the error sensor(s) (cancellation path impulse response(s)). The error signals can be provided by microphones, or by some other transducer that can measure the unwanted disturbance (such as an accelerometer for vibration control). The cancellation path impulse response must be determined as described in Section 3.3.2 for the path between each control source and each error sensor.

Adaptive algorithms used to optimise the FIR or IIR filter weights "on-line" in active noise and vibration control systems are essentially derivations of the adaptive algorithms used in systems such as telephone echo-cancellers and adaptive optics in telescopes to cancel unwanted optical "noise" and thus enhance signals from distant stars. The main difference in active noise control systems is the existence of a cancellation path impulse response, which exists because we are now dealing with sound (and its corresponding slow wave speed) rather than electromagnetic waves. Estimation of the cancellation path impulse response is discussed in Section 3.3.2. Here we will derive the FXLMS (filtered-x, least mean squares) algorithm for adapting the weights of an FIR filter, which includes the effects of the cancellation path impulse response. The LMS (least mean squares) algorithm has been used for many years in telephone echo cancelling systems. The addition of the "FX" to make it the "FXLMS" algorithm is a result of the need to include the effects of the acoustic cancellation path (Morgan, 1980; Burgess, 1981). It is called the "filtered-x" algorithm because it requires a filtered version of the reference signal as input, with the filter having the same (or estimated) impulse response as the cancellation path. Of course, the adaptive algorithm used for determining the weights of the FIR filter used to model the cancellation path impulse response does not include the "filtered-x" part; it is the same as the LMS algorithm used in echo-cancellers in telephone systems.

3.3.1 Single-Channel FXLMS Algorithm for FIR Filter Weight Adaptation

3.3.1.1 Feedforward Control

The LMS algorithm is a gradient descent algorithm that operates by adding to the current value of the filter weights a small percentage of the negative gradient of the error surface (the error criterion plotted as a function of the filter weights) to calculate

an "improved" set of filter weights. In active noise and vibration control applications, the error criterion is the sum of the squared values of the error signals. Minimisation of this error criterion will lead to minimisation of the unwanted acoustic or vibration disturbance at the error sensing locations. A squared error criterion is used because if minimisation of the (unsquared) error signal were the control object, a very large negative error signal, which is clearly undesirable, would result. An error surface corresponding to an FIR filter with just 2 weights is illustrated in Figure 3.7. In practice, many more than two filter weights are used, resulting in a multi-dimensional error surface, which cannot be illustrated easily.

The error surface shown in Figure 3.7 is a hyper-paraboloid that has the

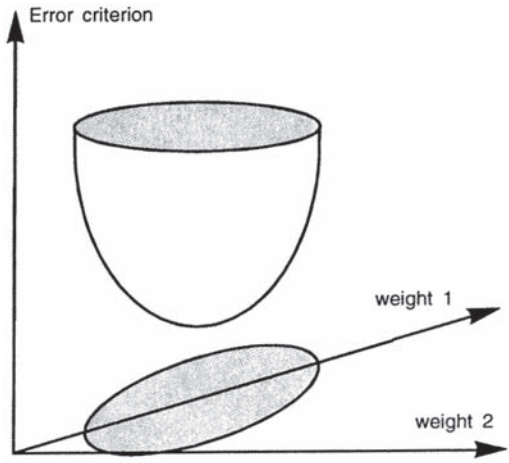

Figure 3.7 Typical plot of mean square error as a function of two weights in the digital control filter.

appearance of a "bowl". There is a single combination of weight values (corresponding to the bottom of the "bowl") that will minimise the error criterion. The purpose of the adaptive algorithm is to find this optimum set of filter weight values (thus minimising the error criterion) by making iterative changes to existing estimates of the weight values.

An intuitive understanding of a gradient descent algorithm may be obtained by imagining a ball being placed at some point on the side of the bowl and then released. The ball then rolls down the sides of the bowl, eventually coming to rest (after some oscillation) at the bottom. This is exactly what one would like an algorithm to do to find the optimum set of filter weights. When first released, the ball rolls in the direction of maximum (negative) change in the slope, or gradient, of the error surface. If the position of the ball at discrete points in time were examined after its release, it would be found that the ball's new position is equal to its old position (one discrete point in time ago) plus some distance down the negative gradient of the bowl. This heuristic argument may be formalised and expressed mathematically as a gradient descent algorithm.

A gradient descent algorithm attempts to iteratively converge down the sides of

the "error bowl" to the optimum set of weight coefficients by adding to its existing estimate a portion of the negative gradient of the error surface at the location defined by this estimate. Mathematically, the process may be expressed as:

$$\boldsymbol{w}(k+1)=\boldsymbol{w}(k)-\mu\nabla J(k) \tag{3.2}$$

where $\nabla \boldsymbol{J}$ is the gradient of the error surface at the location given by the current weight coefficient vector, $\boldsymbol{w}$(k), and μ is the convergence coefficient (a positive number), which defines the portion of the negative gradient to be added. The weight coefficient vector elements are the control filter weights and it can be written as:

$$\boldsymbol{w}(k)=[w_0(k)\ w_1(k)\ w_2(k)\ \ldots\ldots\ w_{L-1}(k)]^{\mathrm{T}} \tag{3.3}$$

For the two weight error surface shown in Figure 3.7, the weight coefficient vector will only have 2 elements; that is, L=2 in Equation (3.3).

Consider for simplicity a system with only a single error sensor. Let the contribution to the error signal $e(k)$ at any time instant k be $p(k)$ from the primary (or unwanted) noise source and $s(k)$ from the control source. Then at any time, k, the error signal is given by:

$$e(k)=p(k)+s(k) \tag{3.4}$$

The gradient of the error surface (error criterion plotted as a function of the filter weights as in Figure 3.7) is calculated by differentiating the error criterion, $J(k)=e^2(k)$, (square of the error signal) with respect to the filter weights. For a single error sensor system, noting that the unwanted noise component $p(k)$ of the error signal is independent of the digital filter weights, differentiation produces the following expression:

$$\Delta \boldsymbol{w}(k) = \frac{\partial e^2(k)}{\partial \boldsymbol{w}(k)} = 2e(k)\frac{\partial e(k)}{\partial \boldsymbol{w}(k)} = 2e(k)\frac{\partial s(k)}{\partial \boldsymbol{w}(k)} \tag{3.5}$$

The preceding equation shows that the gradient of the error surface at the location of the current filter weight values is equal to twice the product of the current error signal sample $e(k)$ and the partial derivative $\partial s(k)/\partial \boldsymbol{w}(k)$ of the control source component of the error signal with respect to the filter weights. The error signal component of the gradient estimate is obtained simply by sampling the error signal. However, obtaining the second term is a little more complicated and requires the following procedure. The controller output signal, $y(k)$ (at time sample k) is given by:

$$y(k) = \boldsymbol{w}^{\mathrm{T}}(k) * \boldsymbol{x}(k) = \sum_{i=0}^{L-1} w_i(k)x(k-i) \tag{3.6}$$

where $\boldsymbol{x}(k)=[x(k)\ x(k\text{-}1)\ \ldots\ldots\ x(k\text{-}L\text{+}1)]^{\mathrm{T}}$ represents the reference signal samples, $\boldsymbol{w}(k)$ represents the filter weights and was defined in Equation (3.3), and L is the number of filter weights for the main control filter. Referring to Figure 3.8, the control source contribution, $s(k)$, to the error signal, $e(k)$ at time k is given by:

$$s(k) = [\boldsymbol{w}^{\mathrm{T}}(k)\boldsymbol{x}(k)] * \boldsymbol{c}(k) \approx \boldsymbol{y}(k) * \hat{\boldsymbol{c}}(k) = \sum_{i=0}^{M-1} \hat{c}_i(k)y(k-i) \tag{3.7}$$

where, $\boldsymbol{y}(k)=[y(k)\ y(k\text{-}1)\ \ldots\ldots\ y(k\text{-}M\text{+}1)]$ and

$\hat{\boldsymbol{c}}(k)=[\hat{c}_0(k)\ \hat{c}_1(k)\ \ldots\ldots\ \hat{c}_{M-1}(k)]^T$ are the coefficients of the FIR filter used to model the cancellation path (between the control output and the error sensor input to the controller) and $\boldsymbol{M}$ is the number of filter weights for that filter. The quantity, $\hat{\boldsymbol{c}}(k)$, represents the estimated (with $\boldsymbol{c}(k)$ the actual) impulse response function of the cancellation path (the time domain equivalent of the transfer function in the frequency domain) and * is the convolution operator. If there were no cancellation path (as is the case for the algorithm used to estimate the cancellation path impulse response or impulse response), then $s(k)=y(k)$.

Referring to Equation (3.7), the quantity, $s(k)$ may also be written as:

$$s(k)=[\boldsymbol{w}^T(k)\boldsymbol{x}(k)] * \boldsymbol{c}(k) \sim \boldsymbol{w}^T(k) * \boldsymbol{f}(k) \tag{3.8}$$

where $\boldsymbol{f}(k)$ is the filtered reference signal given by:
$\boldsymbol{f}(k)=[f(k)f(k\text{-}1)\ \ldots\ldots\ f[k\text{-}M\text{+}1)]^T$ and the j^{th} term in $\boldsymbol{f}(k)$ is given by:

$$f(k-j) = \sum_{i=0}^{M-1} \hat{c}_i(k)x(k-i-j) \tag{3.9}$$

The filtered reference signal, $\boldsymbol{f}$(k), is obtained by passing the reference signal through an FIR filter that models the impulse response of the cancellation path (from the input to the control source to the output from the error sensor) as shown in Figure 3.8.

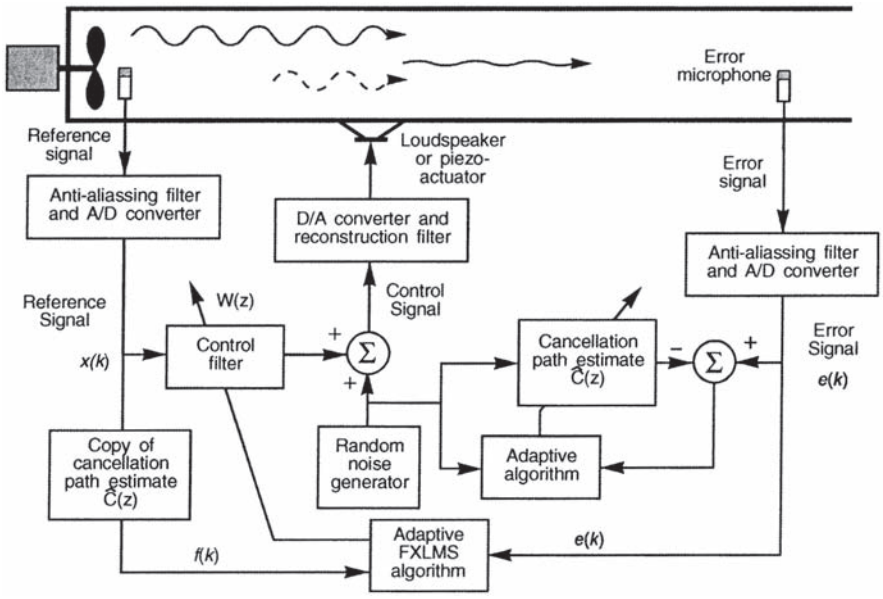

Figure 3.8 Typical control system layout with on-line cancellation path identification.

At this point something needs to be said about notation. Actual quantities are differentiated from estimates of the actual quantities by putting a ^ above the estimated quantities. In the figures, filters are represented by capital letters followed by (z),

such as $W(z)$ or $\hat{C}(z)$, as they are really tapped delay lines. In the equations, the filter coefficients at time k are represented by vectors such as $\boldsymbol{w}(k)$ and $\hat{\boldsymbol{c}}(k)$.

The error signal component of the gradient estimate is obtained simply by sampling the error signal. Using Equation (3.8), the error surface gradient with respect to the filter weight coefficients may be written as:

$$\nabla J = 2e(k)\frac{\partial s(k)}{\partial \boldsymbol{w}(k)} = 2e(k)\boldsymbol{f}(k) \tag{3.10}$$

Using Equations (3.2, 3.6 and 3.10), the adaptive weight update equation can be written as:

$$\boldsymbol{w}(k+1)=\boldsymbol{w}(k)-2\mu e(k)\boldsymbol{f}(k) \tag{3.11}$$

This is the standard FXLMS algorithm, which is used with an adaptive FIR filter. The equation for updating the j^{th} weight of the filter is then:

$$w_j(k+1)=w_j(k)-2\mu e(k)f(k-j) \tag{3.12}$$

where k represents the kth time sample.

The algorithm is implemented in practice by first passing the reference signal, $x(k)$ through an FIR filter, which is a direct copy of the cancellation path estimation filter (FIR filter model) shown in Figure 3.8. The output of the filter is then multiplied by the error signal and the convergence coefficient (see Equation (3.11)) to give the estimate of the change required for each filter weight. The adaptive algorithm effectively calculates the "slope" of the error surface and calculates weights that will cause the error to move down the slope to a smaller value. When the slope is zero, the algorithm will stop converging. Note that for an FIR filter and FXLMS algorithm there is only one minimum on the error surface as opposed to the IIR filter case for which there may be several minima and for which only one of the minima will represent the smallest error.

The filtering of the signal samples in the process of deriving the gradient estimate is what differentiates the active noise and vibration control implementation of adaptive filtering from the other adaptive control implementations, such as those used in telephone echo cancellation. In the latter implementations there is no cancellation path, and so the signal samples in the digital filter are also used in the gradient calculation. The requirement to filter the signal samples to derive the gradient in the active noise and vibration control implementation has led to adaptive algorithm names such as the "filtered-x LMS (or FXLMS) algorithm", which is the active noise and vibration control version of the standard "LMS algorithm".

Selection of a suitable value of convergence coefficient, μ, is extremely important, as it controls both the speed of adaptation and the stability of the adaptive algorithm. If the value of μ is too small, the weights will adapt slowly, and possibly stop adapting before the optimum values are reached. This is because if both the gradient estimate and convergence coefficient are small, then the product (which controls the algorithm) will be even smaller and is likely to become less than the precision of the digital system used for the calculations. If the value of the convergence coefficient is too

large, the weights will either oscillate with too large an amplitude around the optimum values or diverge and lead to instability. In a practical digital system, quantisation errors usually dictate that the best value for the convergence coefficient is that which is just below the value that would cause instability. Smaller convergence coefficients just result in the algorithm stopping convergence prematurely and the error as a result of premature stopping is usually greater than the oscillation error resulting from too large a convergence coefficient.

The delay between calculating a new set of filter weights and detecting the effect at the error sensor output has an important influence on the maximum allowable value of the convergence coefficient that will ensure stability of the algorithm. It is often beneficial to update the filter weights at times separated by an interval equal to the delay. This reduces calculation overheads, allows the use of a larger convergence coefficient and does not reduce the overall convergence rate. An important benefit of using a larger convergence coefficient is that the optimum attenuation level is usually increased.

The optimum convergence coefficient must be selected for each application by trial and error. The factors affecting the choice of optimum convergence coefficient are listed below.

- Number of control sources and error sensors (increasing the number requires a smaller convergence coefficient).
- Cancellation path transfer function amplitude (an increased gain in this path requires a reduced convergence coefficient).
- Time delay in the cancellation path (an increased time delay requires a reduced convergence coefficient).
- Digital filter length (increasing the length requires reducing the convergence coefficient).
- Ratio of sampling rate to reference signal frequency (an increased ratio requires a reduced convergence coefficient.
- Random vs tonal noise (tonal noise requires a smaller convergence coefficient).
- System amplifier gains (increasing gains requires reducing the convergence coefficient).
- FIR vs IIR filter (a larger convergence coefficient may be used for an FIR filter for the same application).
- Errors in the estimate of the cancellation path transfer function (particularly phase). Larger errors require a smaller convergence coefficient. No value of convergence coefficient is satisfactory if the phase error exceeds approximately $N \times 90$ degrees, where N is the number of error sensors (control channels) in the system. Errors in the transfer function amplitude estimate have a smaller but still significant effect; if the gain estimate is too high, then the convergence coefficient must be reduced.

In commercial systems, convergence coefficients are usually adjusted manually by starting with a small value and gradually increasing it until satisfactory and stable convergence rate is obtained. Although it is difficult to set and adjust the convergence coefficient automatically (because the optimum value depends on the parameters mentioned above), it can be done to a limited extent and various means of doing this

are discussed by Kuo and Morgan (1996). The most common method is to use the normalised FXLMS algorithm, which uses the following equation to adjust the convergence coefficient, essentially weighting it in proportion to the reference signal power.

$$\mu = \frac{\beta}{\boldsymbol{x}^{\mathrm{T}}(k)\boldsymbol{x}(k)} \tag{3.13}$$

The quantity $\boldsymbol{x}(k)$ is the reference signal vector equal in length to the number of taps in the control filter and is defined following Equation (3.6). The quantity β is a constant between 0 and 2 that depends on the particular application and is set by trial and error as the control system is set up. In practice, it is necessary to set a lower allowable limit on the product $\boldsymbol{x}^T(k)\,\boldsymbol{x}(k)$ to ensure that the convergence coefficient does not get too large.

3.3.1.2 Delayed FXLMS Algorithm

If a single sinusoidal signal is to be controlled, the cancellation path can be modelled as a pure delay, $z^{-\Delta}$. The purpose of the delay is to align the reference signal to the error signal for use by the control filter weight update algorithm. The weight update expression for the delayed FXLMS algorithm is then:

$$\boldsymbol{w}(k+1)=\boldsymbol{w}(k)-2\mu e(k)\boldsymbol{x}(k-\Delta) \tag{3.14}$$

3.3.1.3 Feedback Control

A very similar algorithm as discussed in Section 3.3.1.1 may also be used with an adaptive feedback system, as illustrated in Figure 3.9. Note that for the adaptive feedback algorithm shown in Figure 3.9, no reference signal is required. In fact, a pseudo-reference signal is synthesised from the error signal. The FIR (control) filter weight update equation is written as:

$$\boldsymbol{w}(k+1)=\boldsymbol{w}(k)-2\mu e(k)[c(k)*\boldsymbol{x}^1(k)]=\boldsymbol{w}(k)-2\mu e(k)\boldsymbol{f}^1(k-1) \tag{3.15}$$

Note that the adaptive feedback controller just discussed cancels only the predictable parts of the primary signal, whereas, feedforward controllers cancel all components of the noise that appear in both the reference and error signals.

The cancellation path modeller shown in the figure is used to estimate the impulse response, $\boldsymbol{c}(k)$ (transfer function in the frequency domain), between the control signal out of and the error signal into the electronic controller. The operation of this part of the system is discussed in detail in Section 3.3.2.

A multi-channel version of the adaptive feedback algorithm is discussed by Kuo and Morgan (1996).

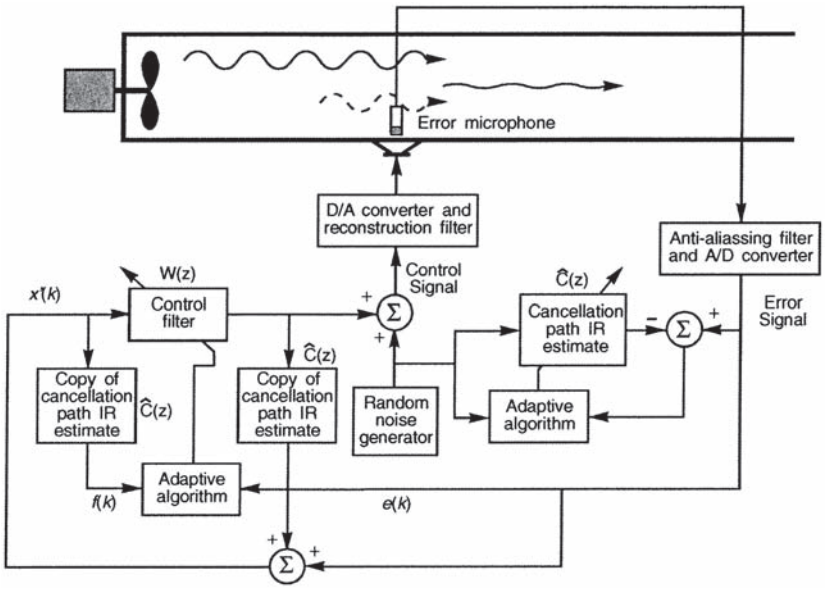

Figure 3.9 Adaptive feedback controller with on-line cancellation path identification.

3.3.1.4 Hybrid Feedforward/Feedback Control

Hybrid feedforward/feedback systems are combined systems that use both a reference and error signal to generate the control output. Note that a feedforward system uses only a reference signal to generate the control output; the error signal is only used by the filter weight update algorithm and is not used directly to generate the control signal. A configuration for a hybrid system is illustrated in Figure 3.10. The long acoustic time delay between the control source and error sensor for the hybrid configuration means that the feedback part of the controller can only act on the predictable components of the noise. The feedforward part will cancel those parts of the error signal that are correlated with the reference signal and the feedback part of the controller will act on all periodic components of the noise at the error sensor, whether or not they are correlated with the reference signal. Thus, the feedback part reduces the energy in the spectral peaks of the error signal, leaving the feedforward part to concentrate on the other parts of the spectrum, resulting in a considerable overall performance improvement when compared to just a feedforward system.

The weight update equations for the filters shown in Figure 3.10 are:

$$\boldsymbol{w}_a(k+1)=\boldsymbol{w}_a(k)(1-\mu a)\ -\mu \boldsymbol{f}(k)e(k) \tag{3.16}$$

$$\boldsymbol{w}_b(k+1)=\boldsymbol{w}_b(k)(1-\mu a)-\mu \boldsymbol{f}^{\mathrm{T}}(k)e(k) \tag{3.17}$$

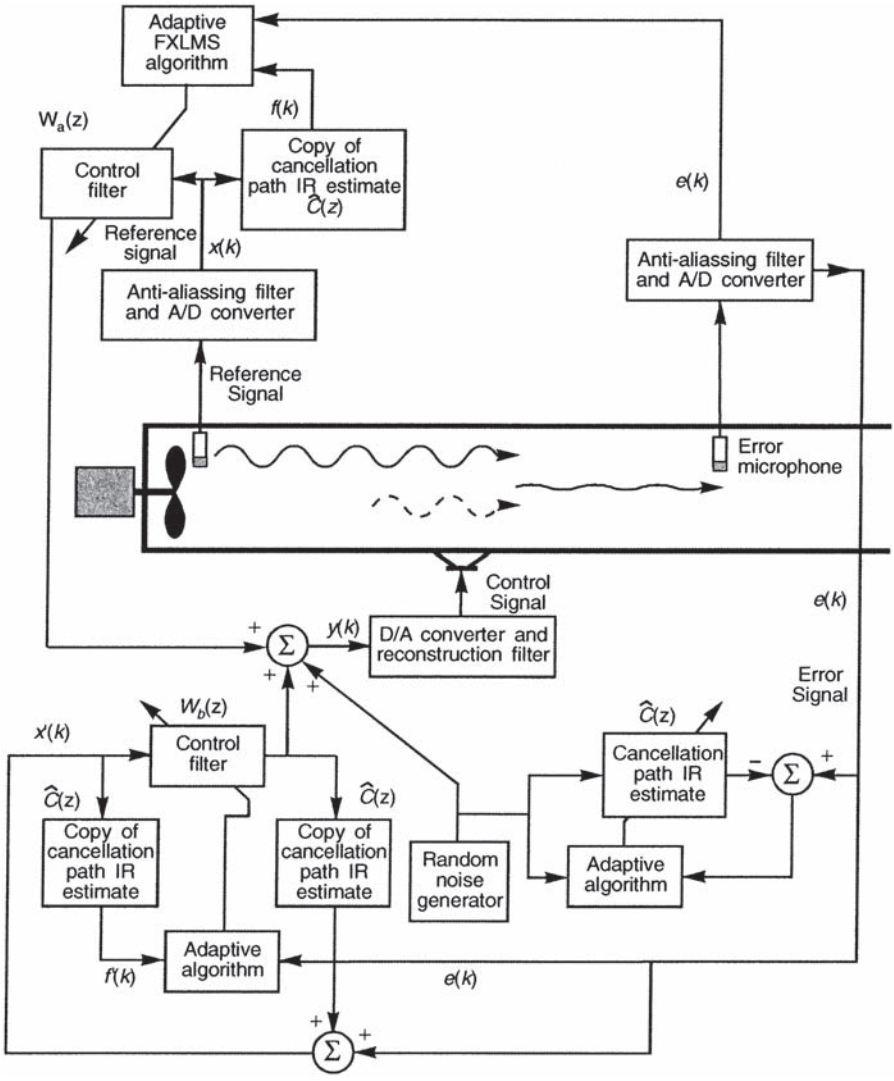

Figure 3.10 Configuration for hybrid feedforward/feedback control system.

3.3.2 Cancellation Path Transfer Function (or Impulse Response) Estimation

The electroacoustic transfer function(s) between the electrical input to the control source and the electrical output from the error sensor(s) is an essential input into adaptive algorithms commonly used to update the control filter weights, as emphasized in Section 3.3.1. To be more correct, what is actually needed by the

traditional time domain controller is the impulse response function, which is the time domain equivalent of the transfer function in the frequency domain. To be even more precise, the controller actually needs a finite impulse response (FIR) filter inserted between the reference signal and the control algorithm to "filter" the reference signal before it is used by the algorithm, as illustrated in Figure 3.8. The effect of this filter is represented by the term, $\boldsymbol{c}(k)$, in Equation (3.8).

The performance of the adaptive algorithm in optimising the control filter weights is only weakly dependent on the accuracy of the estimate of the cancellation path transfer functions. Errors in the transfer function amplitude affect the allowable maximum convergence rate of the control algorithm, so it takes longer to reach an optimum. If the phase error in the transfer function estimate exceeds 90 degrees (for a single channel system), the adaptive algorithm will become unstable. In practice, it is better to limit the error to less than 45 degrees. For multi-channel systems, the phase requirement surprisingly becomes less restrictive as the number of channels increases. From the preceding discussion it may be concluded that it is only necessary that the modelling process produce a reasonable approximation of the actual transfer function, but that increased accuracy in the transfer function measurement will, in some cases, result in improved control system performance.

As the cancellation path transfer function (or impulse response) for a particular system can change with time, it is often necessary to be able to determine it "on-line" on a reasonably regular basis. Reasons for the cancellation path transfer function variations include temperature changes that affect the speed of sound between the control source and error sensor, air flow rate changes in duct systems, dirt build-up on loudspeakers and microphones and ageing of the electro-acoustic components. However, on-line determination of this transfer function (or impulse response) introduces a set of new problems that will become apparent later in the discussion in this section.

Figure 3.11 illustrates the principle of cancellation path impulse response modelling. In most cases, an FIR filter is the most appropriate filter type to implement, and an adaptive algorithm is used to adjust the filter weights so that the impulse response of the FIR filter matches that of the cancellation path. The filter weights are adapted using a gradient descent algorithm, which is a little different to the algorithm used to update the control filter weights (see Section 3.3.1). The difference results from the absence of an electro-acoustic transfer function in the arrangement shown in Figure 3.11. As can be seen from the figure, the modelling signal is used directly in the calculation of the error signal, without having to first pass through speakers, microphones, filters, etc.

The modelling signal shown in Figure 3.11 can be introduced random noise that is uncorrelated with the reference signal or it can be the control signal itself. The advantage of using the control signal is that no additional noise has to be introduced into the system that will limit system performance. The disadvantage is that the modelling signal is highly correlated with the reference signal and this causes errors in the transfer function (or impulse response) measurement. Both types of cancellation path modelling will be discussed here and then a comparison between the two will be made.

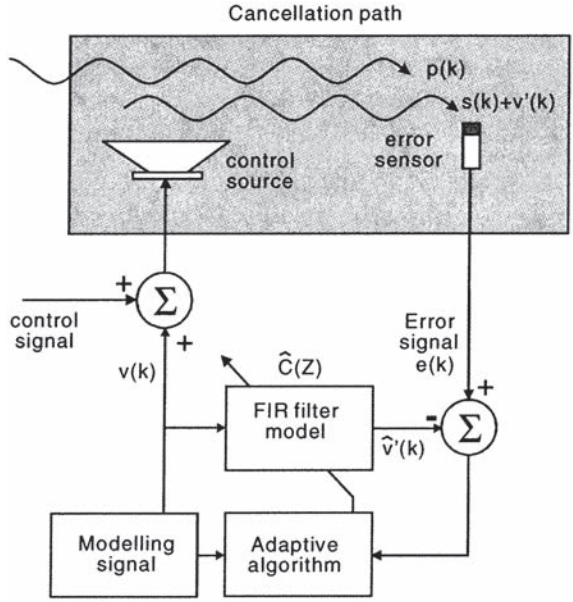

Figure 3.11 Cancellation path modelling arrangement.

3.3.2.1 Random Noise Modelling Signal

The random noise modelling signal is usually either white or pink pseudo-random noise. The advantage of using pseudo-random noise is that it is uncorrelated with the primary noise, which reduces the chance of bias in the model. Unfortunately the use of either type of random noise results in an additional, uncontrollable disturbance being introduced into the system. Fortunately, the amplitude of the modelling disturbance can usually be quite small and still produce an adequate model (say, 30 dB below the peak signal levels at the error sensor as a result of the primary noise, the reduction of which is the control objective).

The filter weight update equation for the filter in Figure 3.11 with both the primary and control sources operating is:

$$w(k+1)=w(k)+\mu v'(k)e(k) \tag{3.18}$$

where:

$$e(k)=p(k)+s(k)+v'(k)-\hat{v}'(k) \tag{3.19}$$

The presence of the uncorrelated primary and control source contributions at the error sensor ($p(k)+s(k)$) degrades the impulse response function estimate accuracy and strong tones in these signals can cause the error to be sufficiently large that the

main control system will become unstable. If the primary source is turned off, no control signal will be introduced and the only signal emitted by the control source will be the pseudo-random noise modelling signal. Thus if the primary source (and thus the control signal) are turned off when the modelling is undertaken, then there is obviously no problem and an excellent estimate of the impulse response of the cancellation path will be obtained. Alternatively, the pseudo random noise signal could be increased to a sufficient level to obtain an adequate model of the cancellation path but this can affect the perceived performance of the controller.

Another way to minimise the influence of the primary and control signals, and allow the controller to remain operating is to use an additional adaptive filter to cancel the primary and control signals as described by Kuo and Morgan (1996, page 224) and Hansen and Snyder (1997, page 483) and referred to as extended identification. This filter uses the reference signal as input and produces an output signal that cancels the components of the error signal that are correlated with the reference signal.

Even if an additional adaptive filter is used, and the primary source is left running as well as the control signal, it is preferable to turn off the control filter adaptation while the impulse response of the cancellation path is being determined and ideally, the impulse response should be measured at relatively infrequent intervals. The interval that is required between consecutive measurements will depend on the application, but in general it need not be nearly as often as the control filter is updated. It has also been found that the overall system performance is improved if the first few filter taps in the impulse response model are set to zero (Snyder, 1999) to reflect the actual delay in the cancellation path.

3.3.2.2 Overall Modelling

Another approach to cancellation path modelling is to use the actual control signal as the modelling signal (instead of the pseudo-random noise) and inject it into the cancellation path model. This approach can lead to high degrees of signal bias, which requires treatment using the extended identification procedure mentioned above. An arrangement for this is illustrated in Figure 3.12 (Kuo and Morgan, 1996). Note that the adaptive algorithms for the primary path and cancellation path estimates are LMS algorithms, not FXLMS. There are three adaptive filters shown in the figure: one is the control filter and the other two model the cancellation path and the primary path, respectively. This arrangement is referred to as "extended ID" due to the additional adaptive filter used to remove the primary path from the cancellation path model.

Note also that the figure shows an off-line state and an on-line state. The idea is to begin with the off-line state when the control system is first turned on. For this state, one or more of the control filter weights must be non-zero and the primary source must be operating or else there would be no modelling signal. The delay, z^{-L}, in the reference signal path is equal to the delay through the control filter. This is to minimise the correlation between the reference signal and the modelling signal. In the on-line state, the control filter is being updated as well as the cancellation path and primary path modelling filters and the control signal is correlated with the reference signal. This

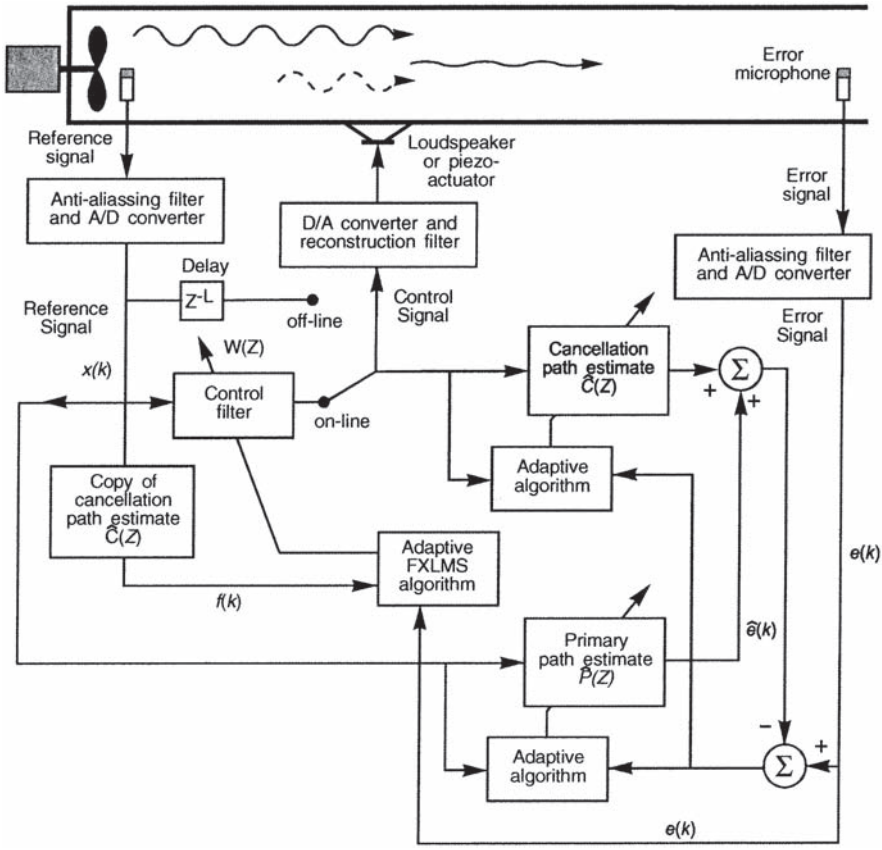

Figure 3.12 Control system with overall modelling of the cancellation path and extended ID to separate out the primary signal.

results in the cancellation path and primary path models being less accurate than if the two signals were not corrrelated. This is acceptable, provided the cancellation path or primary path do not change too much from the initial estimate made in the off-line configuration. If a significant change in either of these paths is detected, then the control filter weight update is suspended and the controller is switched to off-line mode until good estimates of the two paths are obtained.

As the controller converges to the optimum control filter weight values, the error signal becomes smaller and this results in increasing errors in the cancellation path model. Eventually, the errors will become so great that the controller will begin to diverge and the control source output level will increase. This event could be used as a means of determining when to switch to "off-line" mode and measure an accurate cancellation path model. If the increase in control source output level were a result of a change in the primary signal, then a new, accurate cancellation path model is also required, and the switching to "off-line" mode is still the correct controller action. Alternatively, if the cancellation path modelling is occurring continuously,

the increased control output will result in a better modelling signal (as it will be larger in amplitude than the primary source signal at the error sensor), which, in turn, will result in a better cancellation path model and allow the controller to converge again. Unfortunately, this could result in an error signal that cycles from loud to quiet on a regular basis.

3.3.2.3 Comparison of Pseudo-Random Noise and Overall Modelling Approaches

The use of pseudo-random noise reduces the noise reduction performance (especially the perceived performance) of an active noise cancellation system as it increases the residual noise level after cancellation. In practice, this can be reduced by using extended modelling as discussed in Section 3.3.2.1 and by leaving the control source (but not its adaptive filter update) running during the modelling procedure. This will reduce the level of the pseudo-random noise required if the primary source cannot be turned off.

For systems where the primary noise frequency content is changing (eg as a result of a changing engine speed), the overall modelling technique will cause problems as it only produces an accurate cancellation path model for the frequencies in the control (and thus the primary) noise signal. If these change rapidly, the cancellation path modeller will not be able to keep up and the model estimate will always be lagging the true model. This can result in control system instability.

The cancellation path estimate using the overall modelling technique has to be updated more often than the control filter because it is so sensitive to the primary noise content. However, the estimate determined using pseudo random noise only need be updated when there is a large change in the cancellation path, and in some systems, this may not occur very often.

3.3.3 Leaky Single-Channel FXLMS Algorithm

Long term operation of the gradient descent algorithm of Equation (3.11) in a digital control system will lead to system instability due to bias arising from the accumulation of quantisation errors. Fortunately, it is relatively simple to fix this problem by removing a small portion of the current weight values with each new weight calculation (referred to as tap leakage). When tap leakage is implemented, the gradient descent algorithm becomes:

$$\boldsymbol{w}(k+1)=\boldsymbol{w}(k)[1-\mu a]-2\mu e(k)[\boldsymbol{c}(k)*\boldsymbol{x}(k)] \tag{3.20}$$

where a is some small positive number, referred to as a leakage coefficient. The above weight update equation is derived by modifying the error criterion from $J=e^2(k)$ to:

$$\boldsymbol{J}=e^2(k)+a\|\boldsymbol{w}(k)\|^2 \tag{3.21}$$

where $\| \boldsymbol{w}(k) \|$ is the vector norm or length of the entire filter filter weight vector, $\boldsymbol{w}(k)$ at time, k.

An additional benefit of tap leakage is that it can be shown mathematically (Kuo and Morgan, 1996) that it is equivalent to including a control "effort" term in the cost function that is minimised by the control algorithm (as the weight values in the adaptive filter are proportional to the control source output). This can be used to minimise any tendency for the control sound sources to be over-driven. It is useful to note that rather than use Equation (3.20), which represents a weighting proportional to the square of the control effort (see Equation (3.21)), to provide tap leakage, a more stable, faster converging algorithm often results when tap leakage proportional to the fourth power of the control effort (or weight coefficient amplitudes) is used. That is, the cost function becomes:

$$\boldsymbol{J}=e^2(k)+a\|\boldsymbol{w}(k)\|^4 \tag{3.22}$$

The weight update equation for the jth weight in this case is then:

$$w_j(k+1) = [1 - \mu\alpha w_j^2(k)]\, w_j(k) - 2\mu e(k) f(k-j) \tag{3.23}$$

It can be seen from Equation (3.23) that 4th power tap leakage is effectively variable tap leakage. As the filter weight values get larger, the tap leakage effect gets larger. This is why the algorithm works better, because it increases the tap leakage effect when it is most needed.

3.3.4 Multi-Channel FXLMS Algorithm

Similar algorithms to those just derived can also be derived for multi-channel systems. However, this is beyond the scope of what is intended here and is adequately covered in a number of advanced books (Nelson and Elliott, 1992, Kuo and Morgan, 1996 and Hansen and Snyder, 1997).

However, the filter weight update equation for a multi-channel system will be given here as it is of particular interest for the implementation of practical multichannel systems. Using the same terminology as before, the equation for the n^{th} control filter weight update for a multi-channel system with one reference sensor, N control sources and M error sensors is:

$$\boldsymbol{w_n}(k+1) = \boldsymbol{w_n}(k) - \mu \sum_{m=1}^{M} \boldsymbol{f_{nm}}(k)\, e_m(k), \qquad n = 1,2...,N \tag{3.24}$$

where $\boldsymbol{f}_{nm}(k)$ is the reference signal, filtered by the impulse response (time domain equivalent of the transfer function in the frequency domain) between control output, n, and error sensor, m. It has been defined for m=n=1 by Equations (3.8) and (3.9) and the text in between. Note that this quantity is calculated using an estimate of the actual impulse response function, based on the cancellation path measurement described in Section 3.3.2.

It is also possible to have a system with more than one reference signal (for example, to control noise in a twin engined aircraft cabin). The algorithm appropriate for such a system (with multiple error sensors and control sources) is presented by Kuo and Morgan (1996).

Multi-channel versions of the cancellation path models discussed in Section 3.3.2 are discussed by Kuo and Morgan (1996, page 234).

3.3.5 Frequency Domain FXLMS Algorithm

For some types of primary signal (eg tones spread a long way apart in frequency), the convergence of the time domain adaptive FXLMS algorithm can be very slow. One approach to overcome this problem is to convert the signal to the frequency domain using a hardware Fast Fourier Transform (FFT) processor and implement the adaptive algorithm in the frequency domain, with one algorithm for each frequency bin. The frequency bins are then combined together using an Inverse Fast Fourier Transform (IFFT) to provide the control signal. A significant improvement in convergence rate can be achieved in this way as a different convergence coefficient can be used for each algorithm and thus each frequency bin. The arrangement for an active control system using a frequency domain algorithm is illustrated in Figure 3.13. The reference signal,

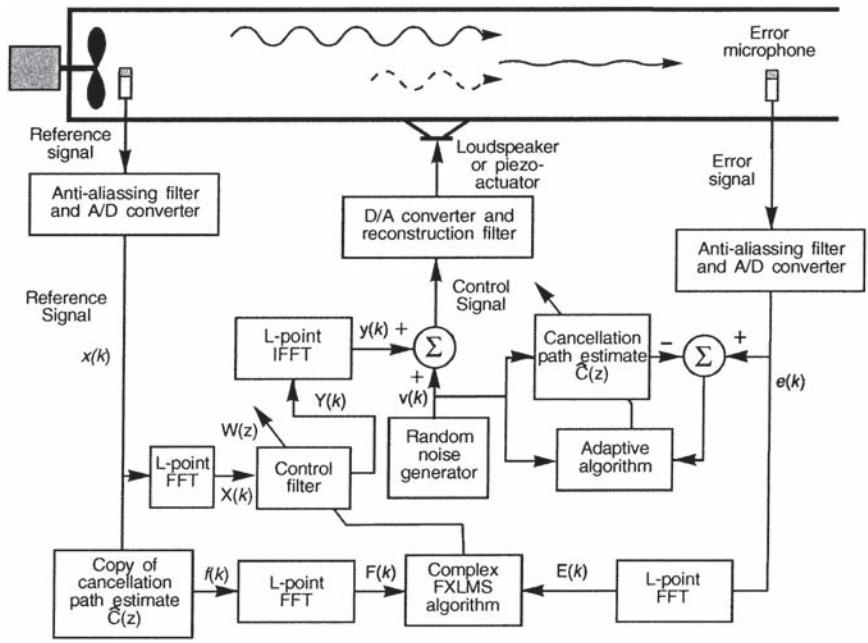

Figure 3.13 Configuration for frequency domain active control.

$\boldsymbol{x}(k)$, is filtered by an estimate of the cancellation path impulse response, $\boldsymbol{c}(k)$, to give $\boldsymbol{f}(k)$ prior to executing the FFT. The signal, $\boldsymbol{f}(k)$, is stored in an L-point data buffer in readiness for performing an L-point FFT. The vectors involved are:

$$\boldsymbol{f}(k)=[f(k)f(k\text{-}1) \ldots\ldots f(k\text{-}L\text{+}1)]^{\mathrm{T}} \tag{3.25}$$

and the Fast Fourier transformed vector is:

$$\boldsymbol{F}(k)=[F_0(k)\ F_1(k)\ .....\ F_{L-1}(k)]^T=\text{FFT}[f(k)] \tag{3.26}$$

The same vector formulation is used for the error signal $\boldsymbol{e}(k)$ which is also stored in an L-point data buffer and transformed using an FFT. The filter weight coefficients are frequency domain quantities and are updated using the complex FXLMS algorithm as follows, with upper case indicating frequency domain quantities:

$$W_l(k+1) = W_l(k) - \mu_l(k)F_l^*(k)E_l(k) \tag{3.27}$$

where the * denotes the complex conjugate and the above equation, consisting of complex variables (except for μ) represents two equations, one to calculate the real part and one the imaginary part of the complex weight coefficient. Note that one update equation is needed for each of the L frequency bins. The convergence coefficient is normalised with respect to the signal power and is different for each frequency as the signal power is different for each frequency bin. The normalised convergence coefficient is given by:

$$\mu_l(k) = \frac{\mu}{\hat{P}_l(n)}, \quad l = 0,1,2,.....,(L-1) \tag{3.28}$$

where the convergence coefficient, μ is set by trial and error for each application. The quantity, $P\hat{}_l(n)$ is a low pass filtered estimate of the power of $X_l(k)$. It is updated after every block of L samples and is given by (Kuo and Morgan, 1996, page 256) as:

$$P\hat{}_l(k)=(1\text{-a})P\hat{}_1(k\text{-}L)+a\,|\,X_l(k)\,|^2 \tag{3.29}$$

where a defines the filter cut-off frequency.

The block processing requirement of the frequency domain implementation causes delays that make it unsuitable for cancelling random noise. Some researchers have tried with limited success to ameliorate this problem by performing an FFT at each sample with just one element in the block changing between each FFT. Nevertheless, the frequency domain approach is really only suitable for periodic noise for which the processing delays are unimportant.

3.3.6 Filtered-U RLMS Algorithms for IIR Filters

Kuo and Morgan (1996) and Hansen and Snyder (1997) also deal with the more complicated case of derivation of a gradient descent algorithm suitable for the more complex IIR filter. The latter case will be considered briefly here as it is used in many active noise control applications (especially those involving resonances or acoustic feedback to the reference sensor), because it provides better results than those obtained using an FIR filter. In this case, the weight update algorithm is the filtered-u RLMS algorithm (Eriksson and Allie, 1987). This can be written for the feedforward filter coefficients, $\boldsymbol{a}$, as:

$$\boldsymbol{a}(k+1)=\boldsymbol{a}(k)\text{-}2\mu e(k)\boldsymbol{f}_x(k) \tag{3.30}$$

and for the feedback coefficients as:

$$\boldsymbol{b}(k+1)=\boldsymbol{b}(k)-2\mu e(k)\boldsymbol{f}_y(k) \tag{3.31}$$

where the quantities $f_x(k)$ and $f_y(k)$ are the filtered reference and control signals, respectively, and are given by $\boldsymbol{f}_x(k)=[f_x(k)\, f_x(k\text{-}1)\, ...\, f_x(k\text{-}\boldsymbol{M}+1)]^T$ and $\boldsymbol{f}_y(k)=[f_y(k)f_y(k\text{-}1)\, ...\, f_y(k\text{-}M+1)]^T$, respectively, where the j^{th} element of $\boldsymbol{f}_x(k)$ is:

$$f_x(k-j) = \sum_{i=0}^{M-1} c_i(k)\, x(k-i-j) \tag{3.32}$$

and the j^{th} element of $\boldsymbol{f}_y(k)$ is:

$$f_y(k-j) = \sum_{i=0}^{M-1} c_i(k)\, y(k-i-j) \tag{3.33}$$

3.3.7 Genetic Agorithms

For non-linear control filters (see Figures 3.5 and 3.6), a gradient descent algorithm will not work and the simplest weight update algorithm available is the genetic algorithm. The genetic algorithm can also be used to update IIR and FIR filter weights, but in general for these latter two cases, its performance is not as good as that of a gradient descent algorithm. The main advantage (in addition to it being able to address non-linear filter structures) of the genetic algorithm is that it is inherently stable and it requires no knowledge of the cancellation path transfer function (or impulse response function), which means that the on-line system identification of the cancellation path can be eliminated. As the genetic algorithm and filter structure are non-linear, they are capable of generating frequencies, not present in the reference signal, which may be used to cancel frequency components arising from the non-linear distortion in the control source output. The one big disadvantage of the genetic algorithm is its slowness in converging. This is a result of the averaging time required for performance measurement, which is at least half the period of the lowest frequency signal encountered in the error signals, which is the lowest frequency to be controlled if a suitable high pass filter is used. A typical arrangement of an active noise control system employing a genetic algorithm is shown in Figure 3.14.

The genetic algorithm is an optimisation/search technique based on evolution, and is essentially a guided random search. It has been applied to many optimisation problems, and in the field of active sound and vibration control it has also been used to optimise the placement of control sources (Wang, 1993, Katsikas et. al., 1993, Baek and Elliott, 1993, Tsahalis et. al., 1993 and Rao et. al., 1991). Here, we discuss how the genetic algorithm may be used to adapt the coefficients of a digital filter (Wangler and Hansen, 1993, 1994).

Use of the genetic algorithm enables any filter structure to be treated as a “black box” that processes reference signals to produce control signals, based on different sets of filter weights. Basic genetic algorithm operation requires the testing of solutions (sets of filter weights), which involves loading the filter weights into the filter and subsequently evaluating the performance of the filter in minimising a cost

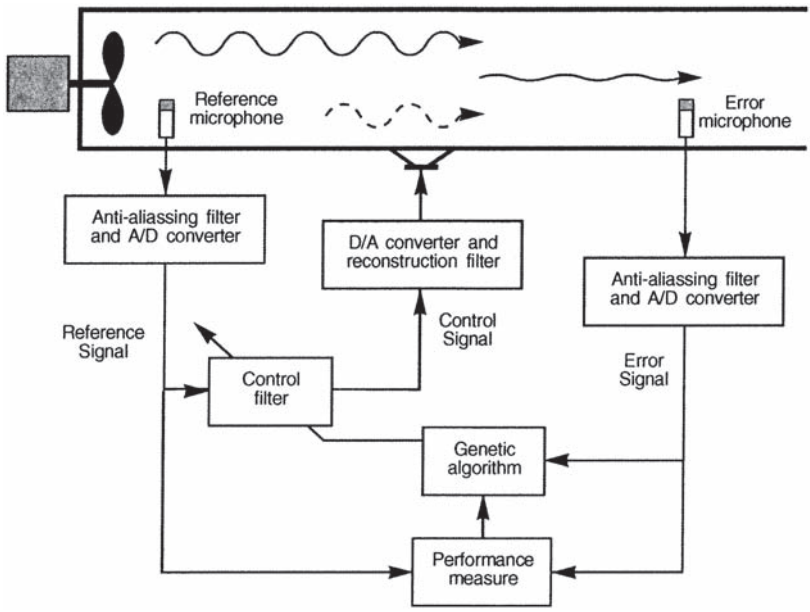

Figure 3.14 Genetic algorithm implementation of an active noise control system.

function based on the error sensor outputs. The genetic algorithm in essence combines high performance solutions while also including a random search component.

Implementation of the genetic algorithm described here has three basic stages: fitness evaluation, selection and breeding. Fitness evaluation requires the testing of the performance of all individuals in the population. Here an individual is considered to be a separate set of filter weights, with the fitness of the individual being a measure of the filter's performance when these weights are used for the filter output calculation. The population then consists of a collection of these individuals. Selection involves killing a given proportion of the population based on probabilistic 'survival-of-the-fittest'. Killed individuals are replaced by children, who are created by breeding the remaining individuals in the population. Typically 70% of the population are killed, with the remaining 30% forming the mating pool for breeding. For each child produced, breeding first requires probabilistic selection of two (possibly the same) parent individuals, with fitter individuals being more likely to be chosen. The probability of selection is high for parents of "good" fitness and low for parents of "poor" fitness. For optimal results, it is best to vary the probability distribution depending upon the stage of convergence that the algorithm has reached. Typical probability distributions used at the beginning and at the end of convergence are illustrated in Figure 3.16, where it can be seen that in the beginning, there is a heavy selection bias (or high selection pressure) towards the fitter individuals.

Application of the crossover and mutation operators on the parent pair produces the new child, as illustrated in Figure 3.15. The crossover operator combines the

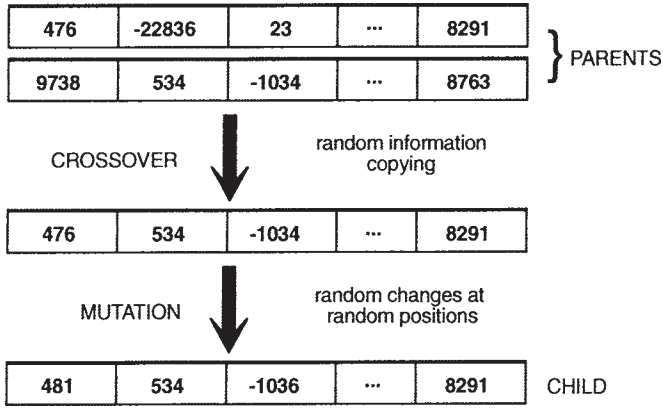

Figure 3.15 Illustration of cross-over and mutation operations for producing a child from two parents.

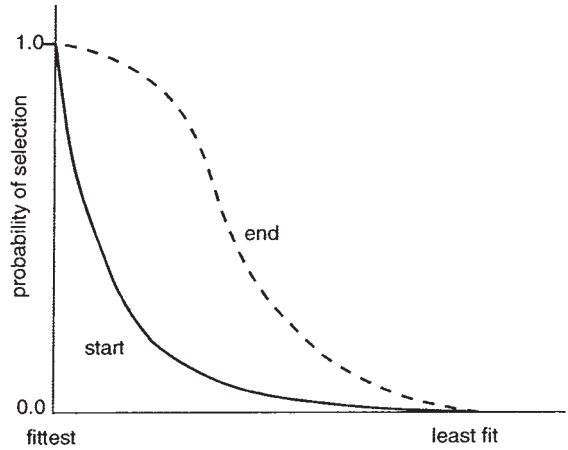

Figure 3.16 Typical probability distributions used for parent selection for breeding.

information contained in two parent strings (or two sets of filter weights) by probabilistic copying of information from either parent to each corresponding string element (or single filter weight) of the child being produced. In this case, the probability of copying a particular weight value to the child from either of the two parents is the same. Mutation introduces random copying 'errors' during the information copying stage of crossover, and gives the algorithm a random search capability.

Mutation plays a minor role in the implementation of the genetic algorithm in standard optimisation problems, in that it is used to replace lost bits in the binary encoding of the problem. As binary data have only two states, small mutation probabilities work well with the 'standard' implementation where data loss is minor.

This is not the case in the implementation most suited to active noise and vibration control, where a weight string is used instead of binary encoding (Wangler and Hansen, 1994). Here, mutation is necessary to maintain population diversity (differences between individuals) and also to allow 'homing in' on optimal solutions, as the population data corresponding to one weight in the string will not fully represent the weight's entire data range. However in practice it is necessary to place bounds on the allowed range of mutation (mutation amplitude), the optimal bounds being somewhat problem dependent.

Two selection processes are carried out during the operation of the genetic algorithm, namely the choice of individuals to be killed, and the choice of parents during breeding (see Figure 3.17). Both selection processes have been implemented using a simulated roulette wheel, where each segment (or slot) on the roulette wheel is allocated a size proportional to the individual's probability of being chosen (selection probability), which is allocated according to Figure 3.16. Each spin of the roulette wheel results in one "winner" being selected. Selection probabilities are

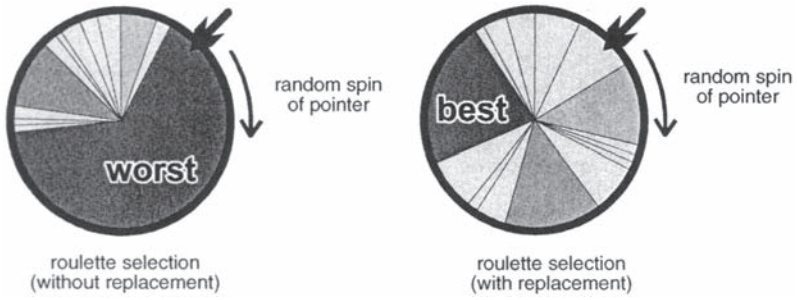

Figure 3.17 Simulated roulette wheel for selecting individuals of a population to be "killed" and those to be "parents" of the next generation.

assigned such that low performance individuals are more likely to be killed, and such that high performance individuals are more likely to be chosen as parents for breeding. Selection without replacement is used for killing, where once an individual is chosen it is removed from the roulette wheel. For breeding, selection with replacement (no removal) is used for choosing the parents, hence the entire mating pool is used in the selection of each parent for each child.

Many aspects of the genetic algorithm used in standard optimisation implementations have been changed to give the desired on-line optimisation performance required for active noise and vibration control (Wangler and Hansen, 1994), as discussed in the subsections to follow.

3.3.7.1 Killing Selection Instead of Survivor Selection

Choosing individuals to be killed rather than those to survive allows higher survival probabilities to be realised for the higher performing individuals. This enables greater

selective pressure (bias towards survival and breeding of the higher performance individuals) to be applied, which can be used to give faster convergence when high levels of mutation are used to sustain population diversity. Use of killing selection also allows the best performing individual to be assigned a killing probability of zero.

3.3.7.2 Weight String Instead of Binary Encoding

The "genetic code" of each individual is normally encoded as a binary string from the problem variables; in this case, it would imply that each weight would be coded as a binary string and the strings connected together to form a complete individual or set of weights, with the crossover and mutation operators working at the single bit level. Mutation of the upper bits of weight variables would result in large jumps in weight values when filter weights are encoded in this way, which significantly degrades online performance. To alleviate this problem in active noise and vibration control systems, a weight string is used with elements taking values of the filter weights and with the crossover and mutation operators applied using whole weight values as the smallest operational element.

3.3.7.3 Mutation Probability and Amplitude

Application of mutation to whole weight values enables a limit to be placed on the deviation of filter weight values about their current values, which gives control over the spread of the filter's performance. Mutation is applied to all child string variables at a given probability (mutation probability, typically 20 to 30%). The weights chosen to be mutated are modified by a random change in value (see Figure 3.15), which is limited to a specified range (mutation amplitude). For best results the mutation amplitude should be relatively high at the start of convergence and low towards the end. Typical values range from 15% of the maximum possible weight value (at the start of convergence) to 0.01% of the maximum possible weight value (at the end of convergence).

3.3.7.4 Rank-Based Selection (Killing and Breeding)

Rank-based selection removes the scaling problems associated with fitness proportionate selection (assigning selection probabilities proportional to fitness values), and gives exceptional control over selective pressure (Whitley, 1989 and Whitley and Hanson, 1989). Rank-based selection, used by Whitley and Hanson (1989) for breeding (parent selection) has been extended in the active noise and vibration control application to include killing selection. Selection probabilities, for both killing and breeding, are assigned based on the rank position of each individual's performance. This essentially means that the individuals are sorted into order from best to worst performance, then each allocated a fixed selection probability

(probability of being chosen) based on their position in this list. The performance evaluation method used thus becomes irrelevant as long as the rank positions are the same (or similar). Separate (adjustable) probability distributions are used for killing and parent selection, with selection for killing being more probable for lower ranked individuals and selection to be a parent being more probable for higher ranked individuals.

3.3.7.5 Uniform Crossover

Uniform crossover nearly always combines the information of two parent strings more effectively than one or two point crossover (Syswerda, 1989). One point crossover is where a position along the string is selected at random, and information is copied (to the child being created) from one parent for the first part of the child string and from the other parent for the second part. Similarly two point crossover involves selecting two points along the string, and copying from one parent between these two points, and from the other parent for the rest of the child string. In uniform crossover each position along the child string is produced by randomly copying from either parent, with both parents being equally likely to be chosen as the information source. For active noise and vibration control problems it has been found that it is best to use a modified form of uniform crossover (Wangler and Hansen, 1994), for which the probability of copying information from the lower ranked parent is supplied, and whole weight values are the smallest elements that are copied (compared to single bits for binary encoded strings) (see Figure 3.15).

3.3.7.6 Genetic Algorithm Parameter Adjustment

As suggested by De long (1985), adjustment of the operating parameters (probabilities, population size, etc) can improve the performance of the algorithm. The adjustable parameters used in the active noise and vibration control implementation discussed here (population size, survival ratio, killing and breeding rank-probability distributions, crossover probability, mutation probability, and mutation amplitude) provide good control over the stages of adaptation needed when good on-line performance is required.

3.3.7.7 Performance Measurement

To evaluate the fitness of an individual (set of filter weights) in minimising the error signal it is necessary to average the mean square error signal over a period of time greater than the period of the lowest frequency signal present. There should also be a delay of twice this between each fitness (or performance) evaluation to allow any transient effects resulting from implementation of the previous individual (set of weights) to subside.

It is interesting to note that the genetic algorithm can handle any form of performance measure, including a measure of power or intensity, whereas previously discussed algorithms, because of the instantaneous nature of their cost functions, cannot use power or intensity error criteria easily.

In multi-channel systems, the performance measure for the genetic algorithm would be the sum of the average squared error measured by each error sensor. For applications involving "more important" and "less important" error sensors, it is easy to weight the signal from individual error sensors accordingly.

3.4 WAVEFORM SYNTHESIS

Waveform synthesis is a control structure that was invented by Chaplin and his co-

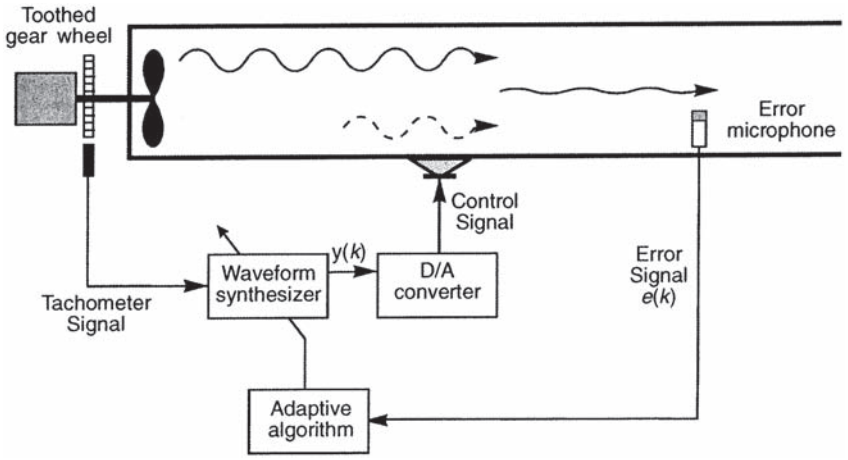

Figure 3.18 Configuration for control using waveform synthesis.

workers (Chaplin et al., 1983) in 1979 and is illustrated in Figure 3.18. The waveform synthesizer in the figure produces a waveform that is intended to cancel the noise arriving at the error microphone. The cancelling noise waveform is stored in the waveform synthesizer as samples, $w_n(k)$, n=1, ... N-1, in contiguous memory addresses, where k is the current time index, n represents a particular sample and N is the total number of samples in one complete waveform (or one period). The synchronisation pulse signal from the tacho is used to increment a memory address pointer and the value in that particular part of the memory is output at that time through a D/A converter and low pass filter. The output remains constant until the waveform synthesizer receives the next synchronisation pulse, which moves it to the next memory address containing a different value. The output, $y(k)$ prior to the D/A converter is then:

$$y(k)=w_{j(k)}(k) \tag{3.34}$$

where $j(k)$ represents the $[j(k)]^{th}$ element of the waveform samples, $w_n(k)$, n=1, ... N-1, at time, k.

The adaptation unit samples the error microphone signal once each time it receives a pulse from the tacho. It then calculates a new value for the waveform corresponding to that part in the cycle and inserts it into the correct memory address. As there is some delay between when the signal is fed to the loudspeaker and subsequently received by the microphone, a time off-set, Δ, needs to be subtracted from the memory address pointer. The final algorithm used by Chaplin (after reporting a number of others is:

$$w_n(k+1) = \begin{cases} w_n(k) + \mu e(k), & n = (k - \Delta) \\ w_n(k) & \text{otherwise} \end{cases} \tag{3.35}$$

3.5 IMPORTANT CONTROLLER IMPLEMENTATION ISSUES

The three constituents of the electronic part of an active control system, the digital filter, the adaptive algorithm, and the cancellation path impulse response modeller, must all be implemented on some form of microprocessor. Further, the signals that are input to, and output from, the three constituents must pass through some form of analog to digital, or digital to analog, converter. This section will briefly discuss some of the issues associated with selection of microprocessors and converters for practical active noise control system implementation.

3.5.1 Microprocessor Selection

The only practical type of micro-processor for the implementation of digital adaptive controllers is the DSP (digital signal processor). These processors are specialised with enhanced support for mathematical computation and this is of particular benefit to active noise control systems where the filter weight calculations involve a large number of multiplications.

There are a wide range of DSPs, with a correspondingly wide range of prices and features. Two principle variables are data format (fixed point versus floating point) and precision (16 bit versus 32 bit). On the low end of the price scale are 16 bit fixed point units. These should only be used in mass consumer goods products involving the reduction of single tonal noise. They are not suitable as general purpose controllers. In particular there are problems with quantisation errors and there may be problems with some IIR filter implementations, where individual weights in the feedback part of the filter can have a magnitude greater than 1 (not allowed by default in a fixed point unit). The use of double precision or block floating point calculations can ease these problems but these are a poor alternative to a floating point DSP. The additional price of a floating point chip is a few hundred dollars, but the associated electronic design and programming is much more complex and adds considerably to the final cost of the controller. In most cases, 16 bit precision is adequate, but 32-bit precision eases problems associated with dynamic range and quantisation errors.

3.5.2 Converter Type and Group Delay Considerations

Mathematically, the group delay $\tau(\omega)$ of a given component is defined as:

$$\tau(\omega) = -\frac{\mathrm{d}}{\mathrm{d}\omega}\theta(\omega) \tag{3.36}$$

where $\theta(\omega)$ is the phase response of the transfer function of the component at frequency ω. Thus the group delay through a system component can be determined by measuring the slope of the frequency response function phase plot (output/input) of the component. The local slope of the frequency response phase function is a good approximation to the group delay at that frequency. Physically, group delay is a measure of the time it takes for a signal to pass through a component.

Group delay is important in adaptive feedforward control systems because it has a significant influence on the electronic control system stability as well as the minimum separation distance allowed between the reference sensor and control source if broadband noise is to be controlled. An example is a system where noise is propagating in a duct and an upstream microphone is used to supply a reference signal. If the group delay through the digital system and loudspeaker control source is five milliseconds, then for sound travelling at 343 ms^{-1} to be controlled, the active control system must be at least 1.7 meters in length. That is, once the reference sensor senses the incoming sound, the sound will travel 1.7 meters in the time it takes the controller to output a control sound at the control sound source.

Group delay also influences the stability of adaptive algorithms used in feedforward active control systems. As there is a finite time delay between the derivation of a control signal and its "appearance" in the error signal, there is a delay between a change in filter weights and its effect being measured. When the weight adaptation is done at time intervals shorter than this delay the stability of the adaptive algorithm is reduced.

The group delay through the A/D and D/A converters and associated anti-aliasing filters is dependent on the converter type. For successive approximation converters, which can cost hundreds of dollars for 16 bit accuracy (the appropriate accuracy for an active noise control system), the group delay is very small and much less than the delay through the associated anti-aliasing filter. The delay through an anti-aliasing filter can be calculated from the following relationship (assuming a filter cut-off frequency of one third of the sample rate),

$$\tau \approx 3MT/16 \text{ seconds} \tag{3.37}$$

where T is the sample period (reciprocal of sample rate in Hz) and M is the number of poles in the anti-aliasing filter (typically between 4 and 8). Note that the delay through the reconstruction filter on the controller output is calculated using the same relationship. An additional delay of approximately one sample period, T, is usually allowed for the processing time of the control filter. The actuation delay associated with the control source is often very significant and can be measured easily by exciting the loudspeaker with an electrical impulse and noting the delay between excitation input and measurement by a microphone.

For sigma-delta A/D converters, which cost tens of dollars for 16 bits, the group delay is approximately 30 samples (including the delay through the in-built anti-aliasing filter) and thus is dependent on the sample rate. For the latter converter type, to minimise group delay, it is necessary to sample the incoming signal at the highest possible rate, then pass it through low pass digital filters (the group delay of which may be calculated using the equation above) and down-sample in software to the optimum rate for the particular frequency range that the active noise control system is to address. Note that for good results, the sample rate of the data used in the control algorithm and control filters should be between 4 and 100 times the frequency of the signal to be controlled (with the optimum being approximately 10 times). Adaptation of the controller at the lower frequency end of the above scale (100fs) tends to be very slow, while at the other end of the scale, the performance deteriorates rapidly. Typical maximum sample rates of low cost sigma delta converters are 40,000 Hz to 50,000 Hz.

Note that a 16 bit A/D converter implies a dynamic range of 96 dB. In practice, however, several of the available bits are useless, owing to signal noise, quantisation noise, and the non-use of the full dynamic range of the device, which means that the actual dynamic range available is often only about 50 dB. Thus use of less accurate (than 16 bit) A/D converters is not recommended.

3.5.3 Digital Sampling Rate

An important factor in the overall performance of a controller is the sampling rate used by the A/D converters at the digital/analog interface. Sampling rate also affects other controller parameters such as the optimum length of the control filter and the optimum convergence coefficient.

If the sampling rate is too fast, the required filter length to achieve a particular result will be excessive. For tonal disturbances, a sample rate that is too high results in digital filter weights of large magnitude (both positive and negative), resulting in a controller output that is calculated by adding and subtracting large numbers of similar magnitude. This results in an imprecise controller output and thus poor performance. The only way to reduce the magnitudes of the weights, while keeping the sample rate constant, is to increase the length of the filter. However, this has the undesirable effect of reducing the adaptive algorithm stability.

For broadband disturbances, a high sample rate results in a large number of weights being required to digitally represent the broadband impulse response of the system being controlled. Long control filters have the undesired effects of reduced system stability (which can sometimes be compensated for by reducing the algorithm convergence coefficient) and an increase in the computational overhead and memory requirements of the DSP.

In a previous section, the “bowl-shaped” nature of the error surface for a gradient descent algorithm adapting the weights of an FIR filter with just two weights was discussed. For multiple weights, the error surface becomes multi-dimensional, corresponding to multiple “bowl” axes some of which have steep sides and some of which have shallow sides. The optimum value of the algorithm convergence

coefficient is a function of the "steepness" of the "bowl", As the bowl becomes steeper, the convergence coefficient must be smaller or the algorithm will become unstable. On the other hand if the slope is shallow, an algorithm with a convergence coefficient that is too small will stop converging before it reaches the optimum weight values. If some of the principle axes of the "bowl" are steep and some are shallow, there will be competing demands on the optimum value of the convergence coefficient and the algorithm will either be unstable or stop converging before an optimum value is reached. The variation in slopes of the error surface corresponding to the various principle axes is mainly a function of the system sample rate. As the sample rate increases, so too does the slope variation.

The generally accepted optimum sample rate in active noise and vibration control systems is approximately 10 times the frequency of the noise or vibration to be controlled. The control system performance decreases as the sample rate increases or decreases relative to the optimum value. At the lower end, the control system will still work to some extent for frequencies that are 1% of the sampling frequencies. For frequencies less than this, the control system performance is characterised by poor adaptive algorithm stability and slow convergence for both fixed point and floating point processors. There are additional problems for fixed-point processors as the filter weights can become larger than normally allowed. At the higher end, the control system will still provide some noise reduction for frequencies up to about 30% of the sampling frequency. For frequencies that are higher than this, the adaptive algorithm is simply ineffective in converging to an optimum set of weight coefficients. Thus it can be seen that at best an active noise control system can operate over a frequency range for which the maximum frequency is 30 times the minimum frequency, with decreased performance expected near the ends of the range. One possible way of extending the frequency range over which acceptable performance is obtained is to use a control system design methodology based on multi-rate filtering principles, where multiple algorithms and filters, running at multiple sample rates, are used with each filter/algorithm combination being responsible for a narrow part of the frequency range over which noise reduction is required.

In summary, a poorly selected sample rate can:

- reduce the final level of noise attenuation obtained;
- reduce system stability, especially if the control filter is updated at a rate approaching the sample rate; and
- cause optimal filter weights to have widely varying values, which impacts on the convergence rate.

3.5.4 Algorithm Considerations

Generally, the convergence coefficient chosen for the cancellation path identification must be larger than that used for generating the control signal. Also, if the control signal is used as the cancellation path modelling signal, it is necessary to update the filter weights for the cancellation path identification much more often than for the

control filter. If these latter two guidelines are not followed, then the system is likely to become unstable.

Also, better results are obtained by updating the control filter at intervals no shorter than the delay in the cancellation path. This allows a larger convergence coefficient to be used and theoretically, the convergence rate should be the same as when the control filter is updated every sample. This can be understood by imagining that it takes an amount of time equal to the cancellation path delay time before the effect of a weight change made by the controller can be detected by the controller, so any filter weight changes done in the meantime are being done "blind" with no way of determining their effect until quite a few more weight updates have been done. However, in practice, using a larger convergence coefficient often produces a smaller mean square error due to the quantisation errors associated with digital multiplication. With a small convergence coefficient, the term that increments the filter weights in Equation 3.20 will effectively become a digital zero before the same term with a larger convergence coefficient. Thus the larger convergence coefficient will produce a better control result.

3.5.5 Accuracy of Controller Output

The controller output accuracy is a function of the accuracy of the A/D and D/A converters, the size of the signal relative to any noise in the system (physical system or control system) and the accuracy of the microprocessor. Often the most influential factor is the second one; acoustic or electrical noise in the system that is not correlated with the noise to be controlled. The accuracy required of the control signal in terms of producing the desired phase of the cancelling signal is illustrated in Figure 3.19 for the control of tonal sound radiation from a vibration surface.

The required amplitude accuracy is approximately related to the phase accuracy by a phase error of 1° having the same effect as an amplitude error of 0.1dB. The figure illustrates why it is extremely difficult to achieve more than about 20 dB noise reduction in practical situations involving sound sources, which have outputs that vary slightly with time.

3.5.6 Estimation of The Potential of ANC Without Using a Controller

There are many laboratory or field situations where it is desirable to determine the potential benefit of active noise control without needing to purchase a controller. The first thing that can be done is an on-site measurement of the coherence between the reference and error signals. This can be done using a spectrum analyser (with a number of averages) and the resulting coherence can be used to estimate the maximum achievable performance of an ideal active noise control system. This is:

$$NR(f) = 10\log_{10}\left[\frac{1}{1-\gamma^2(f)}\right] \quad \text{dB} \tag{3.38}$$

where $NR(f)$ is the maximum noise reduction in dB that is achievable at the error sensor and $\gamma^2(f)$ is the coherence value (between 0 and 1.0) obtained from the spectrum analyser at frequency, f.

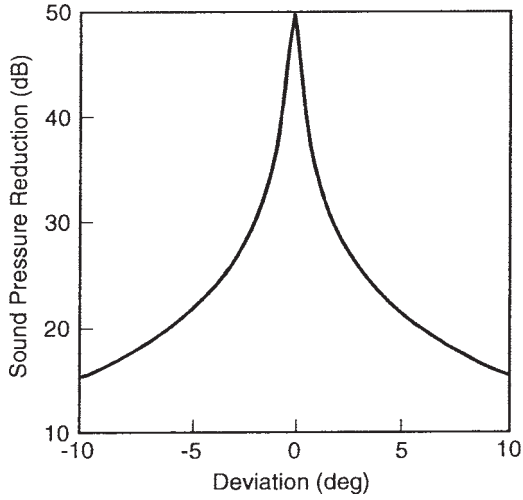

Figure 3.19 Effect of controller phase inaccuracy on the sound pressure radiated by a simply supported lightly damped panel excited at 320 Hz.

When multiple error sensors are to be used, a good estimate of the overall performance of an active noise control system can be determined by measuring the primary source signal at all error sensors and the transfer functions between all control sources and all error sensors to be used in the final system. This method is described in Appendix A under the heading, "Quadratic Optimisation". Of course, if the number of error sensors is equal to the number of control sources, the calculation will return an infinite amount of attenuation at each error sensor. However, if there are more error sensors than control sources, the calculation will return the optimal attenuation that would be possible at each error sensor. More importantly, the method can be used to estimate the sound pressure at locations other than the error sensors. In addition, it is possible to insert a small percentage error (e.g. 1 %) in the transfer function amplitudes used to estimate the optimum control source strengths to represent the limited dynamic range and accuracy of the digital controller that will be used in the final system.

Both of the above mentioned procedures should be carried out for any potential field application before the purchase of a commercial controller is contemplated.

3.5.7 Controller Processor Overload

Even though current digital signal processors are capable of handling a huge processing load, it is still easy to overload any control system by not paying sufficient

attention to its optimisation. To illustrate how increasing the number of channels in a multi-channel controller can quickly overload a controller, consider a 10-channel system.

Recall that the input reference signal must be filtered by the impulse response estimate of the cancellation path, $\boldsymbol{f}_{zm}(k)$, before being used by the control algorithm. For a multi-channel system the control algorithm that updates the filter weights is:

$$\boldsymbol{w}_n(k+1) = \boldsymbol{w}_n(k) - \mu \sum_{m=1}^{M} \boldsymbol{f}_{nm}(k)\, e_m(k), \qquad n = 1,2...,N \tag{3.39}$$

From this equation it can be seen that if 100-tap filters are used, the number of multiplications needed to derive the weights to update the control filter is given by:

$$N_m = N_{ct} \times N_c \times N_e \times N_{irt} = 1{,}000{,}000 \tag{3.40}$$

where the quantities on the right of the equation represent number of filter taps in each control filter, number of control output channels, number of error sensors and number of filter taps in each cancellation path filter, respectively. This requires a minimum of 1 million clock cycles. In addition, passing the reference signal through each control filter requires another 1,000 multiplications, a few orders less than the algorithm requirements. Calculating the transfer function filter weights requires 10,000 multiplications for each iteration. It can be seen that doubling the filter lengths will multiply the number of multiplications needed by four. Use of external memory to due to limitations of on-chip DSP memory will slow the process down by at least a factor of four.

Thus, it is important to minimise the number of control channels if the controller is to converge to the optimum reasonably quickly or be able to track a rapidly changing input signal. It is also important to minimise the number of control and cancellation path filter weights for each application.

3.5.8 Number of Error Signals

It is extremely important to minimise as far as possible, the number of error and control channels in an active noise control system so that convergence speed and stability are maximised, as discussed in Chapter 3. This does not mean that the number of sensors or control actuators needs to be less than desired for control of the physical system. Rather, some clever ways have to be devised to divide the system into a number of smaller independent controllers or combine the error sensors (and control actuators) into groups so that the controller only receives one input from each group. This is why shaped sensors are of such interest. When applied to sense acoustic radiation modes on a vibrating structure that is radiating or transmitting sound, they offer the opportunity of providing a few error signals that when minimised will provide the same results as many discrete sensors providing many separate

error signals. Shaped actuators offer the same potential for reducing the number of output channels of the controller. Discrete sensors can provide similar results to shaped sensors if a sufficient number are used and pre-processing electronics provide a single input to the controller. The main problems are cost and the additional pre-processing electronics that are required.

In many large systems, not all error sensors are affected significantly by all control sources. This provides the opportunity to partition a large controller with many channels into a number of smaller controllers with fewer channels. This is especially relevant when acoustic error sensors are used that differ greatly in their distance from particular control sources. However, much care must be taken when this is done, as even small contributions to an error sensor in a particular subset from a control source not included in that sub-set can cause system instability if the small contribution is correlated with the other control signals in the sub-set. An example of gross partition to provide multiple simple controllers rather than one complex controller is the application of active noise control systems to reduce noise in the vicinity of passengers' heads in mid-size and large aircraft cabins. A separate controller is used for each headrest to provide a zone of cancellation in the immediate vicinity of the headrest only, with minimal influence on neighbouring headrests (Carme and Valentin, 1997).

CHAPTER FOUR

ACTIVE NOISE CONTROL SOURCES

4.1 INTRODUCTION

Since active noise control became a practical reality, commercial installations have suffered from insufficient sound source robustness. The robustness requirements necessary to ensure the survival of the sound source obviously differ from one installation to another and clearly active control sources in air conditioning ducts will have different requirements to those in an industrial air handling system in which the environment is very hostile. The sources needed to generate the anti-noise must be capable of producing noise levels similar to those produced by the unwanted noise source. Typical acoustic sources include loudspeakers and horn drivers. Vibration sources are used sometimes to control the vibration of surfaces that are radiating the unwanted sound. Typical vibration actuators are piezoelectric patches, piezoelectric stacks, magnetostrictive actuators, electrodynamic shakers, inertial shakers, electromagnetic actuators, hydraulic and pneumatic shakers.

4.2 ACOUSTIC SOURCES

4.2.1 Loudspeakers

Current loudspeaker technology is such that loudspeakers used for active noise control will have a life of many years provided they are kept clean and cool. In dirty, hostile industrial environments where the noise levels to be controlled are high, satisfying these requirements is a challenging exercise in mechanical design. To aid the ANC system designer, loudspeakers are available with aluminum or fibreglass cones and also with protection of the coil area from contaminants. Most loudspeakers will not function for extended periods in ambient temperature environments above about 50°C. Another problem is associated with the use of small backing enclosures for the purpose of maximising the low frequency output of the loudspeakers. This practice often results in overheated and eventually burnt out speakers unless they are driven at a small fraction of their rated capacity or unless adequate cooling is provided.

At low frequencies and high sound levels, noise source volume velocities are large. Consequently, for active noise control at low frequencies the important parameter for specification of a control sound source is volume displacement capacity, rather than power handling capacity.

In cases where the required volume velocity exceeds the capability of available speakers, (usually associated with 200–400 watts of electrical power), the number of speakers at each control source location can be increased (for example, by placing them around the perimeter of a duct cross section at the desired axial location and driving them all with the same control signal).

Commercial software is available to design speaker enclosures to provide maximum output power over a narrow frequency range or lesser output power over a much wider frequency range. Loudspeaker enclosures generally need drain holes to prevent water build-up caused by cyclic heating and cooling of enclosures, especially those located outdoors. The drain holes must be sufficiently small not to affect the stiffness of the enclosure at the frequencies of interest or alternatively must be taken into account in the design of the enclosure. Also, the enclosures must be vented with a small hole so that the static pressure on the front face of the speaker cone is equal to the static pressure acting on the rear surface. When very low frequencies are being considered, these vent holes must also be taken into account in the design of the enclosure.

A loudspeaker enclosure design that satisfied the requirements of a cool, clean loudspeaker, even though it was being used to control noise radiated from an 80 m high stack containing wet, corrosive sludge with temperatures varying from 100°C to 180°C is illustrated in Figure 4.1 (Hansen et al., 1996). As shown in the figure, a copper tube containing chilled water was wrapped around each speaker coil and in addition, refrigerated air was used to purge the space between the speaker cone and the stack as well as the speaker enclosure. It was found that it was essential for the refrigerated purging air to be present, even when the ANC system was switched

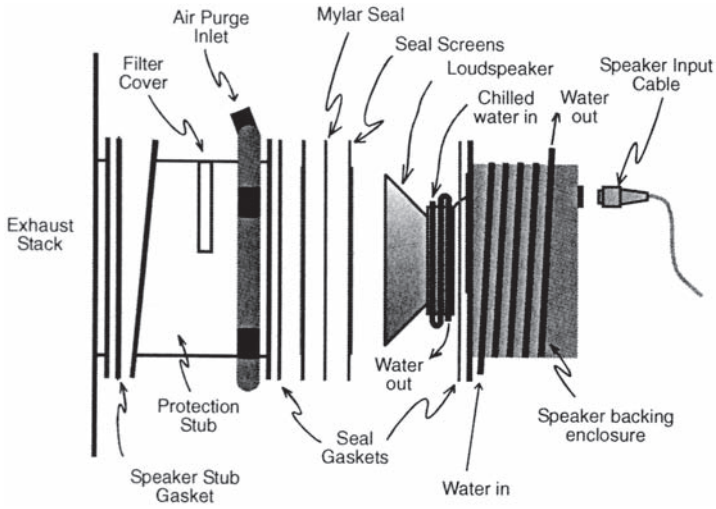

Figure 4.1 Industrial loudspeaker enclosure with a single port for a dirty, hot environment.

off. When this did not happen on one occasion, the loudspeaker suspension became soft and sagged, resulting in the coil touching the magnet. When the cooling air was turned on again, the suspension regained its original stiffness but remained distorted. Thus when the loudspeaker was energised, the coil rubbed on the magnet and after a short time, the coil insulation rubbed off causing a short circuit and a failed speaker.

Another requirement, which is sometimes overlooked, is the provision of a connecting tube to equalise the static pressure on the front and rear faces of the speaker cone. Failure to do this will greatly increase the distortion of the output and reduce the available cone motion, especially in cases where there is a reasonably high vacuum in the duct on which the speaker is mounted as a result of air flow through the duct.

In many cases, the noise to be controlled is at the upper limit of capability for continuous loudspeaker operation, which results in a serious problem of loudspeaker non-linearity. The non-linearity is heard as higher harmonics of the noise being cancelled and this can negate the subjective benefit of active control in practical installations. The non-linearity problem can be minimised by keeping cone excursions small, which may be achieved by only driving loudspeakers at a fraction of their capacity or by clever design of the speaker enclosure. In these cases some effort needs to be devoted to the design of the speaker enclosure to maximise the output in the frequency range of interest. Blondell and Elliott (1996) have investigated the use of ported speaker enclosures to minimise speaker non-linearities while at the same time providing a large volume velocity output. In cases where the loudspeaker has to be attached to a duct, the duct acoustics affect the output and the design of Blondell and Elliott (1996) is inappropriate. A better design in this case is a double cavity, fully enclosed speaker with a single port as illustrated in Figure 4.2. A design such as this has been used by the author as an

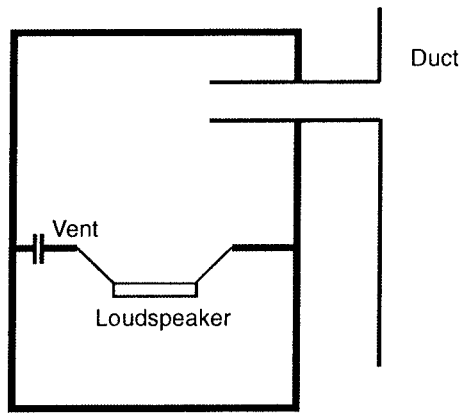

Figure 4.2 Low frequency, high volume velocity, speaker enclosure design.

active control source to reduce a 30–40 Hz random noise problem in an air conditioning system in a high rise building.

4.2.2 Tuned Cavity-Backed Panels

In terms of the usual active noise control requirement for a large volume displacement over a broad frequency range, it is difficult to beat a conventional loudspeaker. However, there are special applications for which a conventional loudspeaker may not be the best noise source choice. One special application is the control of tonal noise radiated outdoors, such as that radiated by a large electric power transformer. In an effort to minimise the number of control sources required, large panels (1 m×0.5 m) have been used (Li et al., 1997) as shown in Figure 4.3.

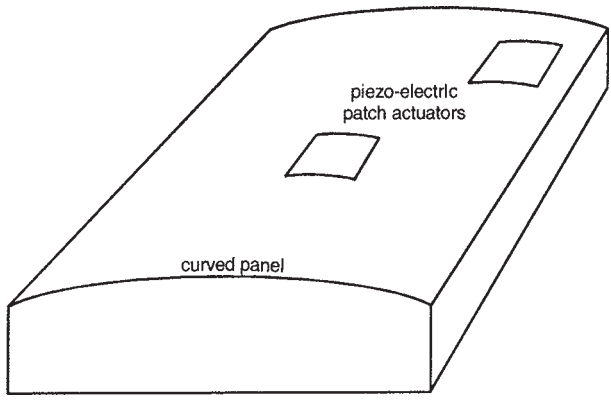

Figure 4.3 Curved panel sound source with rigid backing cavity.

The panels are tuned to have an acoustically efficient mode resonating at 100 Hz and another at 200 Hz (or 120 Hz and 240 Hz respectively, in North America). The panels are driven by piezo-electric patch actuators. If the actuators are too close to a vibration node, then the force required to excite the panel sufficiently will be too great, whereas if the actuators are placed too close to a vibration antinode, the large amplitude may result in cracked actuators. Thus a compromise is necessary. In addition, it is wise to curve the panel in one dimension so that it looks like part of a cylinder. This enables the extensional motion of the piezo-electric crystal to couple better with the normal motion of the panel to which it is attached. The curvature of the panel also makes it easier to design it so that its most efficiently radiating modes resonate at 100 and 200 Hz (or 120 and 240 Hz in North America). The panel should also be mounted over a closed cavity to prevent sound from the back interfering with that radiated from the front, thus maximising the radiation efficiency at the design frequencies.

In the design of the panels to achieve resonance frequencies of 100 Hz and 200 Hz, it is important that there is some means of compensating for the effect of manufacturing errors. This was achieved by designing panels to resonate at a slightly higher frequency than desired and then placing lumped masses on the panel and changing the depth of the backing cavity. In this way it is possible to manufacture a panel with two acoustically efficient resonances at frequencies of 100 Hz and 200 Hz respectively. It was also found that the panel radius of curvature had to be relatively large—at least three times the panel width.

An example of the response of a curved panel sound source designed to control electrical transformer noise is shown in Figure 4.4, in which part (a) is the response after manufacture and part (b) is the response after tuning. Note that the design resonance frequencies were 100 and 200 Hz for the two most efficient modes (1,1 and 1,3). Coincidentally, there is a third mode with a strong response very close to 300 Hz, which is also a problem frequency in the transformer noise spectrum. The panel was 1 m×0.5 m in size and made from 1.6 mm thick aluminium sheet with a radius of curvature of 2.7 m. When tuned the backing cavity was 58 mm deep.

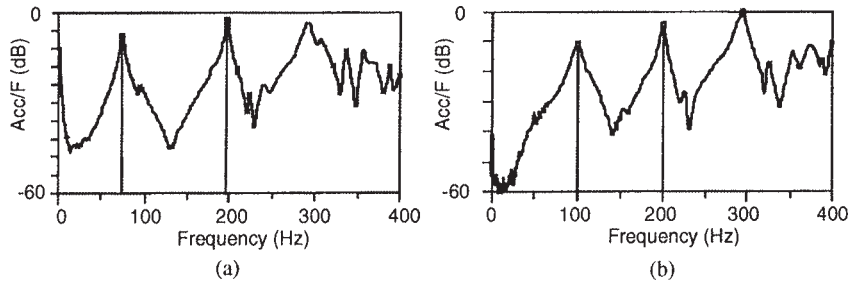

Figure 4.4 Untuned and tuned curved panel (with backing cavity) response.

As can be seen by the data in Figures 4.5 and 4.6, it is possible to tune the 1,1 mode without affecting the 1,3 mode greatly and vice versa by adding mass in strategic places on the panel and changing the depth of the backing cavity.

4.2.3 Acoustic Boundary Control

There are three types of acoustic boundary control that have been reported in the literature directed at reducing the sound transmitted into an enclosure through a bounding structure. One involves the use of an array of acoustic sources close to the structure boundary inside the enclosure to generate a sound field which "unloads" the structure (Jayachandran et al., 1998; Hirsch and Sun, 1998 and Jayachandran and Sun, 1998). The authors showed that such an array could

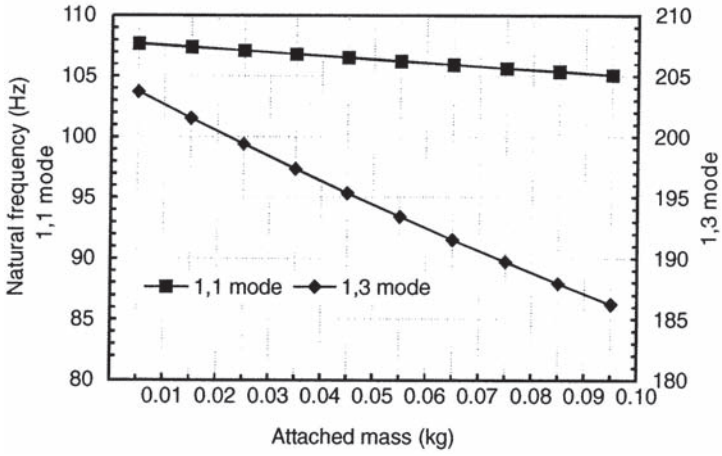

Figure 4.5 Effect of mass on the the 1,3 mode antinode on the resonance frequencies of the 1,1 and 1,3 modes.

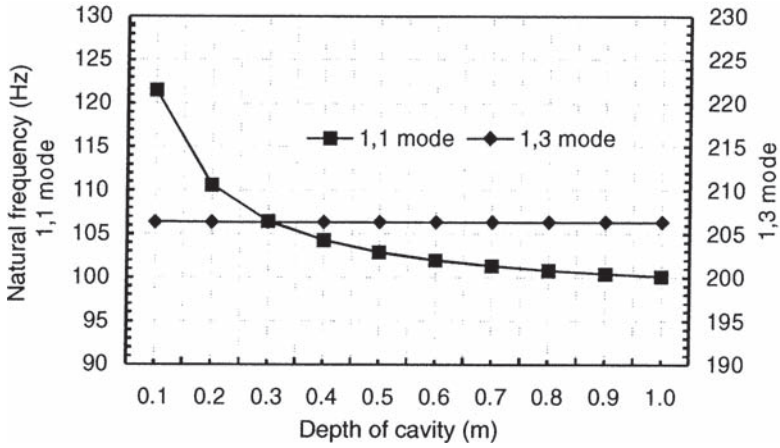

Figure 4.6 Effect of cavity depth on the resonance frequencies of the 1,1 and 1,3 modes for the curved panel sound source.

outperform structural control sources, even if the system response were dominated by structural modes. They have analytically calculated performance bounds that may be expected from this kind of control.

The second type of boundary control involves the use of active foam mounted on the interior of the structure (Gentry et al., 1997; and Guigou and Fuller, 1998) consisting of cylindrically curved PVDF film embedded in partially reticulated polyurethane acoustic foam to form a "smart skin". Interior sound levels are reduced by a combination of passive absorption of the foam and acoustic unloading of the

structure as a result of driving the embedded PVDF film. The authors used the skin to reduce noise transmitted into a Cessna Citation III fuselage.

The third method, introduced by Fuller, et al. (1998) involves the use of a "smart skin" arrangement that does not use acoustic foam but instead uses PZT actuators configured in such a way as to amplify their displacement normal to the surface on which they are fixed. PZT bimorphs are used together with a thin diaphragm as shown in Figure 4.7. When the bimorph is activated, the tip moves out or in, causing he diaphragm to bend up or straighten as shown by the dashed line in the figure (for activation of a single bimorph).

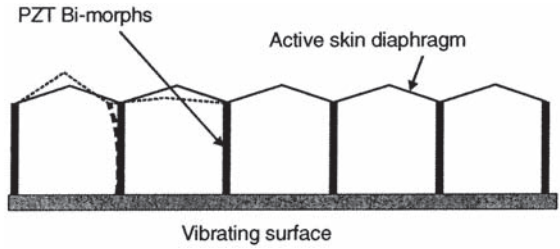

Figure 4.7 Active skin concept (after Fuller et al., 1998).

4.2.4 Tuned Resonator

For the tuned resonator type of control source the resonance frequency is tuned by the output of an active noise controller. The control could take the form of a moveable piston which changes the volume and hence resonance frequency and thus the control effect of the resonator. A different type of tuned absorber uses a loudspeaker, microphone and feedback control system (Darlington and Avis 1996).

4.2.5 Compressed Air Sources

Compressed air sources are often necessary when very high level sound is to be controlled ((Blondel and Elliott, 1997, Obier and Pfeifer, 1997). Optimum design of these sources is still the subject of research.

4.3 VIBRATION SOURCES

It is possible to reduce a radiated sound field by controlling the vibration of the structure generating the sound as discussed in the preceding sections. However, as also mentioned, it is not sufficient to minimise the amplitude of the normal vibration modes of the structure; generally it is necessary to minimise radiation modes.

Radiation modes are vibration modes that are orthogonal with respect to the radiated sound field as opposed to normal vibration modes that are orthogonal with respect to the structural vibration field. Reduction of the amplitude of a normal structural vibration mode is guaranteed to reduce the overall vibration amplitude of the structure, but not the sound radiation. In fact, reducing the amplitude of a single structural vibration mode may actually result in increased sound radiation. On the other hand, reducing the amplitude of a radiation mode is guaranteed to reduce the radiated sound field but not necessarily the overall structural vibration amplitude. Radiation modes can be derived as a combination of normal vibration modes in various proportions that are frequency dependent. They have resonances and mode shapes that are different to the values for the normal structural modes and they are discussed in more detail under "sensing" in the next section.

4.3.1 Piezo-Electric Patch Actuators

It is interesting to note that piezo-electric patches bonded to a structural surface generate vibration by extending and contracting in response to an applied cyclic voltage, which in turn generates a cyclic bending moment in the structure at the point of attachment of the actuator. Kim and Jones (1991a) showed that there was an optimum thickness of piezo-electric actuator, which was dependent on the thickness of the structure being excited. The induced bending moment as a function of actuator thickness is illustrated in Figure 4.8 for a PZT crystal actuator bonded to one side of a simply supported steel plate. It can be seen from the figure that very little is gained by making the actuator thickness greater than about 20% of the plate thickness. Note that this optimum assumes the ratio of voltage/actuator thickness (or electric field) can be held constant, which means that much higher

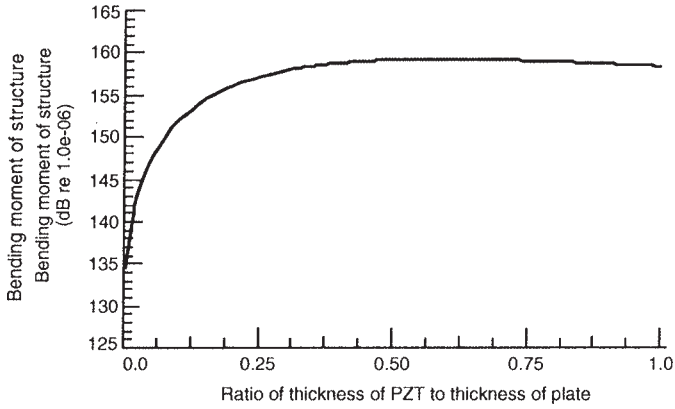

Figure 4.8 Applied bending moment as a function of plate thickness.

voltages will be needed for the thicker actuators. If the voltage applied to the actuator is assumed to be constant, then it is better to use the thinnest actuator that can be driven comfortably by the available voltage. Special high impedance amplifiers capable of outputs of 150 V to 1000 V (depending on the actuator thickness) must be used, although it is possible to drive the patches with normal power amplifiers connected to the actuator through a step-up transformer.

4.3.2 Piezo-Electric Stack and Magnetostrictive Actuators

For very heavy structures, greater bending moments can be induced by using piezo-electric stack or magnetostrictive actuators mounted between the structure and the flange of an angle section as illustrated in Figure 4.9(a) or between the ends of a channel section as shown in Figure 4.9(b), with the base of the channel bonded to the structure. Piezoelectric stacks are made from layers of piezoelectric discs stacked together and magnetostrictive actuators are made from a terfenol rod mounted inside a coil that carries the actuating signal. Both types of actuator are capable of producing large forces and are discussed in detail by Hansen and Snyder (1997). Again, piezo-electric stack actuators need a high impedance, high voltage amplifier, whereas the magnetostrictive actuators need a low impedance power amplifier capable of handling a high inductive load.

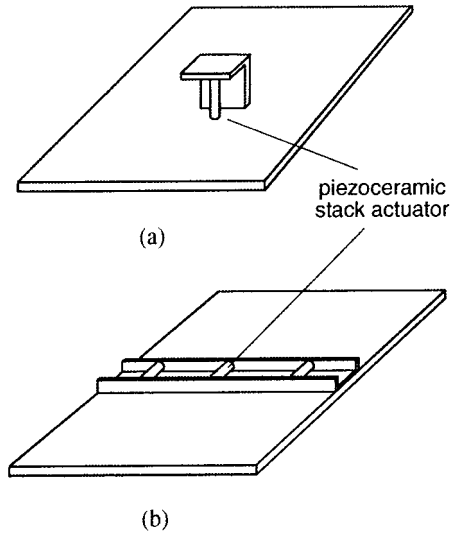

Figure 4.9 Mounting configurations for stack actuators to apply a bending moment to a structure.

4.3.3 Inertial Actuators

Another low-cost type of actuator to control vibrating structures that has become available recently is the inertial actuator. This actuator is similar to an electrodynamic shaker, except that the part that moves is the heavy part containing the permanent magnets while the coil remains stationary. These devices are low in cost because they are mass produced for the car audio industry. When attached to door panels in cars, they vibrate the entire vehicle and greatly enhance the bass response of the sound system. A photo of three such actuators stacked together is shown in Figure 4.10. Each of the actuators has been tuned for maximum output over a narrow frequency range and the stack of three covers three different frequency ranges. Typical maximum force outputs are 100 N rms for 40 W of input power. Tuning the actuators is done by adjusting the stiffness of the suspension shown on the far right of the photograph.

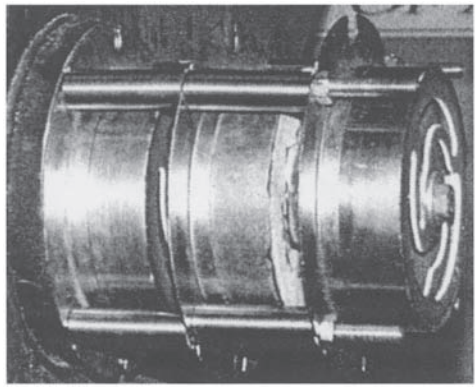

Figure 4.10 Three inertial actuators stacked together.

One disadvantage of these low cost actuators is the relatively high level of harmonic distortion that they exhibit. This can compromise the performance of the active control system with which they are used, unless a non-linear controller is used or the actuators are driven at levels well below their rated output.

4.3.4 Distributed Vibration Actuators, Shaped Vibration Actuators and Actuator Grouping

When using vibration actuators to achieve minimisation of radiation modes, it is possible that some vibrational energy will "spill-over" into higher order modes that are not being sensed. Of course, this problem can be minimised by sensing sufficient radiation modes, but it can also be addressed by using actuators that are fixed to the radiating surface and shaped so that they only excite the radiation

modes that are being sensed by the shaped error sensors. The use of shaped or distributed piezo-electric actuators bonded to the radiating surface has been the subject of a considerable amount of past work (Burke and Hubbard, 1987, 1988, 1991). Their use has been shown to reduce modal spillover and improve controllability.

Early control of sound radiation with distributed actuators relied on the use of judiciously placed actuators. These were optimised in the sense that the boundaries of the actuators extended along the nodal lines of the modes desired to be suppressed (Dimitriadis and Fuller, 1991) and were relatively successfully in reducing modal spillover to a limited extent. Sun et al. (1996) designed a PZT modal actuator for a cylindrical shell that had control authority only for the structural modes which efficiently coupled to the acoustic modes. In doing so they were able to reduce modal spillover and reduce the interior noise levels without increasing the structural vibration.

For distributed structural actuators to make a significant impact on the noise reduction of an enclosed or radiated sound field, it is necessary to use a considerable number of actuators, especially for modally dense structures. This in turn leads to many-channel controllers with their associated instability problems and slow convergence. Thus there has been considerable interest in developing ways of grouping actuators so that several can be driven by the same control signal (Ahn and Balachandran, 1998). In some configurations, fixed phase delays and attenuators are used so that each actuator in a group does not necessarily receive the same signal as any other. However, the relative phase and amplitude of the signals fed to all actuators in a particular group do not change as the controller changes the signal supplied to each group. Another strategy uses a "biologically inspired control" approach (Fuller and Carneal, 1993) in which a small number of signals are sent from an advanced, centralized controller and are then distributed by local simple rules to multiple control actuators.

Using the reciprocal relationship that exists for any piezoelectric transducer it is possible to create modal actuators from the same expressions as used for modal sensors (see Chapter 5). These produce the same benefits that the modal sensors exhibit, namely a reduction in modal spillover and improved controllability due to un-coupling of the modal response. PZT as a shaped modal actuator poses significant difficulties because of the brittle nature of the material. Subsequently more flexible materials have been used such as PVDF and although PVDF does not have sufficient control authority at low frequencies for most practical applications, it has been used successfully in the control of very flexible lightweight space structures (Bailey and Hubbard, 1987; Choi, 1995).

Because of the lack of control authority, researchers have looked at alternative materials. One such material which shows great promise for modal actuators is an elastomeric piezoelectric solid commonly referred to as *piezo-rubber*. Being relatively flexible, piezo-rubber can be used to form non-planar transducers easily without the need for casting and grinding; unfortunately, the lack of material availability has kept the research interest low (Lafleur et al., 1991 and Shields and Lafleur, 1997).

4.3.5 Tuned Vibration Absorbers

The tunable vibration absorber relies on an active control system to tune the stiffness (and sometimes the damping) of a variable stiffness vibration absorber so that the tonal sound field radiated by a vibrating structure is minimised.

4.3.6 Other Types of Vibration Actuator

Other types of vibration sources to control sound radiation from vibrating structures include electrodynamic shakers, electromagnetic actuators, proof-mass actuators, shape memory alloy actuators, hydraulic actuators and pneumatic actuators. These are all described in detail by Hansen and Snyder (1997). Many of the actuators have non-linear characteristics and care must be taken either to not drive them too hard or to use a nonlinear control filter structure and associated algorithm (Wangler and Hansen, 1994). The use of shape memory alloy wire is interesting as it can act indirectly to reduce structural sound radiation. This is done by embedding shape memory alloy wire in the structure (usually made of composite material) which will change the structural stiffness characteristics on application of a voltage (Liang and Rogers, 1991). This in turn will result in a change in the sound radiation characteristics of the structure.

CHAPTER FIVE

REFERENCE AND ERROR SENSING

5.1 MICROPHONES

The most common sensors used in active control applications are microphones. In modern digitally based control systems, the frequency response of the microphone used for providing either the reference signal or error signal to the controller is not very critical as any lack of flatness in amplitude or phase is taken into account in the system identification algorithms, and can be compensated in the weights used in the control filter. For this reason, it is common to find relatively inexpensive microphones used in active control systems. The two most common types are the piezo-electric microphone and the inexpensive prepolarised condenser (electret) microphone. The latter microphones may be purchased with power supply for tens of dollars or without cable or power supply for less than $5. Thus multiple error microphones (for which the outputs are summed) may be used economically to improve system reliability. The author has used these microphones in very dirty environments using the holder incorporating an air purge system as illustrated in Figure 5.1. The additional noise at the microphone location resulting from the air purge is dependent on the speed of the air flow over the microphone. For the case considered here it was about 85–90 dB, which was sufficiently below the duct noise that it was not a problem, as duct noise levels varied from 112 dB to 138 dB.

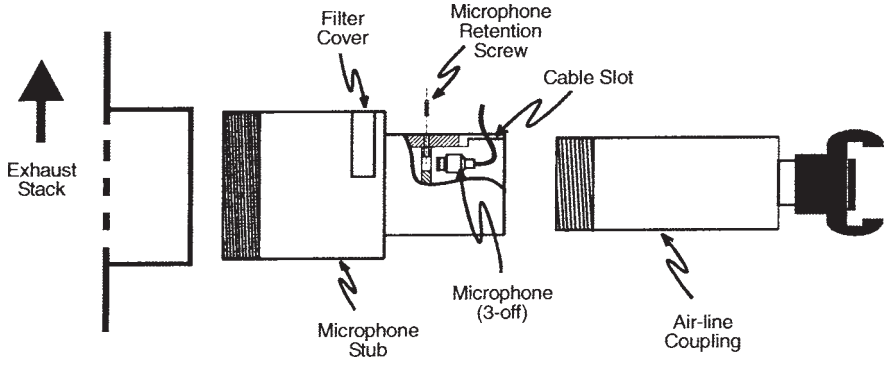

Figure 5.1 Microphone holder with air purge.

Even when the microphones became covered in sludge (due to a malfunction in the air purge supply), they all continued to operate. If noise control is required over a specified frequency range, then better results are obtained if the reference or error

signal is filtered (with either an analog or digital filter) so that unwanted frequencies are discarded prior to the signal being used in the control algorithm.

In many cases aerodynamic pressure fluctuations caused by fluid flow, and travelling with the speed of the flow, contaminate the microphone signals and reduce the achievable noise reduction. This problem can be ameliorated by using turbulence filters (Hansen and Snyder, 1997) if the flow is uncontaminated (see Figure 5.2), or the microphone may be located in a small side branch as illustrated in Figure 5.1. In extreme contamination cases it may be mounted in a side branch and protected by a thin mylar membrane or protected with an air purge system as shown in Figure 5.1.

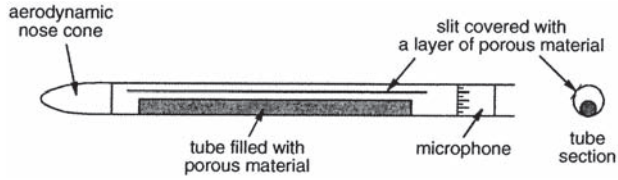

Figure 5.2 Turbulence filter and directional microphone.

To minimise acoustic feedback from the control source to the reference microphone (in cases for which a tachometer signal is unsuitable—see next section), a directional microphone or a directional loudspeaker or both may be used. A directional microphone may be fabricated using two microphones placed a fixed axial distance apart in the wall of the duct with the signal from the one furthest from the control source being delayed by the propagation time for an acoustic wave to travel from one to the other. A directional sound source can be made from two loudspeakers using similar reasoning. Alternatively, a directional probe microphone, which consists of a microphone at one end of a porous tube (or a hollow tube with a slit covered with porous material as shown in Figure 5.2) may be used. This has the added advantage of acting as a turbulence filter as well and for this reason is commonly used for both reference and error microphones in ducts with a mean flow.

A particular probe tube design that works well in practice consists of either a porous ceramic tube (Hoops and Eriksson, 1991) or a sintered metal tube (Bies, 1971). Alternatively a hollow metal tube containing a longitudinal slit running its full length could be used as shown in Figure 5.2. The slit should be covered with porous material having a flow resistance of approximately $2\rho c$ (Neise, 1975). Sometimes it is necessary to use two microphones (between 0.5m and 1m apart) in the probe tube to obtain a reasonable directivity at low frequencies.

To be effective, the end of the probe tube opposite to the microphone must point towards the sound source that is to be measured, regardless of the direction of air flow. This is particularly important for noise control on fan inlets where the air flow is in the opposite direction to the acoustic wave propagation. As discussed previously an IIR filter may be used in the controller in place of an FIR filter to compensate for mild cases of acoustic feedback. However, in many cases, at low frequencies the acoustic feedback is so strong that a directional microphone is also needed to ensure system stability.

To minimise the presence of unwanted extraneous noise in the reference and error signals, the microphone signals are often filtered with band pass filters so only the noise to be controlled is present in both signals. However, for the control of random noise, band pass filtering the reference signal could have a detrimental effect on system performance as a result of the group delay through filter. Thus it should be used with care.

5.2 TACHOMETER REFERENCE SIGNAL

In many cases, it is difficult to obtain an uncontaminated reference signal using a microphone. Many problems are caused by non-acoustic turbulent pressure fluctuations that travel at the speed of the flow but still cause a response from the microphone in the same way as an acoustic wave. Other problems are a result of access difficulty.

If the noise to be controlled is periodic in nature (one or several tones) and is generated by or synchronously with rotating machinery, it is feasible to replace the reference microphone with a tachometer. The tachometer may be magnetic or optical and typically it would output a string of pulses as shown in Figure 5.3. If pointed at the edge of a rotating gear wheel, there would be one pulse generated for each gear tooth that passed the tachometer sensor. Magnetic sensors (or Hall effect sensors) are preferred over optical sensors as they are more rugged and less sensitive to dirt.

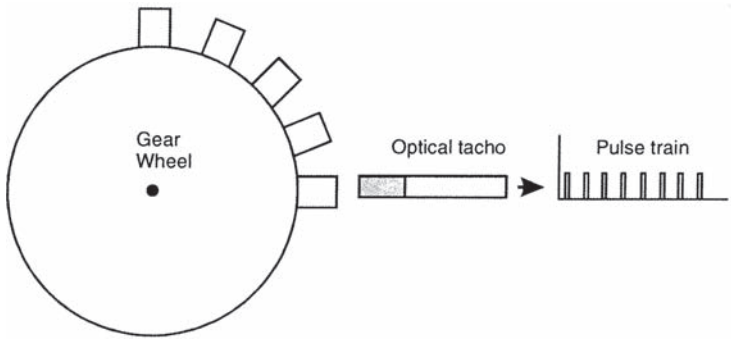

Figure 5.3 Arrangement for optical tachometer reference signal generation.

There are a number of ways of converting the tachometer pulse train into a signal that is useful for an adaptive filter type of active noise control system. Note that for the waveform synthesis method, no pre-processing of the pulse train is necessary. However, the implementation of active control by adaptive filtering is the technique used in commercial controllers and is characterised by a better performance, so it is of interest to discuss the conversion of the tacho pulse signal into sine waves that are suitable inputs to the adaptive filter control system.

It was mentioned in Chapter 3 that the relative powers of the different frequencies in the reference signal spectrum should reflect the relative noise reductions required

at each frequency. Thus it is useful to be able to convert the tachometer pulse train into multiple sine waves corresponding to desired harmonics or sub-harmonics of the pulse frequency, with the relative amplitude of each sine wave able to be set to any desired value.

A number of different ways of generating a multiple sine wave output from a pulse input are discussed in the following sections.

5.2.1 Waveform Synthesis

There are a number of ways to estimate the fundamental frequency if waveform synthesis methods are to be used. For example, auto correlation analysis is suitable for detecting the period from a noisy signal; however, the precision of the frequency estimate is limited by the sampling rate. For a 48 Hz signal sampled at 48 kHz, there are about 1,000 points within one period. So the precision of the estimated frequency is about 1/1,000, while for a 480 Hz signal with the same sampling rate, it reduces to 1/100. Similarly, time domain techniques including the zero cross rate estimation method all have this shortcoming due to the discretization of the continuous signal.

To obtain sufficient frequency precision, a long time data record is necessary. Thus the ZOOM FFT should be used in frequency domain analysis. Normally, FFT algorithms use base band analysis where the frequency range extends from zero up to the Nyquist frequency. The analysis resolution is decided by F_s/N. where F_s is the sampling frequency (two times of the Nyquist rate) and N is the number points in the record. That means for any type of signal, 1 second of data can only offer 1 Hz frequency resolution, no matter what the sampling frequency is. There are two main procedures used for digital zoom. One is called “real-time zoom”, which acts by reducing the sampling frequency after a digital frequency shift. The other is called “non-destructive zoom”, which acts by increasing the record length N. Real-time zoom does not need as long a buffer as non-destructive zoom (10 k words or more). However, it is rare that individual components are so stable in frequency as to be able to justify a resolution of better than 1/4,000 of the centre frequency (Hz) when using real-time zoom. It is only with non-destructive zoom that frequency component definitions to an accuracy of 1/20,000 of the centre frequency (Hz) can be achieved.

Wave form synthesis is characterised by the difficulty in precisely estimating the fundamental frequency. A record length of 10 seconds is needed to get a frequency resolution of 0.1 of the centre frequency. There may be a jump (discontinuous) point in the output wave whenever the detected frequency changes a little; for example, from 100Hz to 100.1 Hz. The advantage of this method is that it can easily generate sinusoidal waves at sub-harmonics and any other harmonics with specified phases and amplitudes. Thus, the method is a good choice when the input signal is very stable.

5.2.2 Filtering

The filtering method uses a low pass filter to filter out the undesired frequency components. Thus, 1/2 harmonic and 2nd harmonic can never be filtered out from a

square wave because there are no such components in it. Fortunately the pulse train from an optical tacho is usually non-symmetrical and thus contains all of the desired components. With specially designed filters to adjust the phases and amplitudes, the relative phase and amplitude of each existing harmonic can be set to any value.

5.2.3 Non-Linear Transformation

Non-linear transformation methods usually are more complicated and are not easy to realize in real time; however, they avoid the difficulty of precise estimation of the fundamental frequency. In a practical implementation, the sampled reference input (tachometer signal) is low pass filtered, then a 1,024 point FFT is implemented to identify the dominant frequency. The frequency so identified is used to set the centre frequency of a digital band pass filter that has a bandwidth similar to the frequency resolution of the FFT. At the same time, the data are passed through the band pass filter that was set up with the previous data set and FTT. The result is a pure (or nearly pure) sine wave output. Automatic gain control (AGC) is used to set the amplitude of the sine wave equal to one. Having obtained a sine wave at the fundamental frequency of the tachometer pulses, non-linear transformations can be used to obtain various harmonics and sub-harmonics as follows:

$$
\begin{aligned}
&\sin(\frac{x}{2}) = (-1)^m \sqrt{\frac{1-\cos x}{2}} \qquad m = \text{int}[\frac{\pi + |x|}{2\pi}] \\
&\cos(\frac{x}{2}) = (-1)^m \sqrt{\frac{1+\cos x}{2}} \qquad m = \text{int}[\frac{|x|}{2\pi}] \\
&\cos(2x) = 1 - 2\sin^2(x) = 2\cos^2(x) - 1 \\
&\sin(3x) = 3\sin(x) - 4\sin^3(x) \\
&\cos(3x) = 4\cos^3(x) - 3\cos(x) \\
&\cos(4x) = 1 - 8\cos^2(x) + 8\cos^4(x)
\end{aligned}
\tag{5.1}
$$

5.2.4 Simple Look-Up Tables

Two types of look-up table methods will be discussed here. One is suitable as a general purpose tool that can be implemented using a DSP and the other is a special application tool that can be implemented using a low cost micro-processor.

The general purpose implementation involves using an optical or magnetic tacho, and measuring the time period between pulses. A look-up table can then be used to generate a sine wave of the same period. Subharmonics can also be generated using look-up tables to generate a single sine wave over more than one pulse period and also to generate a sine wave with one or more periods within the pulse period. The period between two consecutive pulses is measured by the software and that is used to

determine the time interval between copying the values in sequential locations in the look-up table to the output. The accuracy of this interval can only be the time between samples on the DSP, so a very rapidly sampling DSP is needed. The DSP can combine the outputs of a number of look-up tables together, so it is possible to have look-up tables for a large number of harmonics and sub-harmonics and combine the outputs together with any specified relative amplitude. Of course a D/A converter is needed with a low pass filter on the output to minimise the high frequency components caused by discontinuities in the sine waves generated in sequential pulse periods.

For non-general purpose processing electronics, it is preferable to use a fast sampling micro-processor, rather than a DSP. In one particular application that concerned the author, a single engined propeller aircraft, with an existing 149-tooth gear wheel was used with an optical tacho to provide 149 pulses per revolution of the propeller. To reduce harmonic distortion, two pulses were inserted by the electronics between each pulse received from the tacho, using the period measured between the previous two tacho pulses to provide an estimate of the required time spacing for the inserted pulses. The result was a pulse train of 447 per revolution of the propeller. Thus the waveform repeated after a period of 447 pulses. A MATLAB program was written to calculate the required amplitude of the output waveform at 447 equal time intervals. These values were placed in a look-up table that was accessed by the microprocessor at the appropriate place each time a pulse was received. The digital value so accessed was then output to a D/A converter and steep low pass filter (to remove unwanted high frequency contamination).

Several look-up tables were provided to represent different applications and the required table was selected using a manual switch. Each look-up table could be configured to represent a particular combination of propeller blade passing harmonics (numbers and relative amplitudes).

The system consisted of a low-cost microprocessor (<$12) and a D/A converter ($5). The resolution for the digital input was about 200 kHz, (this depends on the speed of the processor) and the sampling frequency of the D/A converter was about 50 kHz.

If the rotational speed of the gear wheel changes too rapidly, it is difficult to insert the pulse evenly between the original tacho pulses because it depends on the precise prediction of the period, which is based on a measurement of the previous period.

5.2.5 Time Domain Measurement

Perhaps the most effective way of generating a sine wave at the same frequency as the tacho pulse signal is to use an extremely fast sampling rate on a floating point digital signal processor (DSP) such as found on the digital interrupt. This could easily be as high as 40 MHz. The number of samples between tacho pulses is measured and then a sine wave of that period is calculated by the DSP and output through a D/A converter sampling at a relatively high frequency (such as 16 kHz). Sine waves of frequencies corresponding to multiples or sub-multiples of the fundamental frequency can also be easily generated. The advantage of this method is that a continuously

phase varying signal is output that does not suffer from any discontinuity if the input signal changes. Practical implementation has shown that this method can produce sine waves with less harmonic distortion than commercial signal generators.

5.3 SOUND INTENSITY

Sound intensity is proportional to the product of sound pressure and particle velocity, with the particle velocity usually being measured by measuring the pressure difference between two closely spaced microphones as explained in Hansen and Snyder (1997).

Sound intensity sensing is often considered to be an attractive alternative to sound pressure error sensing because it actually measures the energy radiated from a sound source to the far field, even when the measurement is made in the near field. Thus, error sensors (sound intensity sensors) can be placed close to the sound source, which increases controller stability and reduces the number of error sensor channels needed to achieve global sound pressure level reductions. Although the use of sound intensity seems to overcome the near field problems associated with using sound pressure, its use raises another set of problems. Errors in relative phase offsets of the two microphones used for a sound intensity measurement are difficult to avoid in low cost microphones and can degrade the results achieved, especially in cases where the phases drift with time, negating any corrections that were made at the time the system was installed. Fortunately for systems with many channels, the phase errors are likely to produce sound intensity errors that cancel out when averaged over many measurements, so the problem may not be as bad as expected.

Nevertheless, experience has shown that sound intensity sensing is unlikely to be a useful cost function for active noise control systems directed at reducing sound radiated from vibrating structures. As well as problems with phase errors in low cost microphones, there is another problem. The sound intensity field close to a vibrating structure generally has a large variation with location and minimising sound intensity at the error sensors tends to produce a negative intensity very locally to the intensity sensor at the expense of large increases in intensity elsewhere. If researchers determine noise reduction by only measuring the field at the error sensors, then the strategy appears to work very well indeed. However, if other intensity sensors are used to investigate the field elsewhere a very different story unfolds. It is found in most cases that the overall radiated sound power increases, even when many intensity sensors are used. Even if the absolute value of intensity is used as the cost function, similar results are obtained and it is found that better results are generally found using near field sound pressure sensing (Berry et al., 1999). However, in spite of its failure as a cost function for the control of sound radiation from vibrating structures, there may be other applications where it is more successful, so the underlying ideas will still be discussed here.

The use of sound intensity as the cost function to be minimised was first published by Hald (1991). He developed the *filtered-x* least mean product algorithm and used it to minimise the sound intensity in front of a loudspeaker for actively reducing the sound radiated by a second (or primary) loudspeaker. In 1994, Sommerfeldt and

Nashif published a more detailed analysis and exposition of Hald's algorithm, although they seemed to be unaware of Hald's work. They also developed an algorithm for the minimisation of energy density (sum of potential and kinetic energies) in an enclosed sound field. In a later paper, Park and Sommerfeldt (1997) extended the energy density approach to the control of a broadband enclosed sound field. It is worth noting that the energy density approach is not appropriate for sound radiation into free space. In the near field of a noise source, normal intensity is a better choice and in the far field, pressure squared is a more effective cost function.

A frequency domain algorithm for minimisation of sound intensity was formulated in 1994 by Swanson (1994) who also demonstrated the importance of using "zero-padding", which means that the last half of the samples in a particular data set must be set equal to zero. When the inverse Fourier Transform is taken to produce a time domain signal (after the necessary arithmetic operations have been performed in the frequency domain), the last half of the resulting time domain data set is also discarded.

In 1995, Kang and Kim (1995) published a paper on the minimisation of sound intensity in a duct for the purpose of minimising the radiated sound power. Their formulation is similar to that of Sommerfeldt and Nashif (1994); however, they do investigate analytically the convergence and stability properties of the algorithm for minimising instantaneous intensity.

Qiu and Hansen (1997) developed an algorithm for controlling sound intensity radiated by electric power transformers based on waveform synthesis. However, the disadvantage of this method is that the A/D clock on the controller must be synchronised with the periodic noise to be controlled.

5.4 ENERGY DENSITY

Energy density is a little different to sound intensity in that it is proportional to the weighted sum of the squared acoustic pressure and squared particle velocity in each of three orthogonal directions.

It has long been known that the energy density in a one-dimensional sound field is approximately constant throughout the field and for 3-D systems with high modal densities it has been shown that the spatial variance of energy density is significantly less than the potential energy (Cook and Schade, 1974). To overcome the observability difficulties that are inherent with microphones as error sensors, such as pressure nodes, Sommerfeldt and Nashif (1991) suggested minimising the energy density at discrete locations. In a numerical simulation the authors found that minimisation of the energy density at a discrete location significantly outperformed the minimisation of squared pressures. Subsequent practical studies using the two microphone technique to estimate the particle velocity in one-dimensional fields (Sommerfeldt and Nashif, 1992, Nashif and Sommerfeldt, 1992, Sommerfeldt and Nashif, 1994, Sommerfeldt and Parkins, 1994) verified the earlier findings and showed that the location of the energy density sensor makes little difference to the controlled levels. Sommerfeldt et al. (1995) extended their earlier work to three dimensions and built

a 3 axis energy density sensor made from 6 electret microphones mounted in a wooden sphere. The preliminary results indicated that controlling energy density has the potential to achieve greater global control than controlling squared pressures. Park and Sommerfeldt (1997) successfully showed that energy density control can also be applied to enclosures excited by broadband noise.

Energy density control has also been applied to the control of a pure tone in a diffuse sound field (Elliott and Garcia-Bonito, 1995; Garcia-Bonito and Elliott, 1995). It was found that minimising both the pressure and pressure gradient along one axis rather than simply pressure, resulted in a significant increase in the 10 dB zone of quiet, from a sphere of diameter $\lambda/10$ around the pressure sensor to $\lambda/2$, for an ellipsoid with its longest axis in the direction of the measured pressure gradient.

Wenjun and Sun (1997) presented numerical simulations showing that 4 energy density sensors were as effective as 32 uniformly spaced micophones in terms of their ability to lead to global noise reduction when used as error signals in an active noise control system. More recently Cazzolato (1999) constructed an energy density sensor using just 4 microphones and showed that it performed as well as a 6-microphone sensor. He undertook some numerical simulations for a rigid-wall enclosure and showed that when a single acoustic source was used to control the interior sound field, the energy density sensor always out performed 4 separate microphones sensing just pressure. However, it was also shown that when the number of acoustic control sources is equal to or greater than the number of microphones in the energy density sensor, global control of the sound field is not as good, and there is also no advantage gained in using energy density sensing over simply summing the squared pressures from all the microphones. The phenomenon of reduced global performance with an increasing ratio of control sources to error sensors is a result of the control sources being able to achieve greater reduction at the sensor locations at the expense of global control and is associated with the control mechanism moving from modal control (of acoustic modes) to modal rearrangement with the consequent reduction in global control. Modal rearrangement, which involves a rearrangement of the phases and amplitudes of the acoustic modes, is the only mechanism whereby the controller can drive the microphone signals to the smallest level possible. The phenomenon is best illustrated graphically in Figure 5.4.

When the enclosure boundaries are flexible, their vibration couples with the interior sound field and this mechanism is the one responsible for many vehicle and aircraft cabin noise transmission problems. Such problems are characterised by external noise being transmitted into the passenger cabin by vibration of the cabin boundaries. Such a coupled vibro-acoustic system is typically the most difficult to treat since the structure tends to excite many more acoustic modes than would an interior noise source emitting the same spectrum of sound, due to interface modal filtering between the structure and the cavity. With more acoustic modes excited, more control sources are required to achieve the same level of control. Also, since the structural modes typically have a shorter wavelength compared to the acoustic modes, acoustic fields excited by the structure tend to exhibit much greater spatial variance, which creates observability problems.

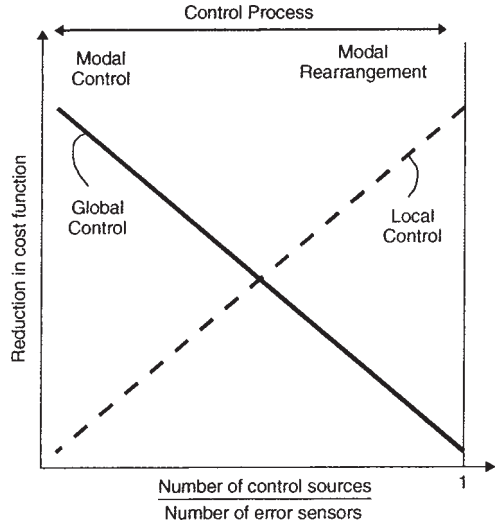

Figure 5.4 Effect of number of control sources on control mechanisms (Cazzolato, 1999).

Two types of control system for minimising the sound transmitted into a rectangular enclosure with 5 rigid walls and a flexible curved panel as its other wall have been investigated (Cazzolato, 1999): interior acoustic control sources; and surface mounted structural control sources. A single primary structural source with unit driving force, was placed in a non-symmetrical position on the curved panel so that all structural modes were excited directly. His results show that if acoustic control sources are used, and if global control is the objective for any cost function derived from discrete sensors, then broadly speaking, there must be a greater number of error sensors than control sources. Any enclosed space excited by structural vibration of its boundaries is particularly prone to modal spillover (energy at any particular frequency transferred from low order modes to high wave number modes), since the primary source does not necessarily efficiently excite the same modes as the acoustic control sources. The level of spillover is considerably reduced when structural vibration control sources rather than acoustic sources are used.

For his enclosure configuration, Cazzolato (1999) calculated the attenuation versus distance resulting from minimisation of the pressure at a single microphone and the energy density sensor using four acoustic control sources and a single structural primary source. His results are shown in Figure 5.5 for a heavily damped acoustic system. The attenuation vs distance from the error sensor has been calculated over the small frequency range of 600 Hz to 700 Hz to allow the separation distance to be normalised to the wavelength. Although energy density control suffers from spillover, the local zone of control is still larger than that achieved when minimising the pressure at a single location. However, both the 10 dB zones of quiet are significantly smaller than they are in an enclosure excited by acoustic sources only, particularly the zone of quiet for energy density control (see Figure 5.6). The reason for the decrease in size

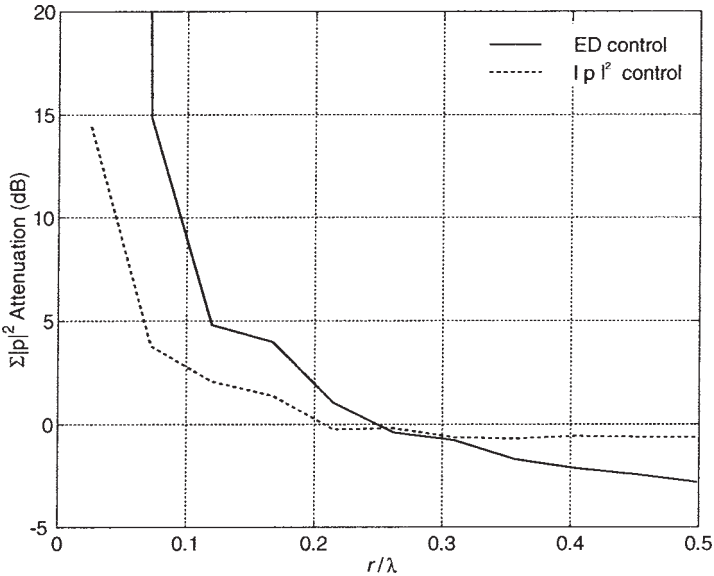

Figure 5.5 Numerical attenuation of squared pressure as a function of distance from the error sensor for a heavily damped acoustic system. Frequency range is from 600 to 700Hz and the separation distance has been normalised to 650Hz (single structural primary source and 4 acoustic control sources) (Cazzolato, 1999).

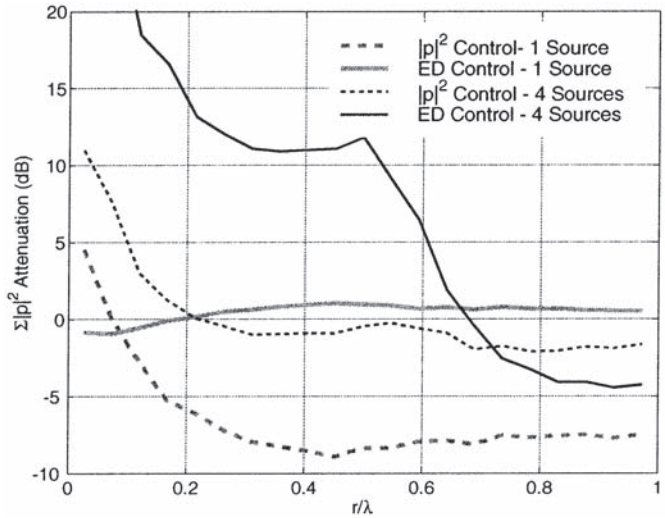

Figure 5.6 Numerical attenuation of squared pressure as a function of distance from the error sensor for a heavily damped acoustic system. Frequency range is from 600 to 700Hz and the separation distance has been normalised to 650Hz (single acoustic primary source and 1 or 4 acoustic control sources) (Cazzolato, 1999).

is because the sound field is driven by high wave number structural modes rather than lower wave number acoustic modes. As a result, the pressure field varies much more rapidly with a change in position and therefore the zone of quiet is reduced.

When the acoustic and structural damping were decreased, it was found that global noise reductions, especially for energy density control, were increased. However, the size of the zone of local control in the vicinity of the sensor for energy density control was decreased, although the size of the zone of local control for pressure control was relatively insensitive to damping as illustrated by comparing the results in Figure 5.7 with those in Figure 5.5.

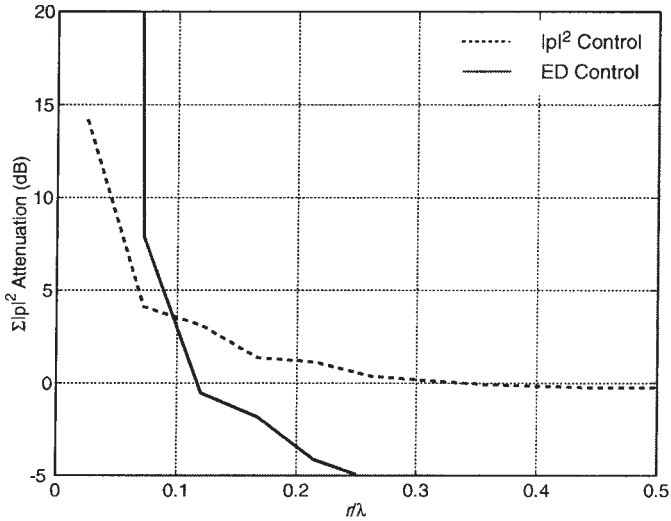

Figure 5.7 Numerical attenuation of squared pressure as a function of distance from the error sensor for a lightly damped acoustic system. Frequency range is from 600 to 700Hz and the separation distance has been normalised to 650Hz (1 structural primary source and 4 acoustic control sources) (Cazzolato, 1999).

In conclusion, it may be stated that when it is desired to obtain zones of reduced noise at a number of locations in an enclosed space, use of an energy density sensor will result in a larger zone of reduced noise level that a microphone at the expense of reduced noise reduction right at the sensor. It was also observed that the type of control source that works best is one that is similar to the type of original primary excitation source; for example, for primary structural excitation a structural control source works best. This is because the control structural sources are more likely to produce a sound field that matches the primary sound field. For energy density to be effective in obtaining global levels of sound reduction in an enclosed field, multiple sensors and control sources are needed, with the number of control sources required being less than the number of sensing elements but more than the number of energy density sensing systems. Multiple energy density sensors result in a reduction of energy "spilled-over" into higher order modes, thus improving the global control result.

5.5 VIRTUAL SENSING

Virtual sensing is the process of minimising the sound field at a location that is away from the error sensor. There are three approaches that have been used in the past to do this and each will be discussed in the following sections. One approach that was introduced by Garcia-Bonito et al. (1996, 1997), is based on measuring the acoustic pressure transfer function between a permanently placed remote microphone and a microphone temporarily located at the observer location. With the temporary microphone subsequently removed, the signal from the permanent microphone was modified with the transfer function to create the virtual microphone. The assumption is implicit that the transfer function does not alter with time and while it is possible that the control system will become ineffective if it changes significantly, Garcia-Bonito et al. (1996) reported acceptable stability when a spherical shape (such as a head) was added to the environment. This approach is discussed in the following paragraphs for pressure (microphone) sensing.

The second approach (Cazzolato, 1999; Hansen and Cazzolato, 1999) is to estimate the pressure at the virtual location in real time using forward difference extrapolation with the signal from a number of remotely placed microphones. This approach would have the advantage that the "virtual microphone" would not need *a priori* information of the control source to pressure transfer functions. This approach will be discussed in the following paragraphs for both pressure and energy density sensing.

The third approach, called model reference control, was first reported by Clark and Fuller (1992, 1993) and it is very similar to the first method mentioned above. They implemented active control of sound radiated by a vibrating structure by using microphone error sensors in the far field and actuators on the vibrating structure. They then measured the "phase-referenced" structural response at the same number of structural locations as they had control actuators. This was called the "desired structural response". The control system then used the vibration sensors at the structural measurement locations as error sensors and adjusted the control signal so that the difference between the desired structural response and the actual structural response was minimised. The above two papers describe the method in detail.

5.5.1 Virtual Sound Pressure (Virtual Microphone)

5.5.1.2 Transfer Function Method

The transfer function method, as described by Garcia-Bonito et al. (1996, 1997), is based on measuring the acoustic pressure transfer function between a permanently placed remote microphone and a microphone temporarily located at the observer location. The theory may be summarised as follows. The total pressure field p_t is the sum of the primary p_p and control pressure fields p_s as follows:

$$p_t = p_P + p_s \tag{5.2}$$

The control source contribution may also be written as the product of the complex acoustic impedance, Z, between the control source location and the error sensor location and the control source strength, q_s. This can be applied to both the actual and virtual microphone locations where the subscripts *a* and *v* apply to the actual and virtual locations respectively:

$$p_a = p_{pa} + Z_a q_s \text{ and } p_v = p_{pv} + Z_v q_s \tag{5.3}$$

The expression for the pressure difference between the two locations is then:

$$p_a - p_v = (p_{pa} + Z_a q_s) - (p_{pv} + Z_v q_s) \tag{5.4}$$

Garcia-Bonito et al. (1996, 1997) state that at low frequencies the spatial rate of pressure change due to the primary field is small enough so we can assume that the primary source pressure component is the same at both the virtual and actual locations. Close to the control sound source, the actual sensor and the virtual error sensor to control source transfer impedance functions are significantly different. The prior measurement of this difference can be used as an operator on the actual error signal to estimate the pressure at the virtual location. Thus:

$$p_v = p_a - (Z_a - Z_v) q_s \tag{5.5}$$

5.5.1.2 Forward Prediction Method

As mentioned previously, this method is based on using forward prediction to determine the sound pressure at a particular location based on actual measurements at two or more remotely located microphones as illustrated in Figure 5.8.

The pressure at point can be approximated by the first order finite difference estimate:

$$p_x' = p_2 + \frac{x}{2h}(p_2 - p_1) \tag{5.6}$$

Using a three-microphone approach it can be seen in Figure 5.9 that the forward estimate in pressure improves (at least theoretically) compared to the estimate from the two-microphone approach.

The pressure at point p_x' can be approximated by the second order finite difference estimate using Lagrange's interpolation formula for unequal intervals; that is:

$$p(x) = \frac{(x-x_2)(x-x_3)}{(x_1-x_2)(x_1-x_3)} p_1 + \frac{(x-x_1)(x-x_3)}{(x_2-x_1)(x_2-x_3)} p_2 + \frac{(x-x_1)(x-x_2)}{(x_3-x_1)(x_3-x_2)} p_3 \tag{5.7}$$

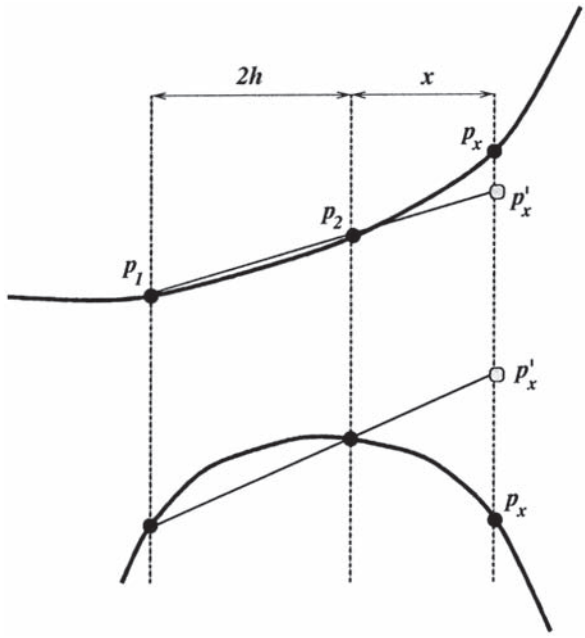

Figure 5.8 Two-microphone forward prediction technique.

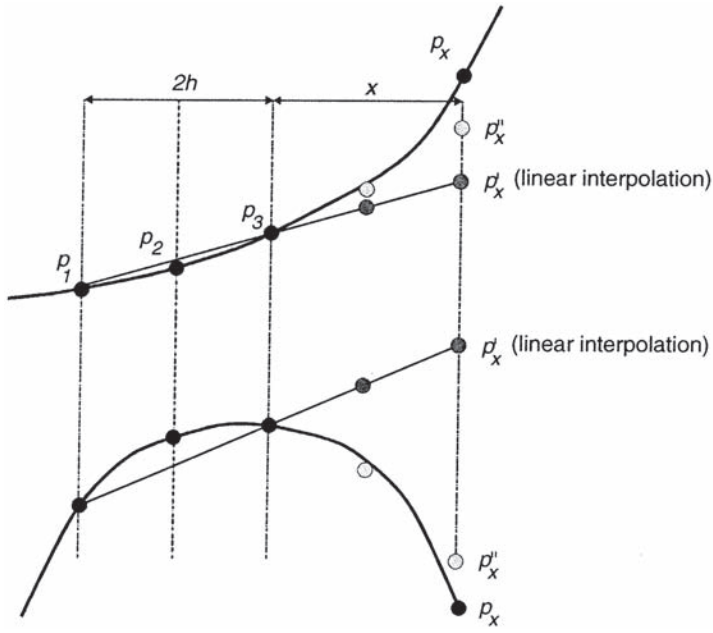

Figure 5.9 Three-microphone forward prediction technique.

Therefore for the system shown in Figure 5.9, Equation (5.7) reduces to:

$$p_x'' = \frac{(x+h)(x)}{(h)(2h)}p_1 + \frac{(x+2h)(x)}{(h)(-h)}p_2 + \frac{(x+2h)(x+h)}{(2h)(h)}p_3 \tag{5.8}$$

Collecting like terms gives:

$$p_x'' = \frac{x(x+h)}{2h^2}p_1 + \frac{x(x+2h)}{-h^2}p_2 + \frac{(x+2h)(x+h)}{2h^2}p_3 \tag{5.9}$$

If $x=h$, then Equation (5.9) reduces to:

$$p_x'' = p_1 - 3p_2 + 3p_3 = p_1 + 3(p_3 - p_2) \tag{5.10}$$

If $x=2h$, then Equation (5.9) reduces to:

$$p_x'' = 3p_1 - 8p_2 + 6p_3 = p_1 - 2(p_2 - p_1) + 6(p_3 - p_2) \tag{5.11}$$

It is possible to have two closely spaced "virtual microphones", which when controlled would create a larger zone of quiet than would be achieved with a single "virtual microphone". It could be possible to define a virtual microphone array to extend the control region even further.

In practice it has been found that background noise that is always present in real measurements causes problems for the 3-microphone estimation technique as it is much more sensitive than the 2-microphone technique. Additional problems occur in ducts as a result of higher order modal contributions affecting the "smoothness" of the plane wave signal. Both of these problems result in the 2-microphone technique providing better control results in practice. A promising alternative is to use the second order equations associated with the 3-microphone technique, but use more microphones and take a least squares approach to obtaining the correct extrapolated pressure.

5.5.2 Virtual Energy Density

Only the forward prediction method will be discussed for energy density as results for the transfer function method applied to energy density have not yet been published. Also only the 2-microphone technique will be considered for the reasons stated in the previous section. The three microphone, second order extrapolation is discussed by Kestell et al. (2000).

The expression for energy density (in a 1-dimensional space) is:

$$E_{Dx} = \frac{p_x^2}{2\rho c} + \frac{\rho v_x^2}{2} = \frac{1}{2\rho c^2}[p_x^2 + \rho^2 c^2 v_x^2] \tag{5.12}$$

For the 2-microphone set-up shown in Figure 5.8, the estimate of the acoustic pressure, p_x' is given by Equation (5.6) and the particle velocity may be approximated by the following equation:

$$v_x' = \frac{p_2 - p_1}{j2h\rho\omega} \tag{5.13}$$

The prime on v_x represents an estimated quantity. The quantity, j=v-1, in the equation, tells us that the particle velocity phase lags the phase of the acoustic pressure gradient between p_1 and p_2, by 90°. Substituting Equations (5.6) and (5.13) into Equation (5.12) gives:
The quantity on the left hand side in the preceding equation may be used as a cost function to be minimised by the active noise control system.

It is anticipated that the use of these virtual sensors as active noise control error sensors will have the following advantages with respect to the more conventional active noise control error sensors:

- The high attenuation associated with local control may be brought directly to the observers ear without intrusive transducers.
- The attenuation zone around the observer may be broadened with the virtual energy density sensor.
- With an algorithm based on separation distance, it may be possible to track the distance between the observer and error sensors and allow the zone of silence to follow the observer.
- Controlling immediately around the head of the observer will allow the use of much smaller speakers (than required for global control).

5.6 VIBRATION SENSING OF SOUND RADIATION

In many applications of active noise control, it is inconvenient to use microphones to provide the error signal for minimising the sound field radiated from or transmitted through a structure. Thus, the use of structural vibration sensors to provide the required error signal, which must be proportional to the radiated sound field strength, is of great interest.

$$E_{Dx} = \frac{1}{2\rho c^2}\left[\left(1 + \frac{x}{2h}\right)^2 p_2^2 - \frac{x}{h}\left(1 + \frac{x}{2h}\right) p_1 p_2 + \left(\frac{x}{2h}\right)^2 p_1^2 - \frac{1}{(2hk)^2}\left(p_2^2 - 2p_1 p_2 + p_2^2\right)\right] \tag{5.14}$$

It is well known that the vibration response of any structure can be represented in terms of vibration modes that are orthogonal with respect to the structural vibration, but which are not orthogonal in terms of their contribution to the radiated sound field. This means that reducing the amplitude of a particular vibration mode will not necessarily reduce the sound radiated from the structure and may even increase it. One way of overcoming the problem is to decompose the structural vibration field into “radiation modes” that are orthogonal in terms of the radiated sound field, but

not in terms of the structural vibration field. An interesting aside is that the radiation modes are each made up of differing combinations of the structural vibration modes with the relative contributions of each vibration mode to a particular radiation mode being frequency dependent. Each radiation mode is characterised by a radiation efficiency and a structural mode shape. Although the calculation of radiation modes is relatively straightforward mathematically, there are a number of practical implementation problems that have provided fruitful topics for recent research. These problems are associated with unambiguous sensing of the radiation modes and the variation in the mode shapes as a function of frequency. One of the advantages of using radiation mode sensors rather than independent microphones (apart from the obvious convenience) is that less controller channels are needed to achieve the same noise reduction and this results in a more stable, faster converging (and hence faster tracking) controller.

The calculation of free space radiation modes for vibrating structures was first illustrated in a paper published by Borgiotti (1990) in which he developed a modal representation for the radiated acoustic power. At a similar time, Photiadis (1990) illustrated the relationship between the radiation mode approach and the wavenumber transform approach for the identification of efficient radiation modes (dominated by supersonic wavenumber components) and inefficient radiation modes (dominated by sub-sonic wavenumber components). Cunefare (1991) used the natural vibration modes of a beam as components of the radiation modes. Although all of the work mentioned essentially derived acoustic radiation modes for a vibrating structure, some confusion existed as a result of the different approaches used and the use of different names such as acoustic modes, weak radiators, singular velocity patterns and eigenfunctions. Since those first three papers, a number of authors have applied the results to the active control of noise radiated by vibrating structures, ranging from beams to cylinders (Baumann et al., 1991, Baumann and Greiner, 1992a, 1992b, Naghshineh and Koopmann, 1993, Naghshineh and Gellrich, 1994, Cunefare and Currey, 1994, Elliott and Johnson, 1993, Burdisso and Fuller, 1993, Currey and Cunefare, 1995, Song et al., 1991, Chen and Ginsburg, 1995, Snyder and Tanaka, 1993). More recently Cazzolato and Hansen (1998) have applied the radiation mode approach to the active control of sound transmission into a cylindrical enclosure and the principle results from this work are summarised here.

A serious obstacle to the implementation of radiation mode control using an active noise control system is the physical measurement of the radiation modal amplitudes and the subsequent derivation of an error signal proportional to the amplitudes. The problem of sensing radiation modes adequately is similar to the problem of sensing vibration modes in an active vibration control system with the added complexity that the radiation modes change shape with frequency. There has been a considerable amount of effort expended in deriving strategies for sensing vibration modes that used continuous PVDF film bonded to the structure and shaped to only measure the mode(s) of interest (Lee and Moon, 1990, Crawley and De Luis, 1987, Lee et al., 1991, Lee, 1990, Lee and Moon, 1989, Burke and Hubbard, 1991, Kim and Jones, 1991, Callahan and Baruh, 1995, Sonti et al., 1995, Sullivan et al., 1996). Of course, similar results can be obtained by measuring the structural

velocity at a large number of discrete locations on the structure and then appropriately weighting each measurement. However this is a very expensive and in most cases an impractical alternative to continuous sensing.

The work on shaped sensors for measuring vibration mode amplitudes has been extended to the measurement of radiation modal amplitudes by a number of authors who have taken into account two important properties of radiation modes. First, it has been found that the frequency dependence of the radiation mode shapes is not very strong, so that it is possible to fix the sensor shape to the correct shape at a particular frequency and obtain good results for a band of frequencies about an octave wide and centred on the design frequency. Second, it has been found that for sound radiation from typical structures at low frequencies (below ka=1, where k is the wavenumber and a is the largest structural dimension), the radiation efficiencies of the radiation modes sharply decrease as the radiation mode order increases. This latter property implies that only a very few radiation modes are necessary to adequately characterise the structural sound radiation.

In the case of planar sound radiators, a number of researchers (Rex and Elliott, 1992, Johnson and Elliott, 1995, Charette et al., 1995) have demonstrated that large reductions in radiated sound power could be obtained by sensing and minimising the total volume velocity over the entire surface of the radiator. It can be shown easily, that this is effectively the same as minimising the first radiation mode and as such is effective only at relatively very low values of ka. Sommerfeldt and Scott (1994) investigated the use of shaped sensors to form a low pass wavenumber filter so that minimisation of the sensor output would effectively minimise the supersonic wavenumber spectrum that is responsible for the radiated sound. Snyder et al. (1993, 1995), Snyder and Tanaka (1993) and Tanaka et al. (1996) investigated the design of 1-dimensional and 2-dimensional modal sensors and demonstrated their application to the reduction of sound radiated by a vibrating panel into free space. Snyder and Tanaka (1993) also briefly investigated the problem of designing shaped sensors for the active minimisation of sound transmission through a rectangular panel into a rectangular enclosure.

More recently, Cazzolato and Hansen (1998) have extended the use of structural error sensing to the active control of sound transmission into a stiffened cylindrical enclosure through the enclosure walls. In their work, the transmitted sound field is derived in terms of structural radiation modes and the implications for structural vibration sensing of the radiation modes is also discussed. Using the modal-interaction approach to the solution of coupled problems, the response of the structure is modelled in terms of its *in vacuo* mode shape functions and the response of the enclosed acoustic space is described in terms of the rigid-wall mode shape functions. The response of the coupled system is then determined by solving the modal formulation of the Kirchhoff-Helmholtz integral equation.

The quantity traditionally minimised in active control strategies for minimising sound transmission into an enclosure is the total time-averaged frequency dependent acoustic potential energy, $E_p(\omega)$, which is effectively the acoustic pressure squared summed over the entire enclosure volume (Nelson et al., 1987):

$$E_p(\omega) = \frac{1}{4\rho_0 c_0^2}\int_V |p(\vec{\mathbf{r}},\omega)|^2 d\vec{\mathbf{r}} \tag{5.15}$$

where $p(\vec{\mathbf{r}}, \omega)$ is the acoustic pressure amplitude at some location $\vec{\mathbf{r}}$ in the enclosure, ρ_0 is the density of the acoustic fluid (air), c_0 is the speed of sound in the fluid and V is the volume over which the integral is evaluated. The frequency dependence of the variables is omitted in the following equations to minimise complexity. The acoustic pressure at any location within the cavity my be expressed as a product of rigid-wall acoustic mode shape functions, φ_i, and the modal amplitudes, p_i, of the cavity as follows:

$$p(\vec{\mathbf{r}}) = \sum_{i=1}^{\infty} p_i \varphi_i(\vec{\mathbf{r}}) \tag{5.16}$$

The acoustic potential energy evaluated using n_a acoustic modes may be written as:

$$E_p = \mathbf{p}^{\mathrm{H}} \Lambda \mathbf{p} \tag{5.17}$$

where $\mathbf{p}$ is the $(n_a \times 1)$ vector of acoustic modal amplitudes and Λ is a $(n_a \times n_a)$ diagonal weighting matrix, the diagonal terms of which are:

$$\Lambda_{ii} = \frac{\Lambda_i}{4\rho_0 c_0^2} \tag{5.18}$$

where Λ_i is the modal volume of the ith cavity mode, defined as the volume integration of the square of the mode shape function:

$$\Lambda_i = \int_V \varphi_i^2(\vec{\mathbf{r}}) dV(\vec{\mathbf{r}}) \tag{5.19}$$

The acoustic pressure modal amplitudes, p, within the cavity, arising from the vibration of the structure are given by the product of the structural modal velocity $(n_s \times 1)$ vector, $\mathbf{v}$, and the modal structural-acoustic radiation transfer function $(n_a \times n_s)$ matrix Snyder and Hansen 1994), $\mathbf{Z}_a$:

$$\mathbf{p} = \mathbf{Z}_a \mathbf{v} \tag{5.20}$$

The l,i^{th} element of the radiation transfer function matrix $\mathbf{Z}_a$ is the pressure amplitude of acoustic model generated as a result of structural mode i vibrating with unit velocity amplitude. Substituting Equation (5.20) into Equation (5.17) gives an expression for the acoustic potential energy with respect to the normal structural vibration:

$$E_p = \mathbf{v}^{\mathrm{H}} \Pi \mathbf{v} \tag{5.21}$$

where the error weighting matrix Π, the elements of which are applied to each error sensor, is given by:

$$\Pi = \mathbf{Z}_a^{\mathrm{H}} \Lambda \mathbf{Z}_a \tag{5.22}$$

The error weighting matrix Π is not necessarily diagonal, which implies that the normal structural modes are not orthogonal contributors to the interior acoustic pressure field. It is for this reason that minimisation of the modal amplitudes of the individual structural modes (or kinetic energy) will not necessarily reduce the total sound power transmission into the enclosure.

As Π is real symmetric it may be diagonalised by the orthonormal transformation:

$$\Pi=\mathbf{USU}^{\mathrm{T}} \tag{5.23}$$

where the unitary matrix **U** is the (real) orthonormal transformation matrix represents the eigenvector matrix of Π and the (real) diagonal matrix **S** contains the eigenvalues (singular values) of Π. The physical significance of the eigenvectors and eigenvalues is interesting. The eigenvalues can be considered radiation efficiencies (or coupling strengths (Bessac et al. 1996)) and the associated eigenvector gives the level of participation of each normal structural mode to the radiation mode; thus it indicates the modal transmission path. The structural radiation modes are orthogonal with respect to sound radiation but not with respect to structural vibration.

Substituting the orthonormal expansion of Equation (5.23) into Equation (5.21) results in an expression for the potential energy of the cavity as a function of the orthogonal radiation mode set:

$$E_p=\mathbf{v}^{\mathrm{H}}\mathbf{USU}^{\mathrm{T}}\mathbf{v}=\mathbf{w}^{\mathrm{H}}\mathbf{Sw} \tag{5.24}$$

where the elements of w are the velocity amplitudes of the radiation modes defined by:

$$\mathbf{w}=\mathbf{U}^{\mathrm{T}}\mathbf{v} \tag{5.25}$$

Equation (5.25) demonstrates that each radiation mode is made up of a linear combination of the normal structural modes, the relative contributions of which are defined by the eigenvector matrix **U**. As the eigenvalue matrix, **S**, is diagonal, Equation (5.24) may be written as follows:

$$E_p = \sum_{i=1}^{n} s_i |w_i|^2 \tag{5.26}$$

where s_i are the diagonal elements of the eigenvalue matrix **S** and w_i are the modal amplitudes of the individual radiation modes given by Equation (5.25).

The enclosure potential energy contribution from any radiation mode is equal to the square of its amplitude multiplied by the corresponding eigenvalue. The radiation modes are therefore independent (orthogonal) contributors to the potential energy and the potential energy is directly reduced by reducing the amplitude of any of the radiation modes. As mentioned previously, the normal structural modes are not orthogonal radiators since the potential energy arising from one structural mode depends on the amplitudes of the other structural modes. The orthogonality of the radiation modes is important for active control purposes because it guarantees that the potential energy will be reduced if the amplitude of any radiation mode is reduced (Johnson and Elliott, 1995). An important property of the radiation modes is that only the first few are sufficiently efficient to have a significant effect on the transmitted

sound field. This greatly reduces the complexity of the physical control system. The eigen value magnitudes for the first few radiation modes for sound transmission into a cylindrical enclosure, 3 m in length 0.9 m in diameter and 1mm thick, excited by a single point force and controlled by a single control force located remote from the primary force are shown in Figure 5.10.

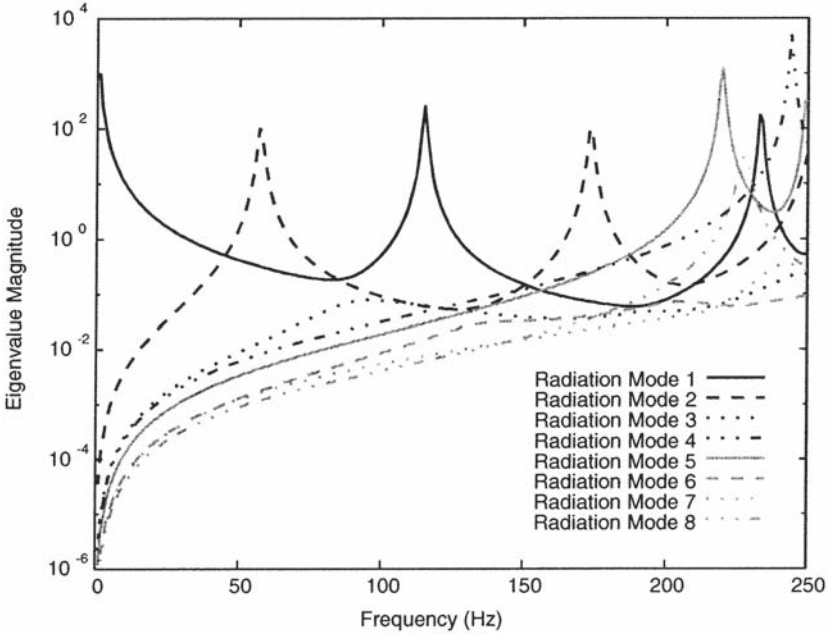

Figure 5.10 Eigenvalue magnitudes for the first few radiation modes that control sound transmission into a cylindrical enclosure (Cazzolato, 1999).

If the structural velocity distribution is sensed with a number of discrete sensors, then the structural velocity levels at these locations are given by the vector $\boldsymbol{v}_e$, which is defined as:

$$\boldsymbol{v}_e = \boldsymbol{\Psi}_e \mathbf{v} = [\boldsymbol{\Psi}_e \boldsymbol{U}]\boldsymbol{w} \tag{5.27}$$

where Ψ_e is the mode shape matrix at the discrete error sensor locations with the number of rows equal to the number of sensor locations, n_e and the number of columns equal to the number of structural modes, n_s used to describe the structural vibration field.

It is possible to show (Cazzolato and Hansen, 1998) that the radiation modal amplitudes are given by:

$$\boldsymbol{w} = \mathbf{Z}_t \boldsymbol{v}_e \tag{5.28}$$

and the radiation mode shapes evaluated at the measurement locations are given by:

$$\boldsymbol{v}_e = \boldsymbol{\Psi}_e \boldsymbol{v} = [\boldsymbol{\Psi}_e \boldsymbol{U}]\boldsymbol{w} \tag{5.29}$$

where $\mathbf{Z}_t$ is the $(n_{rm} \times n_e)$ radiation mode structural transfer function matrix (or modal filter matrix), which relates the vibration velocity levels, v_e, at the discrete error sensor locations to the modal velocity amplitudes of the n_{rm} radiation modes. The elements of each row of this modal filter matrix represent a weighting value, which when applied to the signal from the vibration sensors and summed for all sensors, will provide a measure of the amplitudes of the radiation modes. The radiation mode shapes at the discrete locations are given by $\boldsymbol{\Psi}_e \boldsymbol{U}$.

The practical implementation of the control system may look something like that shown in Figure 5.11, where an accelerometer array would be used to measure the velocity levels on the surface of the shell. The modal filters, $\mathbf{Z}_t$, given by Equation (5.28) would be used to decompose the velocity signal into modal amplitudes of the radiation modes. The frequency weighting (eigenvalue) filters, **S**, would then be used to weight the modal amplitudes to provide inputs to the controller.

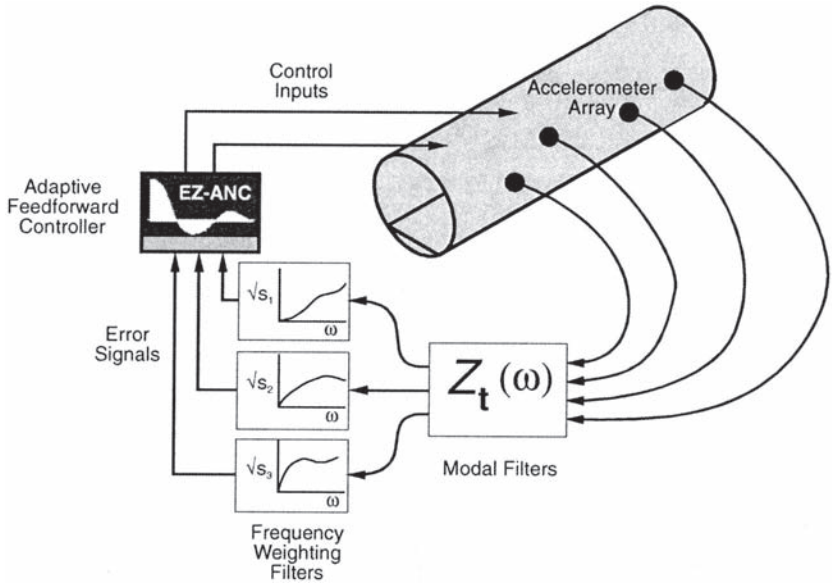

Figure 5.11 Schematic of modal and eigen-fllter for an ANVC system.

The radiation mode shapes are frequency dependent; however, the frequency dependence is not very strong and it can be shown that the discrete sensors may be replaced with shaped PVDF film vibration sensors, attached to the structure and optimised to produce a signal proportional to a radiation mode amplitude at a fixed frequency (Cazzolato and Hansen, 1998). Shaped sensors effectively provide the required modal filtering, thus allowing the modal filters shown in the control system in Figure 5.11 to be eliminated. This approach is effective over a restricted frequency range in which the mode shape variation is small enough to ignore. This process makes implementation of the radiation mode error sensing strategy practical for a

band of noise. Fixing the mode shape at a given frequency is carried out by normalising the eigen vector matrix **U**, at the fixed frequency to form a new eigen vector matrix, $\mathbf{U}_f=\mathbf{KU}$, where **K** is a square but highly diagonal correction matrix. With this approximation, only the frequency dependent eigen value filters (see Figure 5.11) need to be implemented digitally and the modal filter can be implemented with a shaped sensor whose shape is fixed at the optimum for a selected frequency. The shaped sensor is attached to the vibrating structure and is shaped so that it responds to a particular radiation (or eigen) mode.

Figure 5.12 shows some numerical results comparing the minimum interior potential energies achieved by using as cost functions: the interior potential energy; the structural kinetic energy; and the amplitudes of the two dominant radiation modes, where it is assumed that the radiation mode sensor shape is optimised at each frequency. The cylinder was excited by a single point primary force and controlled by a single point control force. As expected, minimisation of the structural kinetic energy is ineffective, but minimising the amplitudes of the two radiation modes is almost as effective as minimising the interior potential energy. It is also clear that the greatest noise reduction occurs at the resonance frequencies of the acoustic modes (57 Hz, 115 Hz, 173 Hz, 220 Hz, 228 Hz, 233 Hz, 244 Hz, 250 Hz and 251 Hz).

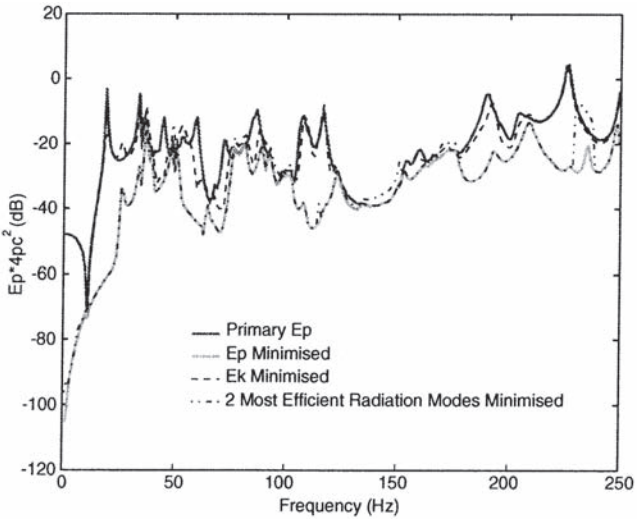

Figure 5.12 Comparison of the effect of using different cost functions on the active reduction of interior acoustic potential energy transmitted into a cylindrical enclosure (Cazzolato, 1999).

In Figure 5.13, similar results to Figure 5.12 are shown, but in this case the distributed sensor shapes are fixed for all frequencies at the optimum value for 57 Hz and 220 Hz respectively. It can be seen that fixing the shape of the first two radiation modes at 57 Hz works well in controlling sound transmission up to about 150 Hz and fixing the shapes at 220 Hz sensor works well at controlling sound transmission above about 70 Hz. Finally results are shown in Figure 5.14 for the first radiation mode sensor shape fixed at the optimum for 117 Hz and the second fixed at the optimum

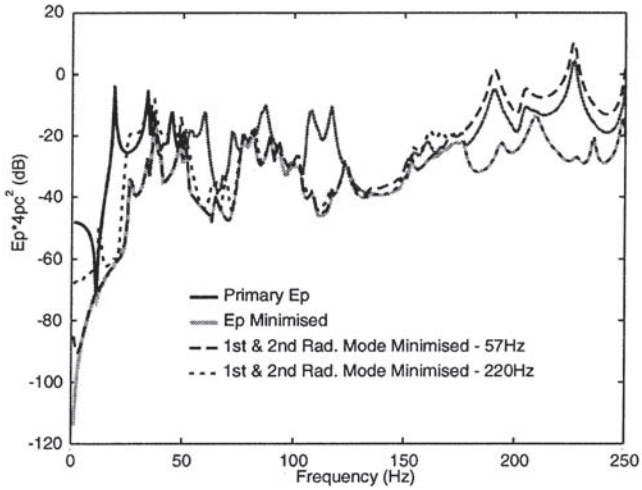

Figure 5.13 Effect of different normalisation frequencies on the active control of sound transmission into a cylindrical enclosure using radiation mode amplitudes as a cost function.

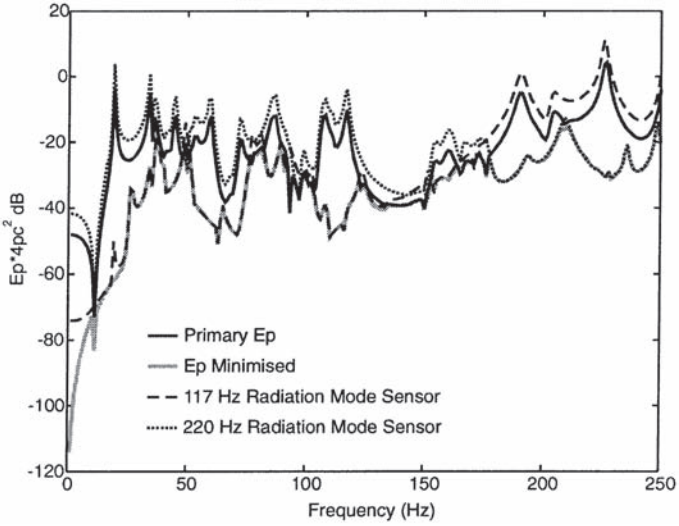

Figure 5.14 Active control of potential energy using single channel fixed frequency radiation modal sensors without a radiation efficiency weighting filter (Cazzolato, 1999).

shape for 220 Hz. The best overall single-channel results would be achieved by using a cross-over network set up so that only the first mode is minimised at low frequencies (below 170 Hz) and the second at high frequencies (above 170 Hz), which effectively requires a single channel controller.

As can be seen from the figure, the results obtained are nearly as good as those obtained by minimising the interior potential energy, which would require many microphones distributed throughout the cavity and a many channel control system.

One interesting discovery made during this research was that the optimum shape for the structural radiation mode sensor, derived using the preceding analysis, was very close to the mode shape of the interior acoustic field to be controlled. In fact, it was found that when the sensor shapes were made the same as the interior acoustic field shape, very similar results were obtained. This finding has enormous impact on the level of effort required to find the optimal sensor shapes for complex enclosures enclosed by structures with high modal densities.

In the future, it is clear that there will be increasing interest in the development of "smart" structures containing distributed actuators and sensors. There is considerable current research effort devoted to the development of suitable strategies for controlling the noise radiated by such structures.

5.7 CONTROL ALGORITHMS FOR VARIOUS SENSING STRATEGIES

5.7.1 Shaped or Distributed Structural Sensors

The control algorithm for minimising radiation modal amplitudes sensed either with continuous or point error sensors is effectively the filtered-x algorithm, which can be used with FIR filters (FXLMS algorithm) or IIR filters (FURLMS algorithm). The quantity that is minimised is the sum of the products of the squared radiation modal amplitudes, $w_{i,}$ and their corresponding radiation efficiencies, σ_i. For an enclosure this is the total interior potential energy and for sound radiation into free space it is the power radiated by the vibrating structure. The error criterion if *n* error signals are used is:

$$J = \sum_{i=1}^{n} \sigma_i | w_i |^2 \tag{5.30}$$

To simplify the analysis and allow ease of comparison between the different algorithms considered here, only a single channel control system will be assumed so that:

$$J=\sigma_1 | w_1 |^2 \tag{5.31}$$

The control system layout for a shaped sensor error signal is illustrated in Figure 5.15.

The filter weight update equation if an FIR filter is used is given by Equation (3.11) or (3.20) in Chapter 3, and if an IIR filter is used, the weight update equations are given by Equations (3.16) and (3.17). Essentially the shaped sensor output (after appropriate signal conditioning) is treated by the controller in a similar way to a microphone.

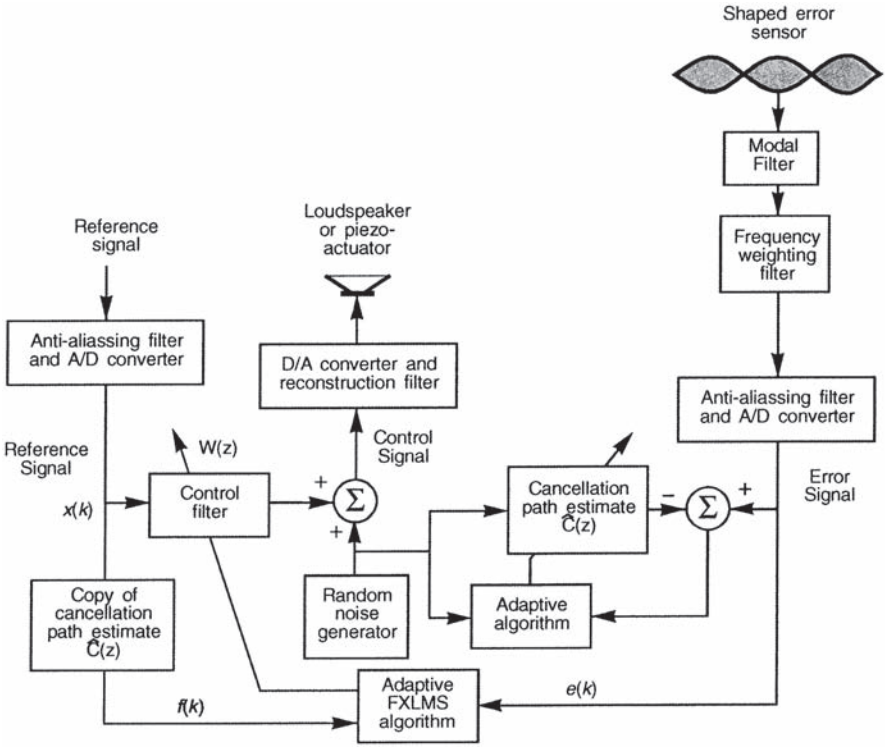

Figure 5.15 Control system layout for shaped sensor error signal and FXLMS algorithm.

5.7.2 Sound Intensity

The control system arrangement used when sound intensity is the cost function is shown in Figure 5.16.

When sound intensity (in one direction) is used together with the least mean product (LMP) algorithm, the weight update equation is a little different to that used for minimising the squared output from shaped sensors discussed in the preceding section. The cost function to be minimised is:

$$J_I = I_a = p_e(k) \times u_e(k) = [Pp(k) + s_p(k)] \text{ x } [p_u(k) + s_u(k)] \tag{5.32}$$

where the product $p_p(k)p_u(k)$ represents the sound intensity at the error sensor due to the primary source alone and $s_p(k)s_u(k)$ represents the control source contribution to the error sensor. Referring to Figure 5.16, the quantities $s_p(k)$ and $s_u(k)$ can be written as:

$$s_p(k) = [\boldsymbol{w}^T(k)\boldsymbol{x}(k)] * c_p(k) = \boldsymbol{w}^T(k)\boldsymbol{f}_p(k) \tag{5.33}$$

$$s_u(k) = [\boldsymbol{w}^T(k)\boldsymbol{x}(k)] \; {}_*c u(k) = \boldsymbol{w}^T(k)\boldsymbol{f}_u(k) \tag{5.34}$$

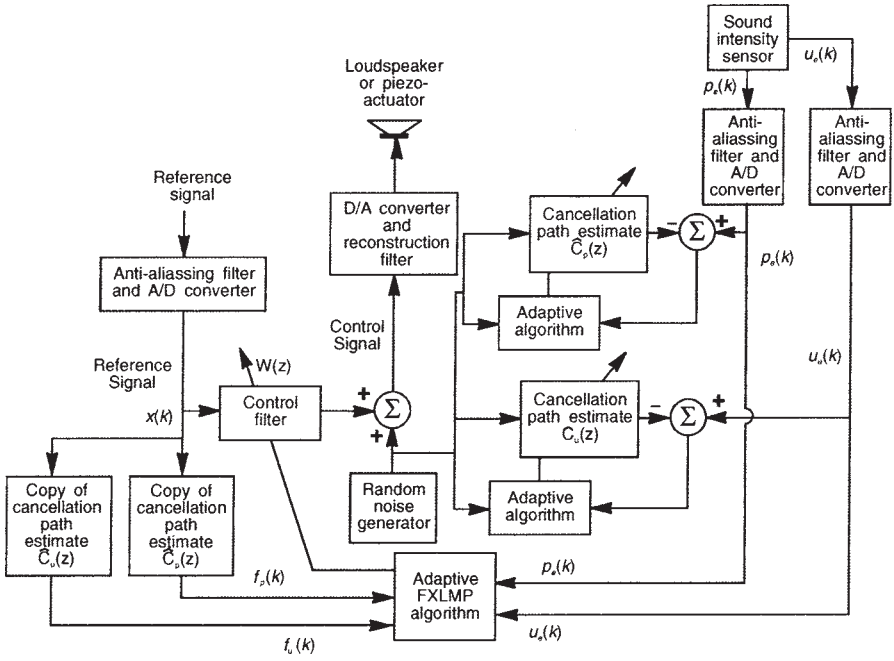

Figure 5.16 Control system layout for sound intensity control with the FXLMP algorithm.

The gradient of the error surface with respect to the weight coefficients may be written as:

$$\nabla J_I(k) = \frac{\partial J_I}{\partial \boldsymbol{w}(k)} = p_e(k)\boldsymbol{f}_{\boldsymbol{u}}(k) + u_e(k)\boldsymbol{f}_{\boldsymbol{p}}(k) \tag{5.35}$$

Thus the weight update equation becomes:

$$\boldsymbol{w}(k+1)=\mathrm{w}(k)-\mu\{p_e(k)\boldsymbol{f}_{\boldsymbol{u}}(k)+u_e(k)\boldsymbol{f}_{\boldsymbol{p}}(k)\} \tag{5.36}$$

which is the result obtained by Sommerfeldt and Nashif (1994). An equivalent equation can be derived for the F-u RLMS algorithm and IIR filter. For the feedforward control filter, the weight update equation is:

$$\boldsymbol{a}(k+1)=\boldsymbol{a}(k)-\mu\{p_e(k)\boldsymbol{f}_{\boldsymbol{ux}}(k)+u_e(k)\boldsymbol{f}_{\boldsymbol{px}}(k)\} \tag{5.37}$$

and for the feedback section it is:

$$\boldsymbol{b}(k+1)=\boldsymbol{b}(k)-\mu\{p_e(k)\boldsymbol{f}_{\boldsymbol{uy}}(k)+u_e(k)\boldsymbol{f}_{\boldsymbol{py}}(k)\} \tag{5.38}$$

where the subscript x refers to the reference signal filtered with a model of the cancellation path and the subscript y refers to the filtered control signal.

Implementing Equation (5.36) in practice is difficult because of the requirement for a measure of the instantaneous particle velocity. If two microphones are used to estimate the particle velocity, then a running time average must be used for the estimate of the particle velocity.

Alternatively, a digital integrator may be used (Park and Sommerfeldt (1997)) as shown in Figure 5.17.

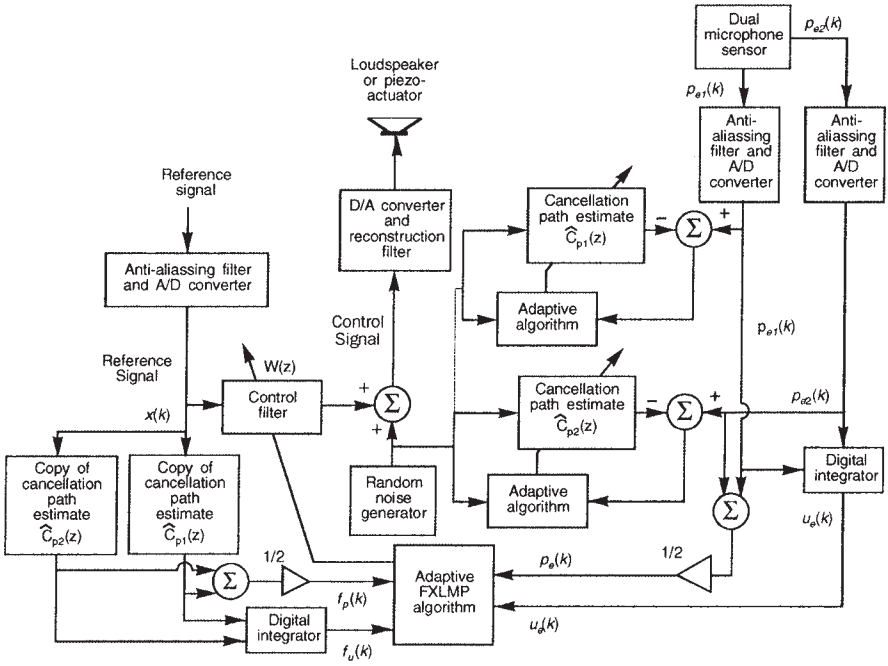

Figure 5.17 Control system layout for sound intensity control with two microphones, a digital integrator and the FXLMP algorithm.

In this case, the velocity may be expressed in terms of the pressures at the two microphones as:

$$u_e(k) = -\frac{1}{\rho} \Xi \left\{ \int_t \frac{p_{2e}(t) - p_{1e}(t)}{\Delta x} dt \right\} \tag{5.39}$$

where the function Ξ denotes the continuous to discrete time transformation. The velocity can be calculated recursively using a digital integrator as follows:

$$\hat{u}_e(k) = \hat{u}_e(k-1) - \frac{1}{f_s \rho \Delta x} [\, p_{2e}(k) - p_{1e}(k) \,] \exp(-1/f_s) \tag{5.40}$$

where f_s is the sampling frequency, ρ is the density of air and Δx is the distance between the microphones. The error sound pressure is given by:

$$P_e(k)=(p_{2e}(k)+p_{1e}(k))/2 \tag{5.41}$$

The actual implementation of the algorithm in this case is shown in Figure 5.17.

5.7.3 Energy Density

When energy density is used as a cost function, the weight update algorithm is different again. However, the control system arrangement is similar to that for sound intensity except that with 3D energy density, velocities in each of the three cartesian coordinate directions need to be measure rather than in just one direction as illustrated in the previous figures. The cost function for energy density in a 3-dimensional space is given by:

$$J_e = \frac{p^2}{2\rho c^2} + \frac{\rho}{2}[v_x^2 + v_y^2 + v_z^2] \tag{5.42}$$

Following a similar procedure as for the intensity error sensing approach, we obtain the following for the gradient of the energy density with respect to the filter weight coefficients:

$$\nabla J_E(k) = \frac{\partial J_E}{\partial \boldsymbol{w}(k)} = \frac{p_e(k)\boldsymbol{f}_p(k)}{\rho c^2} + \rho\left(u_{ex}(k)\boldsymbol{f}_{ux}(k) + u_{ey}(k)\boldsymbol{f}_{uy}(k) + u_{ez}(k)\boldsymbol{f}_{uz}(k)\right) \tag{5.43}$$

where the subscripts *x, y* and *z* refer to velocity in the cartesian *x, y* and *z* coordinate directions, respectively.

The control filter weight update equation for energy density control in a 3-D enclosure is thus:

$$\boldsymbol{w}(k+1) = \boldsymbol{w}(k) - \mu\frac{p_e(k)\boldsymbol{f}_p(k)}{\rho c^2} - \mu\rho\left(u_{ex}(k)\boldsymbol{f}_{ux}(k) + u_{ey}(k)\boldsymbol{f}_{uy}(k) + u_{ez}(k)\boldsymbol{f}_{uz}(k)\right) \tag{5.44}$$

which is equivalent to the result derived by Sommerfeldt and Nashif (1994).

The filter weight update equation for an IIR filter can be derived in a similar way to that done for the intensity case of Equations (5.37) and (5.38). If an energy density probe (such as the one illustrated in Figure 5.18) is used to obtain the velocity and pressure measurements, the instantaneous values may be obtained using Equations (5.40) and (5.41) for each microphone pair. These values can then be converted to the 3 cartesian directions using simple trigonometry.

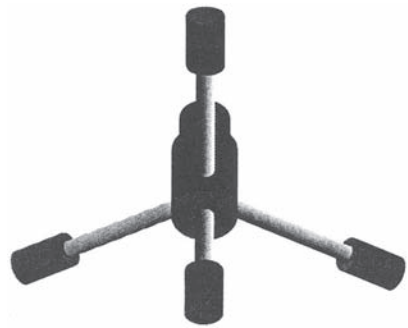

Figure 5.18 4-microphone Energy density probe developed at Adelaide University.

CHAPTER SIX

APPLICATIONS OF ACTIVE NOISE CONTROL

6.1 SOME GENERAL CONSIDERATIONS

In free space, the complexity of the sound field combined with the difficulty of obtaining a reference signal prior to the noise arriving at the control sources means that it is not generally practical to attempt control of broadband or transient noise from large noise sources, although feedback control can be used to obtain noise reductions in local areas at the expense of increased noise levels elsewhere. Tonal noise radiating into free space can be controlled, and a good example of this is the control of the hum from electric power transformers, which is characterised by three or four major tones.

In semi-enclosed spaces, such as characterised by a duct, active control works well up to the point where there are a few higher order modes cut on. It works particularly well at low frequencies when only the plane wave mode is propagating, which is why most commercial active noise control implementations have been directed at this problem. For fully enclosed sound fields, such those characterised by aircraft or vehicle cabins, the maximum achievable noise attenuation is normally predicted as a function of some measure of the presence or otherwise in the space of acoustic "modes". The most useful measure is modal overlap, which is a measure of the density of modes (number of modes per Hz) and the damping associated with each one (Bies and Hansen, 1996). Active control has the potential (with correct control source placement) to work well when the modal overlap is low, where the unwanted noise is predominantly contained in a few lightly damped modes (Elliott, 1989). Generally, it is difficult to achieve global control with just a few sources if this is not the case. Local cancellation to produce "zones of quiet" is a feasible alternative and some success has been achieved in propeller-driven aircraft, for passengers resting their head against seat headrests, at frequencies up to about 350Hz (Carme, 1997).

Use of active absorbers is sometimes contemplated as a means of reducing very low frequency reverberant sound fields at frequencies below which traditional treatment with porous acoustic material (such as fibreglass or rockwool) is ineffective or impractical. The advantage of active absorbers over passive systems such as Helmholtz resonators is that they can adapt to changes in environmental conditions, which result in a change of wavelength in even constant frequency sound fields, and in addition, the active systems can also absorb sound energy over a much wider frequency range.

In the remainder of this chapter, specific application examples that are suitable for active control and examples that are unsuitable will be discussed.

6.2 APPLICATION EXAMPLES

6.2.1 Sound Propagation in Ducts

6.2.1.1 Plane Wave Propagation

Active control of noise propagating in ducts is well suited for the control of low frequency noise where the attenuation which can be achieved using conventional passive silencers may be inadequate. Elements of active systems are usually small and can be mounted in the duct wall, thus minimising air flow pressure losses. This application of active noise control is the oldest and is now the most commercially successful with numerous systems installed in industry in the USA. Typical results achieved are 15–20 dB over two octaves of random noise and 20 to 30 dB for tonal noise. Typical frequencies which are controlled range from 40 Hz to 400 Hz.

Disadvantages of active attenuators are associated with their cost (although this is rapidly decreasing), the need for regular maintenance (speaker replacement every three to five years), the requirement for custom installation and testing by experts, the reduction in performance at frequencies above the first higher order mode cut on frequency and the fact that they often only function well in relatively long (over 3m) sections of duct. Although most installed systems are only intended to control plane wave propagation, the installation of one commercial system which also controls one higher order mode has also been reported (Pelton et al., 1994).

Almost all systems are installed using feedforward control due to its superior performance, although Kuo and Morgan (1996) report a novel configuration for a feedback system that is suitable when the reference signal is contaminated with too much flow noise. Their suggested system is illustrated in Figure 6.1.

Applications of duct noise control include: reduction of noise in air conditioning ducts; reduction of noise in industrial blower systems; and reduction of vehicle exhaust noise. Although vehicle exhaust active mufflers have been demonstrated that perform as well acoustically as their passive counter parts (but without the undesirable pressure drop—see Figure 6.2), they have yet to be used commercially on a widespread basis because of their expense and unreliability (due to the harsh environment). Recent developments involving the use of a radically new type of noise source (Renault et al. 1996) have revolutionised the possibility of practical active control of engine exhaust noise. The device consists of a rotatable flap placed in the exhaust flow and angled up from the exhaust pipe axis by about 12° (see Figure 6.3).

The active control system is used to oscillate the flap back and forth ±3 to 5 °. As might be expected, this device consumes very little power and is reported as being extremely effective. However, work is still necessary to improve the mechanical reliability and also to overcome the excessive exhaust back pressure generated by the valve. Various means such as perforated flapper valves are being investigated to ameliorate this latter problem.

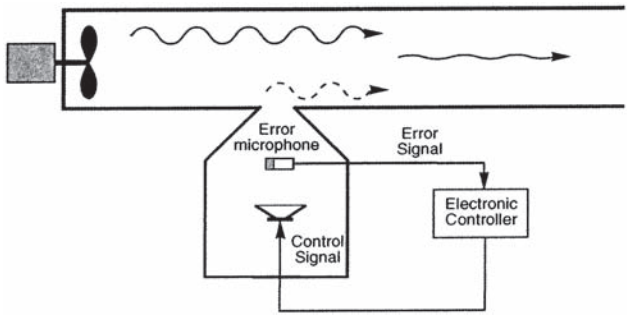

Figure 6.1 Implementation of a feedback system for control of noise propagating in ducts (after Kuo and Morgan, 1996).

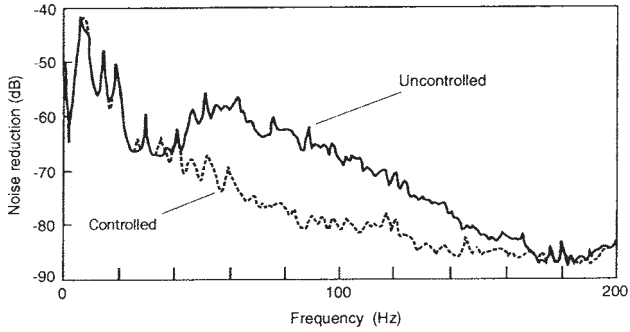

Figure 6.2 Effect of active control on broadband sound propagating in a duct.

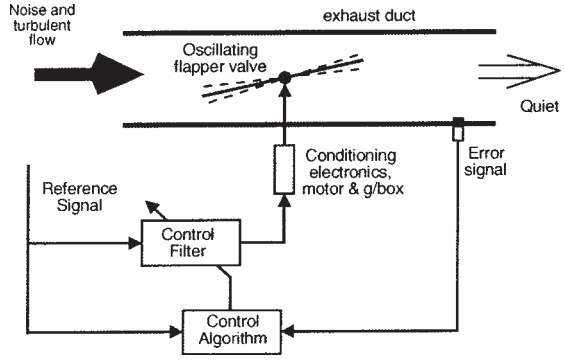

Figure 6.3 Flapper valve ANC source.

6.2.1.2 Higher Order Mode Propagation

Some progress has been reported for the active control of higher order modes in ducts (Pelton, et. al., 1994). It has been shown that for the case of *N* propagating modes, N error sensors and *N* control sources are sufficient to suppress the propagating modes. For large air conditioning ducts, the first cut-on mode may begin to propagate at a frequency as low as 100 Hz. Consequently, to provide active control in such a duct to 200 Hz would require five error sensors and five control sources (as there would be five propagating modes), while active control to 800 Hz would require 64 error sensors and 64 control sources.

Control of one propagating higher order mode has been reported (Eriksson et. al., 1989, Pelton et. al., 1994). A separate adaptive filter was used for each positive and negative portion of the non-uniform pressure distribution associated with the higher order mode. Each filter obtained error information from a separate error transducer and output a signal to a separate loudspeaker. The active control system was reported to reduce tonal noise by 20 to 25 dB at a single measurement location, and broadband noise, above the cut-on of the higher order mode by about 10 to 25 dB.

In many cases it is preferable to use axial splitters in the duct to prevent higher order mode propagation in the vicinity of the controller and then use a single channel independent control system for each splitter section. The splitters need to be sufficiently long to include the reference sensor, control source and error sensor and extend a half wavelength beyond the reference and error sensors.

6.2.1.3 Hybrid Active/Passive Silencers

These silencers for duct systems are of special interest in that they are an example of the effective combination of active (feedback) and passive silencing techniques in the same device (Kruger and Leistner, 1996, Carme et al., 1997). The concept of combining active and passive techniques in vehicle suspensions and vibration isolation systems has been used for some time now and it is clear that future research is likely to extend the concept to other devices and systems for active noise control.

6.2.3 Sound Radiation From Vibrating Structures

Generally it is desired to reduce the total sound power radiated by a vibrating structure rather than the sound pressure at one or two locations. Thus the error sensors must be of sufficient number and arrangement so that they can observe the total radiated sound power. A trade off will almost invariably have to be made between the practical number of error microphones and the need to accurately measure the radiated sound power so that the maximum reduction theoretically achievable with the control source arrangement can be realised.

To control the sound radiated by a vibrating structure, either vibration sources attached to the structure or acoustic sources located in the acoustic medium

surrounding the structure, or a combination of both may be used. Similarly, error sensors may be either structural vibration sensors, which sense the vibration distribution in such a way that the reduction of the error signal results in a reduction in the radiated sound power, or they may be one or more microphones placed strategically in the acoustic medium surrounding the structure.

6.2.3.1 Physical Control Mechanisms

It is of considerable interest to identify the physical mechanisms underlying the active control of sound radiation from a vibrating surface. Only if these are properly understood will it be possible to determine the limitations on the amount of noise reduction that would be achievable with an ideal electronic controller. In one study (Hansen and Snyder, 1991), the effect of various parameters such as control source location, error sensor location, control source type (acoustic or force) panel size, structural damping, excitation frequency and panel response type (resonance or forced) has been evaluated theoretically for a simply supported, baffled rectangular panel vibrating at a single frequency and radiating into free space. The panel was excited off-resonance by a harmonic point primary force at a single frequency between the (2,2) and (3,1) modal resonance frequencies.

Figure 6.4 shows the maximum achievable reduction in radiated sound power as a function of location of a single control force, assuming an ideal electronic controller and assuming that the error sensor(s) can accurately measure the radiated sound power. Even under these ideal conditions it can be seen from the figure that for locations of the control source other than on top of the primary source (which is a trivial case and represents the control source at the centre of the concentrated set of contours shown in the figure) the maximum achievable reduction in radiated sound

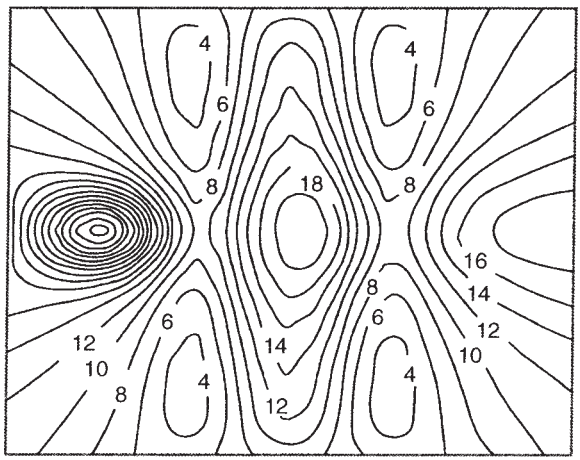

Figure 6.4 Maximum achievable reduction in sound power as a function of control source location on a simply supported panel.

power is 22.4 dB and this will only occur for one location of the control force. Improper location of the control force can result in achievable sound power level reductions as low as 4 dB. The size of the panel depicted in Figure 6.4 was such that the acoustic wavelength corresponding to the excitation frequency was three times the largest panel dimension.

For this test case, two fundamental physical control mechanisms were identified by calculating modal vibration levels on the panel before and after control. With the single control force located at the right hand maximum of Figure 6.4, the control mechanism was modal amplitude reduction; that is, the vibration amplitudes of the modes contributing most to the sound radiation were significantly reduced. It was also found that for the simple case considered here, a single error microphone properly located in the far field of the panel was able to provide an error signal that allowed the sound power to be reduced by an amount very close to the maximum possible.

With the single control force located in the centre of the panel, the dominant control mechanism was found to be that of modal phase rearrangement. That is, the controller rearranged the temporal phases of the radiating modes in such a way as to effectively reduce the overall panel radiation efficiency. This can be better understood if it is noted that the total sound power radiated by a vibrating surface is not the sum of the powers radiated by each mode. Rather, the modes combine together to provide a particular panel velocity distribution that is characterised by a particular radiation efficiency. With this control mechanism, it is likely that the r.m.s. vibration levels on the structure will, in some cases, increase under control, even though the radiated sound power will be reduced.

Increasing the panel size so that it was one rather than one third of a wavelength across had a dramatic effect on the results. The maximum reduction in sound power theoretically achievable with a single control source was reduced from 22.4 to 16.9 dB. Also, the modal rearrangement control mechanism was no longer operative.

Increasing the panel loss factor (vibration damping) from η=0.04 to η=0.2 also had a dramatic effect on the maximum achievable reduction in sound power. Apart from the trivial case of the control source on top of the primary source, the maximum achievable sound power reduction was reduced to 8 dB. Also the modal amplitude control mechanism was no longer effective; control was only achieved by a rearrangement of the relative modal temporal phases.

With acoustic control sources, the mechanism responsible for a reduction in radiated sound power was found to be a change in radiation impedance "seen" by the panel as a result of the presence of the acoustic sources. Thus the acoustic sources act to "unload" the panel. Clearly, it is not possible then for a single small acoustic source to provide a significant reduction in the power radiated by a large structure such as an electrical transformer, as such a source could not acoustically unload the transformer. However this does not preclude the control source from providing local areas of sound cancellation at the expense of other areas of increased sound level.

As well as needing to understand the physical mechanisms involved to design an optimum system to control sound radiation from a vibrating surface, it is also necessary to realise that all vibration modes contributing to the radiation must be both controllable by the control forces and observable by the error sensors. Clearly

a control force located at a modal node cannot control that mode and equally clearly a vibration sensor located at a modal node cannot provide an error signal for that mode. Also an acoustic sensor located at a minimum point in the radiation field generated by a particular mode may not provide adequate error information for that mode. Thus if a single acoustic error sensor is used to provide a signal proportional to the total sound power radiated by a structure, then it is extremely important that it is located so that it can best measure the required quantity. Measurements made using the simple test arrangement just described indicated that the maximum achievable reduction in sound power, could vary from 11 dB to 22.4 dB (for the optimum location of a single control force) dependent upon the location of the far field acoustic error sensor. Clearly, it is desirable to use multiple error sensors.

An important practical application of active control to the reduction of sound radiation from a vibrating surface is the reduction of low frequency tonal noise radiated outdoors by electric power transformers. A number of prototype systems have been demonstrated for actively controlling the tonal noise (100 Hz and 200 Hz) radiated by electric power transformers. Systems include the use of loudspeakers and tuned curved panels as acoustic control sources and piezoceramic patch actuators bonded to the transformer tank to control its noise radiation. Reductions of 10–15 dB have been claimed. However, careful reading of the claims indicates that they refer to the reduction measured at the error sensors and not the global sound power reduction, which is considerably smaller!

6.2.4 Active Headsets and Ear Muffs

It is well known that conventional passive hearing protectors are not very effective in protecting the wearer from low frequency noise, and that communication using standard headsets in noisy areas is extremely difficult. Both active headsets and active hearing protectors enhance hearing protection at low frequencies (usually below 1,500 Hz). Active hearing protectors differ from active headsets in that the former include passive elements to further attenuate mid to high frequency sound (above 250 Hz), and the latter allow radio communication to be heard clearly. As the principles of operation of active headsets and active hearing protectors are similar, the two devices will be treated together here.

The active control of noise at the ear using an active headset or hearing protectors is a similar problem to that of active control of plane wave noise propagating in a duct, in that the problem is one-dimensional. The one-dimensionality of the problem enables good results to be achieved with a single channel control system.

The need for increased performance of passive hearing protectors in a number of applications is well established, especially in the low frequency range where the performance is particularly poor. In addition to the needs in noisy industries such as sheet metal and forging, better hearing protectors are needed for occupants of tracked military vehicles and military aircraft.

Although a number of researchers have been working on the development of active hearing protectors for some time, almost all of the work reported has been in

the form of brief conference papers and patents rather than detailed journal papers. This lack of detailed reporting of particular designs probably stems from the commercial sensitivity of the work. However, two detailed studies have been recorded in the doctoral theses of Wheeler (1986) and Carme (1987), and these along with the paper by Salloway and Twiney (1985) provide some useful insights. In the following sections, various designs of hearing protectors and head sets will be discussed with reference to their principles of operation, practical implementation problems and potential performance.

There are two main types of control system for active hearing protectors and head sets; feedback and feedforward. Each will be discussed in the following sections and the associated advantages and disadvantages will also be considered.

6.2.4.1 Feedback Systems

A typical active feedback system for hearing protectors is illustrated in Figure 6.5. In practice, it is necessary to place the microphone as close as possible to the ear canal as this is where the sound pressure will be minimised.

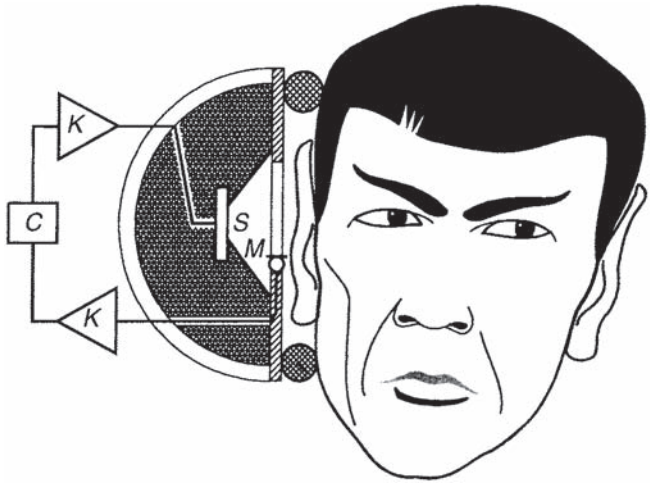

Figure 6.5 Active ear protector using feedback control.
K=amplifier; *C*=compensating filter; *S*=speaker; *M*=microphone.

The design challenge is to develop a compensation filter, *C*, which allows the gain, *K,* to be large without causing the system to become unstable. A feedback system such as the one shown in Figure 6.5 was first suggested by Dorey et. al. (1975), although problems with instability were reported and the feasibility of attenuation of random noise was not established. The work was directed at developing a headset suitable for aircrew, and for this reason it also involved the introduction of a communications signal between the compensating filter and the amplifier.

Typical noise reductions as a function of frequency for a headset designed by Carme (1988) are shown in Figure 6.6. Data for a low cost active headset are shown in Figure 6.7.

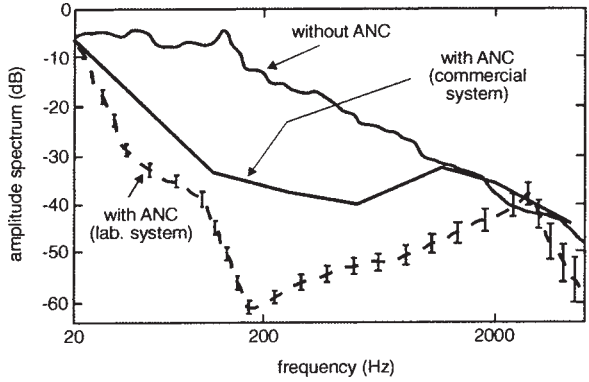

Figure 6.6 Noise reduction as a function of frequency for the feedback controlled active hearing protector.

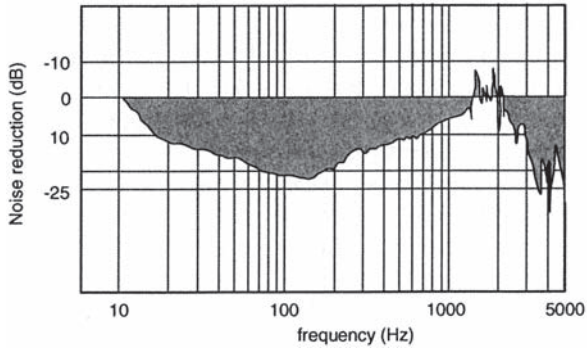

Figure 6.7 Performance of feedback controlled headset used for aircraft passengers.

An arrangement allowing the hearing protector to act as a communications headset is illustrated in Figure 6.8. In the arrangement shown, the communications signal is not affected by the compensation filter, and it is also free from the distortion usually caused by the transfer function of the loudspeaker and cavity, thus resulting in a clear and easily heard signal.

One problem associated with feedback control systems for active head sets is the large variability in the transfer functions of the cavity depending upon who is wearing the device and upon the quality of the acoustic seal between the device and the head. This can result in the onset of instability if an ear protector optimally adjusted for one person is worn by another or if the device slips a little on the wearer's head. Trinder and Jones (1987) claim to have developed a filter that minimises the effect of the

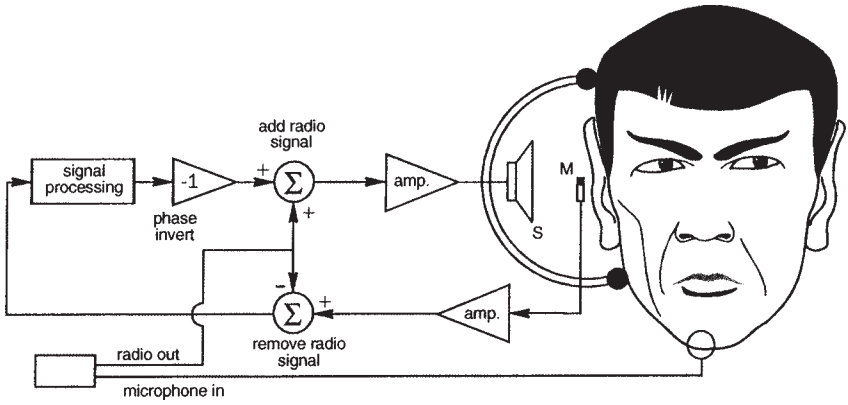

Figure 6.8 Arrangement for a feedback controlled headset intended for radio communication.

acoustic seal on the results and that is also effective for an open backed headset, for which they obtained more than 15 dB of reduction at the ear over a decade in frequency (60 to 600 Hz). It is clear that feedback control systems are effective in significantly reducing broadband noise in ear protectors and their practical application is the subject of much current attention.

Open back headsets are preferable to fully enclosed hearing protectors for pilots and other industrial workers who are required to wear them continuously for long periods of time, as heat build up in the enclosed cavity and the pressure to maintain the acoustic seal causes considerable discomfort to the wearer. Another study by Veit (1988) reported on the effectiveness of a feedback active control system using an open backed headset with the microphone mounted externally. This microphone location was justified because of the low frequency nature of the noise and had the effect of minimising the effect of the compensation network on the radio communication signals incorporated as part of the system. Veit reported maximum noise reductions of 20 dB in one 1/3 octave band and 10 dB over two octave bands (from 250 Hz to 1,000 Hz). The frequency band corresponding to maximum attenuation was adjustable.

Although a considerable effort has been devoted to developing commercial active headsets and hearing protectors using feedback controllers, their use to date has been very limited, possibly due to potential system instabilities caused by high level impulsive noise (with high frequency components) or low frequency pressure pulsations that can overdrive the loudspeaker. Removing the low frequency pressure pulsations by use of a high pass filter is described in a patent by Twiney and Salloway (1990). However, high level impulsive noise in the control frequency range can still result in system instability if the control speaker is over driven as a result.

Current research is addressing these problems and is also investigating the effectiveness of digital feedforward and adaptive feedback systems (Bao and Pan, 1996, Pan et al., 1995). Note that for broadband noise control, feedback system headsets are the best choice. Analog feedback headsets perform better than digital headsets because of the smaller delay in the electronic system. The smaller delays

effectively extend the upper frequency range over which the headset is effective as well as increasing the noise reduction over the operating frequency range. It is clear that active hearing protection for low frequency noise is viable and it is here to stay.

A number of active headsets based on the feedback control approach (using analog electronics) are now commercially available and are very effective up to frequencies of 1,000 Hz. Prices range from $US20 to $US1,000. An industrial quality headset will usually be at least $US300.

6.2.4.2 Feedforward Systems

As discussed earlier, feedforward control systems rely on the availability of a reference signal, which contains information on the frequency content of the noise signal to be attenuated. For an adaptive feedforward system an error microphone provides a measure of the remaining acoustic signal after action of the control loudspeaker and this signal is used to update the filter that operates on the reference signal prior to feeding it to the control source. Two types of adaptive feedforward system are shown in Figure 6.9.

The system shown in Figure 6.9a was first reported by Jones and Smith (1983) and is the subject of a patent awarded to Chaplin et. al. (1987). It will only control periodic noise originating from the noise source attached to the toothed wheel sampled with the tachometer. In practice, this is limited to the fundamental rotational frequency and the first few harmonics. Any random noise or periodic noise originating from other noise sources will not be attenuated. However, in certain applications this may be an advantage rather than a disadvantage. For example, in the mining industry it is desirable to attenuate rotational equipment noise but not the random noise associated with "roof talk" which gives miners some warning of an impending cave-in. It is also feasible to use radio transmitted signals to transmit the reference signal from a transducer on the noisy equipment to the headset.

In other situations, it is desirable to control the random noise component as well and a system that is capable of controlling both periodic and random noise is illustrated in Figure 6.9b. The main problem associated with controlling random noise is the need to ensure that the noise signals arrive at the microphone sufficiently long enough before arriving at the ear to allow the controller to process the signal and send it to the loudspeaker so that it arrives at the same time as the undesirable noise. Satisfaction of this requirement means that for random noise control, the reference microphone must be mounted on a boom pointed towards the noise source. If the direction from which the noise originates is unknown or varies, the boom could be designed so that the microphone location is adjustable. For example, if the microphone were connected to the hearing protector with a ball-joint or if it were on the end of a flexible rod, the user could adjust its location with respect to the hearing protector until the noise was minimised.

Feedforward controllers are advantageous in that the control signals they generate do not attempt to interfere with any radio communication signal which is not sampled by the reference microphone. In Figure 6.9, the communication signal would be

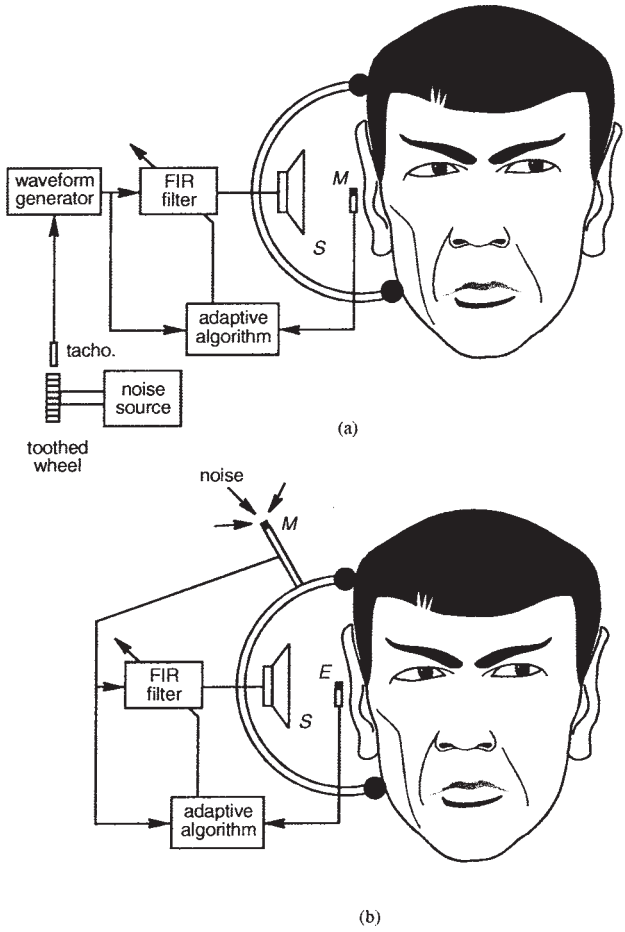

Figure 6.9 Adaptive feedforward control systems for active head sets.
(a) tacho reference signal.
(b) microphone reference signal.
E=error microphone, *M*=reference microphone and *S*=loudspeaker.

introduced immediately prior to the loudspeaker. The same reference microphone or tachometer signal could also be used to drive a second adaptive noise cancelling system to minimise noise in radio communication signals initiated by the wearer of the active hearing protector, using the circuit shown in Figure 6.10.

6.2.4.3 Transducer Considerations

One of the most difficult tasks in the design of an active hearing protector is the design of an appropriate loudspeaker that is capable of producing the required cancelling

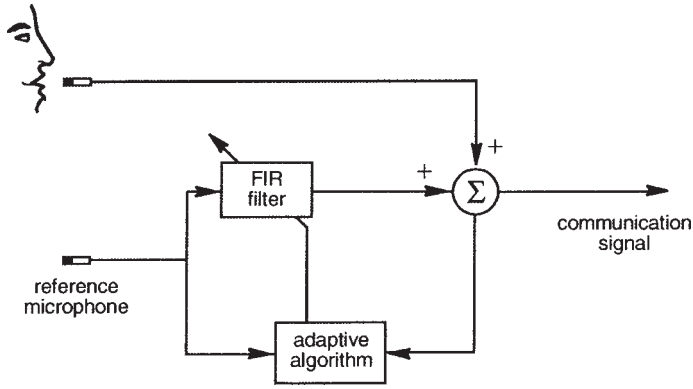

Figure 6.10 Cancellation of unwanted noise in radio communication signal.

signals. The loudspeaker must be small enough to fit in a standard hearing protector and yet perform well at low frequencies. It must also have the required "headroom" to support undistorted speech communication signals at the required level. In an intense noise environment such as found in a tracked vehicle, achieving this performance can be difficult.

Fortunately, procuring a microphone suitable for measuring the unwanted noise is relatively easy, as there are several commercially available miniature electret microphones that are more than adequate for the task.

6.2.5 Sound Transmission Into Enclosed Spaces

When sound is transmitted from the outside of an enclosed space to the inside, such as propeller noise into an aircraft fuselage, the outside disturbance first sets the enclosing structure into motion. The structural vibration modes then couple with the interior acoustic modes, resulting in an energy transfer from the structure into the acoustic space. For structures that are at least of "moderate" size, which constitute the vast majority of enclosed spaces of interest for active noise control, and where the acoustic medium is not particularly dense, such as air, the response of the structural/acoustic system can be considered in terms of the structural *in vacuo* mode shapes, the acoustic cavity rigid-walled mode shapes, and the modal coupling between the two. Not all structural modes will excite all acoustic modes; in fact, quite the opposite. For modal coupling to occur, the product of the structural and acoustic mode shape functions at the structural/acoustic boundary (the wall), integrated over the entire contacting area, must be a non-zero number. For this type of coupled system, the total response can be considered in two regimes; structure-controlled, where the majority of the total system energy is in the shell, and cavity-controlled, where the majority of the total system energy is in the acoustic space. Examples of potential applications of active noise control of interior noise fields include aircraft cabins, diesel generated mining equipment cabins, trucks and cars.

The basic components of an active noise control system to control noise transmitted into an enclosure, are shown in Figure 6.11, where the aim is usually to minimise the acoustic potential energy (or mean squared sound pressure integrated over the enclosure volume). The mean square sound pressure averaged over the enclosure volume is usually approximated with a number of strategically located microphones. The optimum microphone locations are at the locations of the greatest difference in sound pressure between the primary and optimally controlled sound fields (assuming that potential energy was being accurately measured).

In some cases, the aim may be to achieve local areas of high attenuation at the

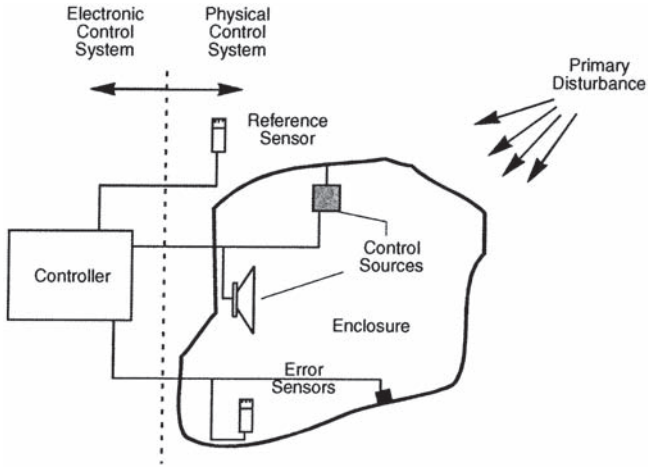

Figure 6.11 Active noise control system for reducing sound transmitted into an enclosed space.

expense of other areas being subjected to increased levels (especially when the physical system is such that global levels of noise reduction are not possible). In this case, the use of energy density sensors (virtual or actual), as discussed in Chapter 5, at the locations of the desired noise reduction is preferable to simple microphones. This is due to the increase in volume over which substantial noise reduction occurs when energy density sensors are used.

When interior acoustic sources are used in an active system controlling sound transmission to produce global attenuation of the interior noise levels, it is tempting to view the physical control mechanism as one of "cancellation", where the goal of the active control system is to excite the acoustic modes in the enclosure with equal amplitude and opposite phase to that of the primary source. However, simple interference of two sound fields would result in large noise reductions at some interior locations at the expense of increased noise at other locations. Implying this as the physical mechanism responsible for global sound attenuation leads to the (in)famous catch-cry of active noise control researchers, "where does the energy go?" (Roebuck, 1990). To find an answer, a closer look at the sound transmission problem is required.

The energy transfer from the structural to the acoustic modes is dependent upon the input impedance of the acoustic modes at the structural/acoustic interface, which is proportional to the acoustic modal pressure at this boundary. In exciting the acoustic modes out of phase with the primary excitation, the control source causes a reduction in the modal pressure at the interface, which in turn acts to decrease this input impedance. Thus, the amount of energy accepted by the acoustic modes is reduced. Further, by reciprocity, the impedance presented to the control sources by each acoustic mode is similarly reduced. Thus mutual unloading of the primary and control noise sources is the impedance mechanism used in the global active control of sound transmission using acoustic sources. When the source of noise is inside the enclosure and the enclosure response is modal (that is, not highly damped), then good interior noise control can be obtained by placing a control source such that it can excite the same modes at the same amplitude as the primary source. The amount of control achieved when the sound field is not too modally dense is illustrated in Figure 6.12 for one and five control sources. Note that at frequencies above 300 Hz in this example, even five control sources become ineffective as the modal density and modal overlap become too high to enable effective control with just a few control sources. Thus,

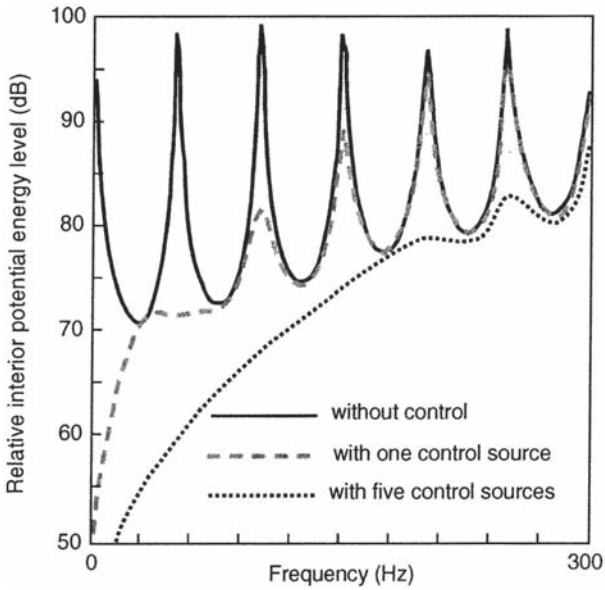

Figure 6.12 Typical noise reductions resulting from a single active noise source in an enclosed space.

when many modes exist in the frequency band to be controlled that the sound field is diffuse or if the enclosed space is acoustically well damped (resulting in only relatively small resonance peaks), it is not possible to globally control the sound field with even a large number of control sources unless they are located within 1/10 of a wavelength of the primary source. This latter condition is similar to the condition

for active noise control in free space. Nevertheless, it is still possible to obtain local zones of cancellation near the error sensors.

Noise levels transmitted into an enclosed space may also be controlled using vibration sources driving the enclosure boundary structure. However, this technique is not likely to be effective if the interior noise levels are a result of noise transmitted into the enclosure through openings or holes in the enclosure boundary. Vibration control sources achieve global sound control by altering the velocity distribution of the structure. This can have two different effects, corresponding to two different physical mechanisms. The first of these, which is the most obvious, is to reduce the levels of vibration which cause the noise (Fuller and Jones, 1987). For a coupled enclosure, this does not necessarily mean reducing the total structural vibration, but rather reducing the vibration levels of the principal noise-producing (coupled) structural modes. This effect, termed modal control, is most prevalent when the response of the system is structure controlled, and is due to an increase in the structural input impedance that these modes present to the external sound pressure excitation field (Pan et al., 1990).

The second effect that vibration control sources can have upon the velocity distribution of a structure, often predominant for a cavity-controlled response, is to alter the relative amplitudes and phasing of the structural modes (termed modal rearrangement) (Pan et al., 1990; Snyder and Hansen, 1991a) without necessarily reducing the overall structural vibration amplitude. This can have the effect of reducing the total modal energy transfer into an individual acoustic mode from the set of structural modes coupled to it, by reducing the coupling efficiency.

There is an interesting sideline arising from this dual-mechanism nature of vibration source active noise control. Initial research directed towards using vibration control sources on aircraft, modelled the aircraft as plain cylinders. The modal coupling characteristics of a plain cylinder are such that essentially, at low frequencies, each acoustic mode is driven by a single structural mode. It was found that when using a limited number of control sources, sound attenuation by modal control near the resonance of either the acoustic or structural mode in a coupled pair was significant. However, off-resonance sound attenuation was poor. Often, modal rearrangement will work off-resonance, but this was not a viable prospect in a plain cylinder, as it required at least two structural modes to be coupled to a single acoustic mode to work. The addition of a floor-like longitudinal partition into the model, however, alters the modal coupling characteristics so as to “turn-on” the modal rearrangement mechanism, improving off-resonance performance. (Snyder and Hansen, 1991a). This phenomenon is very unusual, where adding complexity to the model improves the result!

Because of the differing physical mechanisms involved, it can be shown that acoustic control sources are more effective when the coupled system response is dominated by one or more acoustic modes while vibration control sources are often more effective when the coupled system response is dominated by one or more structural modes.

There is no direct analytical method for the design of the physical part of an active sound transmission control system. There are, however, several concepts that

are commonly employed when analytically assessing the maximum performance of such a system. As for the sound radiation case considered in the previous section, the active noise control system must be able both to excite the modes (structural and/or acoustic) excited by the primary noise source (controllability), and also measure the response of these modes (observability). Ideally, this would lead to the use of one control source and error sensor per mode (Meirovitch et al., 1983), an ideal not practically realisable. It is more desirable to design active control systems using a relatively few, judiciously placed, transducers. For a simple structure, such as a rectangular enclosure, "good" acoustic control source and error sensor placement positions in the corners (where the acoustic modes have antinodes) are obvious. For more complex structures, such as an aircraft fuselage, the optimum arrangement is not so clear, and will depend upon whether the objective is to minimise the acoustic potential energy of the entire enclosure or to minimise the sound pressure level at a fixed number of locations within the enclosure.

It is feasible to use numerical modelling (finite element analysis or boundary element analysis) to express the acoustic potential energy or the sound pressures at the fixed number of error sensors as a function of the control source volume velocities or forces. The problem can then be solved to find the optimum control forces and maximum possible reduction in acoustic potential energy or sound pressure level at the error sensor locations (Pan et al., 1990a-d, Nelson et al., 1987a, Snyder and Hansen, 1991b, 1994a,b). The process can be implemented in a genetic search algorithm to find the optimum locations of the control sources. For the case of minimisation of the acoustic potential energy, the corresponding optimum error sensor locations (which should be no more in number than the control sources) can be found by expressing the problem as one of linear regression and using commercially available software for solution (Snyder and Hansen, 1991c).

Note that an optimum physical system to control sound transmission into an enclosure would probably include both acoustic and vibration control sources as well as acoustic and vibration error sensors. In addition; each error sensor could have a weighting applied to it, depending upon its importance. Thus error microphones located near people may be considered more important then those located further away. Also, vibration levels sensed on the enclosure boundary structure may be given a lower weighting than the interior noise sensors. It is also possible to include control source effort (Snyder and Hansen, 1994a) in the controller algorithm so that no control source is over driven. It is likely that distributed vibration sensors attached to the enclosure boundary structure may be located and shaped so that minimisation of their output will minimise the acoustic potential energy in the enclosure.

Practical applications of active control of noise transmitted into enclosures are discussed in the following sections.

6.2.5.1 Global Reduction of Low Frequency Tonal Noise in Propeller Aircraft

A number of prototype systems have achieved global noise reductions of up to 15 dB at the propeller blade passing frequency (and lesser reductions at frequencies

corresponding to harmonics of the blade passing frequency) in aircraft ranging in size up to to 100 seats and one commercial system that achieves an average reduction of about 6 dB(A) is currently in service in a SAAB 340 aircraft. Reductions of up to 10 dB overall and 20 dB at the propeller blade pass frequency have been achieved on a King Air aircraft (Lord Corporation Web site 1998) using eight loudspeakers and 16 microphones. A commercially available system for a SAAB 2000 propeller aircraft uses a multi-channel controller of 27 loudspeakers and 72 microphones to achieve significant noise reduction of the first four harmonics of the propeller blade passing frequency. Another commercial system, installed on the deHavilland Dash 8 propeller aircraft, relies on actuators attached to the fuselage and does not use any loudspeakers at all. The system produces a noise reduction of 7 dB(A) in interior noise as well as a reduction in the fuselage vibration levels.

Fuller et al. (1997, 1998) have shown that it is possible to reduce noise transmission into the fuselage in a Cessna Citation by using an actively controlled foam skin attached to the interior fuselage surface.

6.2.5.2 Reduction of Interior Noise in Diesel Engine-Driven, Mobile Mining Equipment

Excess levels of low frequency noise in this type of equipment can lead to driver fatigue. However, the heavily damped nature of this space means that global active control of annoying low frequency engine noise is not feasible. Preliminary results indicate that the use of energy density sensing is an excellent way of achieving large areas of local reduction in the vicinity of the occupants' heads. It is even possible to project the zone of control away from the error sensor so that it surrounds the occupant's head (Kestell, et al., 2000). This allows loudspeakers and sensors to be positioned where they will not be noticed by the occupant. Use of more than one sensor and control source can increase the size of the zone of noise reduction quite significantly.

6.2.5.3 Local Reduction of Broadband Noise in Large Aircraft

Experimental systems exist which consist of a loudspeaker and microphone set into the passenger headrest. A single channel control system is used for each headrest and noise reductions of 10–15 dB in the frequency range 100 to 400 Hz have been demonstrated (Carme and Valentin, 1997).

6.2.5.4 Global Reduction of Low Frequency Road Noise in Cars

Between 5 and 7 dB of noise reduction has been achieved up to a frequency of 150 Hz (Bernhard, 1995).

6.2.5.5 Reduction of Low Frequency Sound Transmission Through Double Panel Walls

Experimental systems have been demonstrated for reducing low frequency noise transmission (in the range 80 to 200 Hz) through double panel walls (Pan et al., 1998; Jacob and Moser, 1999; and Paurobally et al., 1999). Similar work has also been done on aircraft fuselages by placing vibration actuators between the outer skin and the inner trim (Fuller 1997, 1998).

6.2.6 Active Vibration Isolation

It is necessary in some cases to vibration isolate mechanical equipment from support structures to prevent the transmission of vibratory energy to these structures and the subsequent noise radiation. As periodic vibratory energy is the most common problem, the following discussion will be restricted to it. Custom active vibration isolation systems have been developed for some special problems and these usually involve a multi-channel feedforward control system driving control actuators that are placed in parallel or in series with an existing passive isolator. Control actuators may be piezoelectric stacks, magnetostrictive rods, electrodynamic shakers, hydraulic shakers or electromagnetic drivers (as in loudspeakers).

Although the general principles of active vibration isolation are similar to those discussed in the previous sections for active noise control, there are some added complexities. For example, equipment support systems usually exert moments and horizontal forces as well as vertical forces on the support structure and these generate longitudinal and shear waves as well as bending waves. Although bending waves are responsible for any appreciable sound radiation, longitudinal and shear wave energy can be transformed to bending waves at structural discontinuities. Thus it is important that the transmission of all wave types through the isolator into the support structure are controlled. For this reason it is necessary for an active isolation system containing multiple actuators to be controlled by a multi channel controller and not by individual single channel controllers for each actuator. This allows the actuators to be adjusted together to minimise some cost function which may be the total vibratory power flow through the isolators to the supporting structure or the mean square vibratory energy at a number of locations on the support structure or even the radiated sound measured at a number of error microphone locations. Applications of active vibration isolation for noise control are discussed in the following sections.

6.2.6.1 Reduction of Engine Noise Transmitted Into Passenger Cars in the Low to Mid-Frequency Range

Because the engine noise is periodic, the reference sensor used in this case is a tachometer on the camshaft. Reductions of 10 to 15 dB(A) have been achieved over a range of engine speeds. Manufacturers are now investigating the possible use of

active engine mounts so that lighter cars can become a reality with no corresponding increase in engine noise levels heard in the passenger compartment.

6.2.6.2 Reduction of Noise Generated by Naval Ships

Active vibration isolation is also being tried out on Naval ships in a number of countries to reduce both interior noise and radiated noise. One example was reported by Winberg et al. (1999).

6.3 EXAMPLES OF APPLICATIONS WHICH ARE IMPRACTICAL

6.3.1 Global Reduction of Broadband or High Frequency Tonal Noise in Large Aircraft

This is currently not possible using standard loudspeaker/microphone systems and a feedforward controller because in the case of broadband noise, a suitable reference signal is not available and for the case of high frequency tonal noise, the sound field is too complex to be cancelled with a reasonable number (and acceptable locations) of control sources and error sensors. However, several researchers are working on various alternative solutions. Fuller et al. (1998) have investigated the possibility of using active skin attached to the fuselage interior to "unload" the fuselage and reduce its ability to couple acoustically with the interior space. They have demonstrated that this treatment can work for low-frequency-propeller tonal noise, but it has not yet been demonstrated for global control of high frequency tonal noise or random noise.

It is possible to achieve local areas of cancellation of low frequency random noise (below 350Hz) in the vicinity of seat headrests by using an independent single channel feedback control system in each headrest. It may also be possible in the future to use individual feedback systems driving actuators fixed to the fuselage to control low frequency broadband boundary layer noise in aircraft (Thomas and Nelson, 1995). Of course the control of low frequency tonal noise is quite feasible as stated previously.

6.3.2 Global Reduction of Broadband or Transient Noise Transmitted into a Building Space

If the transmission paths into the building were restricted to small areas such as windows, then it may be feasible to use active noise control sources in the cavity of a double glazed construction to further reduce low frequency noise transmission, especially at frequencies corresponding to the window cavity resonances. However, it is unlikely that control over a wide frequency range would be possible (Bao et al., 1996). In the more general case where there are multiple transmission paths into the building, the control sources would need to be inside the space where control was

desired. If the room were lightly damped, control of some low frequency resonances would be possible, provided one control source was used for each resonance. However, most building spaces are not lightly damped and also have a high modal density (and thus high modal overlap) in the audio frequency range. Thus it is unlikely that significant global noise reductions would be achieved, even with a large number of control sources.

6.3.3 Reduction of Traffic or Aircraft Flyover Noise Transmitted into a Building

As this noise may be considered random and is generally transmitted into the building by way of a multitude of different paths, its control is impractical for the reasons stated above.

6.3.4 Global Reduction of Tonal or Periodic Noise in a Large Space Such as a Factory That Contains Many Noise Sources

In a large space in the audio frequency range, the acoustic resonance frequencies are so close together that the difference between the peaks and troughs is very small, thus physically limiting the effect of active control, even at room resonance frequencies, to an insignificant amount, regardless of the capability of the controller, unless it is possible to use a sufficient number of control sources near each primary source so that all primary sources are acoustically "unloaded". Note that it is possible to achieve "zones of silence" of up to one tenth of a wavelength in size around pressure sensors and up to one half a wavelength in size around energy sensors when these are used as error sensors in periodic sound fields.

6.3.5 Global Reduction of Broadband Noise in a Large Factory

The lack of availability of a causal reference signal and the complexity of the sound fieldgenerally makes this application impossible for feedforward control and the lack of correlation together with the high degree of complexity in most random industrial noise fields makes the application impractical for feedback control.

6.3.6 Reduction of Broadband Noise Outdoors

This form of active control is physically impractical because of the complexity of the sound field involved and the lack of time for the controller to adapt the control source output to provide the required cancelling field. For a feedforward control system, the reference signal would have to be available early enough for the controller to produce an appropriate cancelling signal at the control source. However, to obtain a 10 dB noise reduction, the control and primary sources must be separated by no

more than 1/10 of a wavelength. If it is assumed that the reference signal comes from a microphone directly in front of the primary source, then to satisfy the 1/10 of a wavelength minimum separation between the primary and control sources, control would be limited to a frequency range below a few tens of Hz. Thus, for practical purposes, feasible control of outdoor noise is limited to periodic noise, such as that radiated by electrical transformers, motors, commercial garden vacuums or any other equipment with rotating parts generating periodic noise. A feedback system may be used to achieve noise reductions at a particular location if the random noise field is highly correlated for time delays corresponding to the processing delay of the controller.

6.3.7 Reduction of Transient Noise Outdoors

In addition to the complexities associated with the control of broadband noise outdoors, the control of transient noise suffers from too short a time for the controller to adapt to the incoming sound field. This latter problem could be somewhat alleviated if the transient events were repetitive (such as a punch press) and a reference signal were available or could be generated artificially based on the previous event and triggered by a sensor that detected the imminent occurrence of the event (such as the initiation of the press movement in the case of a punch press). A sufficient number of control sources would also have to be placed around the noise source to be controlled so that the latter source was acoustically unloaded.

Control at a single point would also be possible for the punch press case described above using a single control source and error sensor.

REFERENCES

Ahn, C.W. and Balachandran, B. 1998. Active control of multiple tones transmitted into an enclosure. *Proceedings of SPIE,* **3329**, pt 1–2, 244–253.

Auspitzer, T., Rafaely, B. and Elliott, S.J. 1996. A fast adaptive feedback controller for active noise control, *Proceedings of Internoise '96*, pp. 1021–1024.

Bailey, T. and Hubbard, J. 1985. Distributed piezoelectric-polymer active vibration control of a cantilever beam. *AIAA Journal of Guidance, Control and Dynamics* **8**, 605–611.

Bao, C. and Pan, J. 1996. Use of adaptive filters in active ear defenders. *Proceedings of Internoise '96*, pp. 1175–1178.

Bao, C., Pan, J. and Guo, J. 1996. Experimental investigation of active sound control of sound transmission through double walls. *Proceedings of The Annual Conference of The Australian Acoustical Society.*

Baumann, W.T., Saunders, W.R. and Robertshaw, H.H. 1991. Active suppression of acoustic radiation from impulsively excited structures *Journal of the Acoustical Society of America* **90,** 3202–3208.

Baumann, D.C. and Greiner, R.A. 1992. Modal identification approach to multi-modal cancellation. *Proceedings of Inter-Noise* 92, pp. 341–344.

Baumann, D.C. and Greiner, R.A. 1992. Number of error microphones for multi-modal cancellation. *Proceedings of Inter-Noise* 92, pp. 345–348.

Bernhard, R.J. 1995. Active control of road noise inside automobiles. *Proceedings of Active '95*, pp. 21–32.

Berry, A., Qiu, X. and Hansen, C.H. 1999. Near-field sensing strategies for the active control of sound radiated from a plate. *Journal of the Acoustical Society of America* **106**, 3394–3406.

Bessac, F., Gagliardini, L. and Guyader, J.-L. 1996. Coupling eigenvalues and eigenvectors: A tool for investigating the vibroacoustic behaviour of coupled vibrating systems *Journal of Sound and Vibration* **191,** 881–899.

Bies, D.A. 1971. *Investigation of the feasibility of making model acoustic measurements in the NASA Ames 40×80ft wind tunnel.* BBN Report 2088 prepared for NASA under contract NAS2–6206, NASA Ames, San Jose.

Bies, D.A. and Hansen, C.H. 1995. *Engineering noise control: theory and practice,* 2nd edn. E&FN Spon, London.

Blondel, L.A. and Elliott, S.J. 1996. Tuned loudspeaker enclosures for active noise control. *Proceedings of Internoise '96*, pp. 1105–1108.

Blondel, L. and Elliott, S.J. 1997. Sub-sonic compressed air sources for active noise control. *Proceedings of Active '97,* p. 347.

Borgiotti, G.V. 1990. The power radiated by a vibrating body in an acoustic fluid andits determination from boundary measurements *Journal of the Acoustical Society of America* **88,** 1884–1893.

Burdisso, R.A. and Fuller, C.R. 1994. Design of active structural acoustic control systems by eigenproperty assignment *Journal of the Acoustical Society of America* **96,** 1582–1591.

Burgemeister, K.A. and Snyder, S.D. 1997. Implementation of modal filters for acoustic sensing of sound power radiation. *Proceedings of the 5th International Congress on Sound and Vibration,* Adelaide, South Australia, pp. 231–238.

Burgess, J.C. 1981. Active adaptive sound control in a duct. *Journal of the Acoustical Society of America* **70,** 715–726.

Burke, S. and Hubbard Jr., J. 1987. Active vibration control of a simply supported beam using a spatially distributed actuator. *IEEE Control Systems Magazine* **7,** 25–30.

Burke, S. and Hubbard Jr., J. 1988. Distributed actuator control design for flexible beams. *Automatica* **24,** 619–627.

Burke, S.E. and Hubbard, J.E., Jr. 1991. Distributed transducer vibration control of thin plates *Journal of the Acoustical Society of America* **90,** 937–944.

Burke, S.E., Hubbard, J.E., Jr. and Meyer, J.E. 1993. Distributed transducers and collocation *Mechanical Systems and Signal Processing* **7,** 349–361.

Callahan, J. and Baruh, H. 1995. Modal analysis using segmented piezoelectric sensors *AIAA Journal* **33,** 2371–2378.

Carme, C. 1987. *Absorption acoustique active dans les cavities.* Doctoral thesis, Faculte des Sciences de Luminy, Universite D'Aix-Marseille II, France.

Carme, C. 1988. A new filtering method by feedback for A.N.C. at the ear. *Proceedings of Internoise '88*. Institute of Noise Control Engineering, pp. 1083–1086.

Carme, C., Delemotte, V. and Montassier, A. 1996. Active noise reduction in turboprop aircraft. *Proceedings of the 4th International Congress on Sound and Vibration,* pp. 1925–1934.

Carme, C. and Valentin, G. 1997. Industrial applications of active seat ANCAS. *Proceedings of the 5th International Congress on Sound and Vibration,* Adelaide, South Australia, pp. 343–350.

Carme, C., Derrien, D. and De Man, P. 1997. Hybrid controller: theory and product. *Proceedings of the 5th International Congress on Sound and Vibration,* Adelaide, South Australia, pp. 375–381.

Cazzolato, B.S. 1999. *Sensing Systems for the Active Control of Sound Transmission into Cavities.* PhD Thesis, University of Adelaide, South Australia.

Cazzolato, B.S. and Hansen, C.H. 1997. Structural sensing of sound transmission into a cavity for active structural-acoustic control. *Proceedings of the 5th International Congress on Sound and Vibration,* Adelaide, South Australia, 2391–2399.

Cazzolato, B.S. and Hansen, C.H. 1998. Active control of sound transmission using structural error sensing. *Journal of the Acoustical Society of America* **104,** 2878–2889.

Cazzolato, B.S. and Hansen, C.H. 1999. Structural radiation mode sensing for active control of sound radiation into enclosed spaces. *Journal of the Acoustical Society of America* **106,** 3732–3735.

Chaplin, G.B.B. 1980. The cancellation of repetitive noise and vibration. *Proceedings of Internoise '80*, pp. 699–702.

Chaplin, G.B.B., Smith, R.A. 1983. Waveform Synthesis-the Essex solution to repetitive noise and vibration. *Proceedings of Internoise '83*, pp. 399–402.

Chaplin, G.B.B., Powell, A.R. and Smith, R.A. 1983. *Method of reducing the adaptation time in the cancellation of repetitive vibration.* US Patent 4,417,098, Nov.22, 1983.

Chaplin, G.B.B., Smith, R.A. and Bramer, T.P.C. 1987. *Method and apparatus for reducing repetitive noise entering the ear.* U.S. Patent 4,654,871.

Charette, F., Guigou, C. and Berry, A. 1995. Development of volume velocity sensors for plates using PVDF film. *Proceedings of Active* 95, pp. 241–252.

Chen, P.-T. and Ginsberg, J.H. 1995. Complex power, reciprocity, and radiation modes for submerged bodies *J. of the Acoustical Society of America* **98,** 3343–3351.

Choi, S. 1995. Alleviation of chattering in flexible beam control via piezo-film actuator and sensor. *AIAA Journal* **33,** 564–567.

Clark, R.L. and Fuller, C.R. 1992a Experiments on active control of structurally radiated sound using multiple piezoceramic actuators *Journal of the Acoustical Society of America* **91,** 3313–3320.

Clark, R.L. and Fuller, C.R. 1992b A model reference approach for implementing active structural acoustic control. *Journal of the Acoustical Society of America* **92,** 1521–1533.

Clark, R.L., Gibbs, G.P. and Fuller, C.R. 1993. An experimental study implementing model reference active structural acoustic control. *Journal of the Acoustical Society of America* **93,** 3258–3264.

Cook, R. and Schade, P. (1974), New method for the measurement of the total energy density of sound waves. *Proceedings of Inter-Noise '74,* pp. 101–106.

Crawley, E.F. and de Luis, J. 1987. Use of Piezoelectric actuators as elements of intelligent structures *AIAA Journal* **25,** 13373–1385.

Cunefare, K.A. 1991. The minimum radiation efficiency of baffled finite beams *Journal of the Acoustical Society of America* **90,** 2521–2529.

Cunefare, K.A. and Currey, M.N. 1994. On the exterior acoustic radiation modes of structures," *Journal of the Acoustical Society of America* **96,** 2302–2312.

Currey, M.N. and Cunefare, K.A. 1995. The radiation modes of baffled finite plates *Journal of the Acoustical Society of America* **98,** 1570–1580.

Curtis, A. 1997. A methodology for the design of feedback control systems for the active control of sound *Proceedings of Active '97,* p. 851.

Darlington, P. and Avis, M.R. 1996. Noise control in resonant sound fields using active absorbers. *Proceedings of Internoise '96,* pp. 1121–1126.

Dimitriadis, E. and Fuller, C. 1991. Active control of sound transmission through elastic plates using piezoelectric actuators. *AIAA Journal* **29,** 1771–1777.

Dimitriadis, E.K., Fuller, C.R. and Rogers, C.A. 1991. Piezoelectric actuators for distributed vibration excitation of thin plates Trans. ASME—*Journal of Vibration and Acoustics* **113,** 100–107.

Dorey, A.P. Pelc, S.F. and Watson P.R. 1975. An active noise reduction system for use with ear defenders. *Proc. 8th Int. Aerospace Symposium.* Cranfield, pp. 24–27.

Eghtesadi, Kh., Hong, W.K.W. and Leventhall, H.G. 1983. The tight coupled monopole active attenuator in a duct. Noise control Engineering Journal **20,** 16–20.

Elliott, S.J. 1989. *The influence of modal overlap in the active control of sound and vibration.* ISVR Memorandum *695.*

Elliott, S. and Garcia-Bonito, J. 1995. Active cancellation of pressure and pressure gradient in a diffuse sound field. *Journal of Sound and Vibration* **186,** 696–704.

Elliott, S.J. and Johnson, M.E. 1993. Radiation modes and the active control of sound power *Journal of the Acoustical Society of America* **94,** 2194–2204.

Elliott, S.J., Stothers, I.M. and Nelson, P.A. 1987. A multiple error LMS algorithm and its application to the active control of sound and vibration. *IEEE Transactions on Acoustics, Speech, and Signal Processing,* **35,** 1423–1434.

Eriksson, L.J. 1990. Computer-aided silencing—an emerging technology, *Sound and Vibration* **24,** pp. 42–45.

Eriksson, L.J. 1991. The continuing evolution of active noise control with special emphasis on duct-borne noise. *Proceedings of Recent Advances in the Active Control of Noise and Vibration,* Virginia Polytechnic Institute and State University, Blacksburg, Virginia, April 15–17, pp. 237–245.

Eriksson, L.J. and Allie, M.C. 1989. Use of Random Noise for On-Line Transducer Modelling in an Adaptive Active Attenuation System. *Journal of the Acoustical Society of America* **85,** 797–802.

Eriksson, L.J., Allie, M.C. and Greiner, R.A. 1987. The selection and application of an IIR adaptive filter for use in active sound attenuation *IEEE Transactions on Acoustics, Speech and Signal Processing* **35,** 433–437.

Eriksson, L.J., Allie, M.C., Hoops, R.H. and Warner, J.V. 1989. Higher order mode cancellation in ducts using active noise control. *Proceedings of Inter-Noise 89,* pp. 495–500.

Friot, E. 1997. Optimal feedback control of a radiating plate under broadband acoustic loading. *Proceedings of Active '97,* p. 873.

Fuller, C.R. 1997. Recent advances in the active control of structurally radiated sound. *Proc. 5th Int. Congress on Sound and Vibration,* Adelaide, Sth. Aust., pp. 103–114.

Fuller, C.R., 1998. Control of sound radiation from structures using active skins. *Proceedings of the FIA 1 Congresso Iberoamericano de Acustica*, Florianopolis, April 4–8, pp. 186–197.

Fuller, C.R. and Carneal, J. 1993. A biologically inspired control approach for distributed elastic systems. *Journal of the Acoustical Society of America* **93,** 3511–3513.

Fuller, C.R. and Jones, J.D. 1987. Experiments on the reduction of propeller induced interior noise by active control of cylinder vibration. *Journal of Sound and Vibration* **112,** 389–395.

Fuller, C.R., Guigou, C. and Gentry, C.A. 1996. Foam PVDF smart skin for active control of sound. *Proceedings of SPIE*, **2721,** 26–37.

Fuller, C.R., Guigou, C. and Johnson, B.D. 1998. Control of sound radiation from structures using active skins. *Proceedings of 1 Congresso Iberoamericano de Acustica,* Florianopolis, Brazil, April 5–8.

Garcia-Bonito, J. and Elliott, S. 1995. Strategies for local active control in diffuse sound fields, *Proceedings of Active '95.* pp. 561–572.

Garcia-Bonito, J., Elliott, S.J. and Boucher, C.C. 1996. A virtual microphone arrangement in a practical active headrest. *Proceedings of Internoise '96,* pp. 1115–1120.

Garcia-Bonito, J., Elliott, S. and Boucher, C. 1997. Generation of zones of quiet using a virtual microphone arrangement. *Journal of the Acoustical Society of America* **101,** 3498–3516.

Gentry, C.A., Guigou, C. and Fuller, C.R. 1997. Smart foam for applications in passive/active noise radiation control. *Journal of the Acoustical Society of America* **101,** 1771–1778.

Goodfriend, M.J. and Shoop, K.M. 1991. Adaptive characteristics of the magnetostrictive alloy, Terfenol-D for active vibration control. *Proceedings of Recent Advances in Active Control of Sound and Vibration,* Virginia Polytechnic Institute and State University, Blacksburg, Virginia, April 15–17, 199–209.

Guigou, C. and Fuller, C.R. 1997. Foam PVDF smart skin for aircraft interior sound control. *Proceedings of SPIE,* **3044**, 68–78.

Guigou, C. and Fuller, C.R. 1998. Adaptive feedforward and feedback methods for active/passive sound radiation control using smart foam. *Journal of the Acoustical Society of America* **104,** 226–231.

Hald, J. 1991. A power controlled active noise cancellation technique. *International Symposium on Active Control of Sound and Vibration,* 285–290.

Hansen, C.H. 1997. Active noise control—from laboratory to industrial application. *Proceedings of NoiseCon 97*, Vol. 2, pp. 3–38 (Sommerfeldt, S.D., Ed.) The Institute of Noise Control Engineering, The Pennsylvania State University.

Hansen, C.H. and Cazzolato, B.S. 1999. Recent advances in the active control of interior noise. *Proceedings of the 6th International Congress on Sound and Vibration,* Copenhagen, July 5–8. pp.85–126.

Hansen, C.H. and Snyder, S.D. 1991. Effect of geometric and structural/acoustic variables on the active control of sound radiation from a vibrating surface. *Proceedings of the Conference on Recent Advances in Active Control of Sound and Vibration,* Virginia Polytechnic Institute and State University, Blacksburg, Virginia, 487–506.

Hansen, C.H. and Snyder, S.D. 1997. *Active control of sound and vibration.* E&FN Spon, London.

Hansen, C.H., Simpson, M.T. and Wangler, C.T. 1996. Application of genetic algorithms to active noise and vibration control. *Proceedings of the 4th International Congress on Sound and Vibration,* St Petersburg, Russia, pp.371–388.

Hansen, C.H. Howard, C.Q. Burgemeister, K.A. and Cazzolato, B.S. 1996. Practical implementation of an active noise control system in a hot exhaust stack. *Proceedings of The Annual Conference of The Australian Acoustical Society.*

Hansen, C.H., Simpson, M.T. and Cazzolato, B.S. 1999. Genetic algorithms for active sound and vibration control. *Proceedings of IEE Inter-Active '99,* (28 pages), http://www.iee.org.uk/Control/active.htm

Hirsch, S. and Sun, J. 1998. Numerical studies of acoustic boundary control for interior sound suppression. *Journal of the Acoustical Society of America* **104,** 2227–2235.

Hong, W.K.W. and Leventhall, H.G. 1983. The tight coupled monopole (TCM) and tight coupled tandem (TCT) attenuators: theoretical aspects and experimental attenuation in an air duct. *Journal of the Acoustical Society of America,* **81,** pp. 376–388.

Hoops, R.H. and Eriksson, L.J. 1991. *Rigid foraminous microphone probe for acoustic measurement in turbulent flow.* U.S. Patent #4,903,249.

Howard, C.Q. 1999. *Active Vibration Isolation,* PhD Thesis, University of Adelaide, South Australia.

Howard, C.Q. and Hansen, C.H. 1997. Finite element analysis of active vibration isolation. *5th International Congress on Sound and Vibration,* pp. 421–427.

Howard, C.Q. and Hansen, C.H. 1998. Finite element analysis of active vibration isolation using vibrational power as a cost function *International Journal of Acoustics and Vibration* Submitted for publication.

Howard, C.Q., and Hansen, C.H. 2000. Calculation of vibratory power transmission for use in active vibration control. *Journal of Sound and Vibration.*

Jakob, A. and Moser, M. 1999. Enhancement of the transmission loss of double panels by means of actively controlling the cavity sound field. *Proceedings of Active '99,* Institute of Noise Control Engineering, New York, pp. 363–374.

Jayachandran, V. and Sun, J.Q. 1998. Impedance characteristics of active interior noise control systems. *Journal of Sound and Vibration* **211,** 716–727.

Jayachandran, V., Hirsch, S. and Sun, J. 1998. On the numerical modelling of interior sound fields by the modal expansion approach. *Journal of Sound and Vibration* **210,** 243–254.

Johnson, M.E. and Elliott, S.J. 1995. Active control of sound radiation using volume velocity cancellation *Journal of the Acoustical Society of America* **98,** 2174–2186.

Johnson, M.E., Sors, T., Rafaelly, B. and Elliott, S.J. 1997. Feedback control of broadband sound radiation using a volume velocity sensor. *Proceedings of Active '97,* p. 1007.

Jones, O. and Smith, R.A. 1983. The selective anti-noise ear defender. *Proceedings of Internoise '83*. Institute of Noise Control Engineering, pp. 375–378.

Kang, S.W. and Kim, Y.H. 1995. Active global noise control by sound power. *Proceedings of Active 95.* Institute of Noise Control Engineering, pp. 465–476.

Kestell, C.D., Cazzolato, B.S. and Hansen, C.H. 2000. Active noise control in a free field with virtual sensors. Part 1: Analytical model. Journal of the Acoustical Society of America.

Kim, S.J. and Jones, J.D. 1991a. Optimal design of piezoactuators for active noise and vibration control. *AIAA Journal* **29,** pp. 2047–2053

Kim, S.J. and Jones, J.D. 1991b. A study of actuators for active control of distributed systems. *Proceedings of NoiseCon 91,* pp. 283–290, Institute of Noise Control Engineering, Tarrytown, New York.

Kruger, J. and Leistner, P. 1996. Effective noise reduction with hybrid silencers. *Proceedings of Internoise '96,* pp. 1097–1100.

Kuo, S.M. and Moran, D.R. 1996. *Active noise control systems.* John Wiley, New York.

Lafleur, L., Shields, F. and Hendrix, J. 1991. Acoustically active surfaces using piezorubber. *Journal of the Acoustical Society of America* **90,** 1230–1237.

Lee, C.K. 1990. Theory of laminated piezoelectric plates for the design of distributed sensors/actuators. Part I: Governing equations and reciprocal relationships *Journal of the Acoustical Society of America* **87,** pp. 1144–1158.

Lee, C.K. and Moon, F.C. 1989. Laminated piezopolymer plates for torsion and bending sensors and actuators *Journal of the Acoustical Society of America* **85,** pp. 2432–2439.

Lee, C.K. and Moon, F.C. 1990. Modal sensors/actuators *Journal of Applied Mechanics* **57,** pp. 434–441.

Lee, C.K., Chiang, W.-W. and OSullivan, T.C. 1991. Piezoelectric modal sensor/ actuator pairs for critical active damping vibration control *Journal of the AcousticalSociety of America* **90,** pp. 374–384.

Li, X and Hansen, C.H. 1999. Active control of sound radiated from structures using near field error sensing. *Proceedings of Active '99,* Fort Lauderdale, December 2–4.

Li, X., Hansen, C.H. and Qiu, X. 1997. Design of Curved Panel Sources for Active Control of Sound Radiated by Transformer. *Proceedings of the 5th International Congress on Sound and Vibration,* Adelaide, South Australia pp. 213–222.

Liang, C. and Rogers, C.A. 1991. Design of shape memory alloy coils and their applications in vibration control. *Proceedings of Recent Advances in Active Control of Sound and Vibration,* Virginia Polytechnic Institute and State University, Blacksburg, Virginia, April 15–17, pp. 177–198.

Lindner, D.K., Baumann, W.T., Ho, F.S. and Bielecki, E. 1991. Modal domain optical fibre sensors for control of acoustic radiation. *Proceedings of Recent Advances in Active Control of Sound and Vibration,* Virginia Polytechnic Institute and State University, Blacksburg, Virginia, April 15–17, pp. 839–850.

Lueg, P. 1933. *Verfahren zur Dämpfung von Schallschwingungen.* German Patent DRP No. 655,508.

Laugesen, S. 1996. A study of online plant modelling methods for active control ofsound and vibration. *Proceedings of Internoise '96*, pp. 1109–1114.

Manolas, D.A., Gialamas, T. and Tsahalis, D.T. 1996. A genetic algorithm for the simultaneous optimisation of the sensor and actuator positions for an active noise and/or vibration control system. *Proceedings of Internoise '96*, pp. 1187–1191.

Meirovitch, L., Baruh, H. and Oz, H. 1983. A comparison of control techniques for large flexible systems. *Journal of Guidance,* **6,** 302–310.

Morgan, D.R. (1980). An analysis of multiple correlation cancellation loopswith a filter in the auxillary path, *IEEE Transactions on Acoustics, Speech and Signal Processing,* **ASSP-28,** 454–467.

Naghshineh, K. and Koopmann, G.H. 1993. Active control of sound power using acoustic basis functions as surface velocity filters *Journal of the Acoustical Society of America* **93,** 2740–2752.

Naghshineh, K. and Gellrich, C.A. 1994. Broadband active vibration control of a beam using experimentally obtained impulse function. *Proceedings of Noise-Con 94,* 373–378.

Nam, H-D., Kim, K-T. and Cheung, W-S. 1996. A multi-channel fuzzy LMS algorithm for active noise control. *Proceedings of Internoise '96,* pp. 1137–1140.

Nashif, P. and Sommerfeldt, S. 1992. An active control strategy for minimising the energy density in enclosures. *Proceedings of Inter Noise '92.* pp. 357–361.

Neise, W. 1975. Theoretical and experimental investigations of microphone probes for sound measurements in turbulent flow. *Journal of Sound and Vibration* **39,** 371–400.

Nelson, P.A. 1996. Acoustical prediction. *Proceedings of Internoise '96*, pp. 11–50.

Nelson, P.A. and Elliott, S.J. 1992. *Active Control of Sound*. Academic Press, San Diego.

Nelson, P.A., Curtis, A.R.D., Elliott, S.J., and Bullmore, A.J. 1987a. The active minimisation of harmonic enclosed sound fields, part 1: Theory. *Journal of Sound and Vibration* **117,** 1–13.

Nelson, P.A., Curtis, A.R.D., Elliott, S.J., and Bullmore, A.J. 1987b. The minimum power output of free field point sourced and the active control of sound. *Journal of Sound and Vibration,* **116,** 397–414.

Nordholm, S. and Nordberg, J. 1997. Delayless, subband echo cancellation. *Proceedings of the 5th International Congress on Sound and Vibration,* Adelaide, South Australia, pp. 319–326.

Obier, T. and Pfeifer, G. 1997. An alternative source for high sound pressures and low frequencies. *Proceedings of Active '97,* p. 689.

Olson, H.F. 1953. Electronic Sound Absorber. *Journal of the Acoustical Society of America* **25,** 1130–1136.

Olson, H.F. 1956. Electronic Control of Noise, Vibration and Reverberation. *Journal of the Acoustical Society of America* **28,** 966–972.

Pan, J. and Bies, D.A. 1990a. The effect of fluid-structural coupling on sound waves in an enclosure—Theoretical part. *Journal of the Acoustical Society of America* **87,** 691–707.

Pan, J., Bies, D.A. and Hansen, C.H. 1990b. The effect of fluid-structural coupling on sound waves in an enclosure-Experimental part. *Journal of the Acoustical Society of America,* **87,** 708–717.

Pan, J. and Bies, D.A. 1990c. The effect of fluid-structural coupling on acoustical decays in a reverberation room in the high-frequency range. *Journal of the Acoustical Society of America,* **87,** 718–727.

Pan, J. and Bies, D.A. 1990d. The effect of a semi-circular diffuser on the sound field in a rectangular room. *Journal of the Acoustical Society of America* **88,** 1454–1458.

Pan, J. et. al., 1995. Application of adaptive feedforward active noise control to hearing protectors. *Proceedings of Active '95,* pp. 1319–1328.

Pan, X., Sutton, T.J. and Elliott, S.J. 1998. Active control of sound transmission through a double-leaf partition by volume velocity cancellation. *Journal of the Acoustical Society of America 104,* 2828–2835.

Paurobally, R., Pan, J. and Bao, C. 1999. Feedback control of noise transmission through a double-panel partition. *Proceedings of Active '99,* Institute of Noise Control Engineering, New York, pp.375–386.

Park, Y.C. and Sommerfeldt, S.D. 1997. Global attenuation of broadband noise fields using energy density control, *Journal of the Acoustical Society of America* **101,** 350–359.

Pelton, H.K., Wise, S. and Sims, W.S. 1994. Active HVAC noise control systems provide acoustical comfort. *Sound and Vibration* July, 14–18.

Photiadis, D.M. 1990. The relationship of singular value decomposition to wave-vector filtering in sound radiation problems *Journal of the Acoustical Society of America* **88,** 1152–1159.

Pottie, S. and Botteldooren, D. 1996. Optimal placement of secondary sources for active noise control using a genetic algorithm. *Proceedings of Internoise '96,* pp. 1101–1104.

Qiu, X. and Hansen, C.H. 1997. An adaptive sound intensity control algorithm for active control of transformer noise. *Proceedings of the 5th International Congress on Sound and Vibration,* Vol. 1, pp. 205–212 (Hansen, C.H. and Vokalek, G., Eds.) International Institute of Acouistics and Vibration, Adelaide, South Australia.

Qiu, X. and Hansen, C.H. 1999. An adaptive waveform synthesis algorithm for active control of transformer noise. *Proceedings of Active '99,* Fort Lauderdale, December 2–4, ??.

Qiu, X and Hansen, C.H. 2000. Secondary acoustic source types for active noise control in a free field: monopoles or multipoles? *Journal of low frequency noise and active control.*

Renault,, S., Micheau, P., Tartarin, J. and Besombes, M. 1996. Industrial applications of pulsed flow,". *Proceedings of Internoise '96,* pp. 1061–1066.

Rex, J. and Elliott, S.J. 1992. The QWSIS—a new sensor for structural radiation control. *1st International Conference on Motion and Vibration Control,* pp. 339–343, Yokohama, Japan.

Roebuck, I. 1990. Energy considerations in active noise control. *Proceedings International Congress on Recent Developments in Air-and Structure-borne Sound and Vibration,* 509–516.

Ross, C.F. 1981. A demonstration of the active control of broadband sound. *Journal of Sound and Vibration* **74,** pp. 411–17.

Salloway, A.J. and Twiney, R.C. 1985. Earphone active noise reduction systems. *Proceedings of the Institute of Acoustics* **7,** 95.

Schirmacher, R. 1996. Application of fast adaptive IIR filter algorithms for active noise control in a kitchen hood. *Proceedings of Internoise '96,* pp. 1193–1198.

Shen, Q. and Jolly, M.R. 1996. Multi-channel normalised X-block algorithm for active noise and vibration control. *Proceedings of Internoise '96,* pp. 1219–1222.

Shen, Q. and Spanias, A.S. 1996. Time and frequency domain X-block least-mean-square algorithms for active noise control. *Noise Control Engineering Journal* **44,** 281–293.

Shields, F. and Lafleur, L. 1997. Smart acoustically active surfaces. *Journal of the Acoustical Society of America* **102,** 1559–1566.

Simpson, M.T. and Hansen, C.H. 1996. Use of genetic algorithms to optimise actuator placement for active control of interior noise in a cylinder with floor structure. *Noise Control Engineering Journal,* **44,** 169–184.

Snyder, S.D. and Burgemeister, K.A. 1996. Performance enhancement of structural/acoustic active control systems via acoustic error signal decomposition. *Proceedings of Internoise '96*, pp. 1141–1146.

Snyder, S.D. and Hansen, C.H. 1991a. The effect of modal coupling characteristics on one mechanism of active noise control. *Proceedings Recent Advances in Active Control of Sound and Vibration.* 708–727.

Snyder, S.D. and Hansen, C.H. 1991b. Mechanisms of active noise control using vibration sources. *Journal of Sound and Vibration,* **147,** 519–525.

Snyder, S.D. and Hansen, C.H. 1991c. Using multiple regression to optimise active noise control system design. *Journal of Sound and Vibration,* **148,** 537–542.

Snyder, S.D. and Hansen, C.H. 1994a. The design of systems to actively control periodic sound transmission into enclosed spaces. Part 1. Analytical models. *Journal of Sound and Vibration,* **170,** 433–449.

Snyder, S.D. and Hansen, C.H. 1994b. The design of systems to actively control periodic sound transmission into enclosed spaces. Part 2. Mechanisms and trends. *Journal of Sound and Vibration,* **170,** 451–472.

Snyder, S.D. and Tanaka, N. 1993. On feedforward active control of sound andvibration using error signals *Journal of the Acoustical Society of America* **94,** 2181–2193.

Snyder, S.D. and Tanaka, N. 1995. Calculating total acoustic power output using modal radiation efficiencies," *Journal of the Acoustical Society of America,* **97,** 1702–1709.

Snyder, S.D. Tanaka, N. and Hansen, C.H. 1993. Shaped vibration sensors for feedforward control of structural radiation. *Proceedings of the Second Conference on Recent Advances in Active Control of Sound and Vibration,* pp. 177–188.

Snyder, S.D., Tanaka, N., Burgemeister, K. and Hansen, C.H. 1995. Direct-sensing of global error criteria for active noise control. *Proceedings of Active 95,* pp. 849–860.

Sommerfeldt, S. and Nashif, P. 1991. A comparison of control strategies for minimising the sound field in enclosures. *Proceedings of Noise-Con '91.* pp. 299–306.

Sommerfeldt, S. and Nashif, P. 1992. Energy based control of the sound field in enclosures. *The Second International Congress on Recent Developments in Air- and Structure-Borne Sound and Vibration,* pp. 361–368.

Sommerfeldt, S.D. and Nashif, P.J. 1994. An adaptive filtered-x algorithm for energy based active control *Journal of the Acoustical Society of America* **96,** 300–306.

Sommerfeldt, S. and Parkins, J. 1994. Active control of energy density in three dimensional enclosures. *Journal of the Acoustical Society of America* **95,** 2989.

Sommerfeldt, S.D. and Scott, B.L. 1994. Estimating acoustic radiation using wavenumber sensors. *proceedings of Noise-Con 94,* 279–284.

Sommerfeldt, S.D. and Scott, B.L. 1997. Active control of structural radiation using wavenumber spectrum measurement. *Proceedings of the 5th International Congress on Sound and Vibration,* Adelaide, South Australia, 239–246.

Sommerfeldt, S., Parkins, J. and Park, Y. 1995. Global active noise control in rectangular enclosures. *Proceedings of Active '95,* pp. 477–488.

Song, L., Koopmann, G.H. and Fahnline, J.B. 1991. Active control of the acoustic radiation of a vibrating structure using a superposition formulation. *Journal of the Acoustical Society of America* **89,** 2786–2792.

Sonti, V.R. and Jones, J.D. 1991. A study of the modal response characteristics of piezo-actuator driven shells for active noise and vibration control. *Proceedings of NoiseCon 91,* pp. 275–282. Institute of Noise Control Engineering, Tarrytown, New York.

Sonti, V.R., Kim, S.J. and Jones, J.D. 1995. Equivalent forces and wavenumber spectra of shaped piezoelectric actuators *Journal of Sound and Vibration* **187,** 111–131.

Sullivan, J.M., Hubbard, J.E.J. and Burke, S.E. 1996. Modelling approach for two-dimensional distributed transducers of arbitrary spatial distribution. *Journal of the Acoustical Society of America* **99,** 2965–2974.

Sun, J., Norris, M., Rossetti, D. and Highfill, J. 1996. Distributed piezoelectric actuators for shell interior noise control. *Journal of Vib. and Acoustics* **118**, 676–681.

Swanson, D.C. 1994. Active control of acoustic intensity using a frequency domain filtered-x algorithm. *Proceedings of Inter-Noise 94*, 1253–1258.

Tanaka, N., Snyder, S.D. and Hansen, C.H. 1996. Distributed parameter modal filtering using smart sensors," *Journal of Vibration and Acoustics* **118,** 630–640.

Thomas, D.R. and Nelson, P.A. 1995. Feedback control of sound radiation from a plate excited by a turbulent boundary layer,", *Journal of the Acoustical Society of America* **98,** 2651–2662.

Tokhi, O. and Wood, R. 1997. Neuro-active noise control using a decoupled linear/nonlinear system approach. *Proceedings of the 5th International Congress on Sound and Vibration,* Adelaide, South Australia, pp. 493–500.

Trinder, M.C.J. and Jones, O. 1987. Active noise control at the ear. *Proceedings of Noise-Con '87.* Institute of Noise Control Engineering, pp. 393–398.

Twiney, R.C. and Salloway, A.J. 1990. Active noise reduction systems reducing unwanted signal enhancement. U.S. Patent 4,953,217.

Veit, I. 1988. A lightweight headset with an active noise compensation. *Proceedings of Internoise '88*. Institute of Noise Control Engineering, pp. 1087–1090.

Wang, B., Fuller, C.R. and Dimitriadis, E.K. 1991. Active control of structurally radiated noise using multiple piezoelectric actuators. *AIAA Journal* **29,** 1802–1809.

Wangler, C.T. and Hansen, C.H. 1994. Genetic algorithm adaptation of non-linear filter structures for active sound and vibration control. *Proceedings of ICAASP '94,* pp. 505–508.

Warnaka, G.E., Tichy, J. and Poole, L.A. 1981. Improvements in adaptive active attenuators. *Proceedings of Internoise '81*, pp. 307–310.

Warnaka, G.E., Poole, L.A. and Tichy, J. 1984. *Active acoustic attenuators.* US Patent 4,473,906, Sept. 25, 1984.

Wenjun, S. and Sun, J.Q. 1997. A study of shell interior noise control. *Proceedings of SPIE* **3041,** 812–818.

Wheeler, P.D. 1986. *Voice communications in the cockpit noise environment—the role of active noise reduction.* PhD thesis, University of Southampton, England.

Winberg, M., Johanssen, S. and Claesson, I. 1999. AVIIS, active vibration isolation in ships; an ASAC approach. *Proceedings of Active '99,* Institute of Noise Control Engineering, New York.

Wise, S.S., Depies, C.R. and Dineen, S.H. 1992. Case histories of active noise control on industrial fans and air handlers used for heating, ventilating and air conditioning. *Proceedings of Internoise '92*, pp. 307–312.

APPENDIX A

A LITTLE MATHS

A.1 INTRODUCTION

The brief overview of mathematics in this appendix is intended to provide background material to help in the understanding of the vector and matrix maths used in the main part of the book.

A.2 VECTORS

In the sense used in this book, vectors represent a string of discrete numbers (for example, the string of control filter weights). A vector is written in bold type and a vector x is defined as:

$$\boldsymbol{x} = \begin{bmatrix} x_1 \\ x_2 \\ \vdots \\ x_n \end{bmatrix} \tag{A.1}$$

The transpose of the vector is defined as:

$$\boldsymbol{x}^{\mathbf{T}} = [\, x_1 \;\; x_2 \;\; \cdots \;\; x_n \,] \tag{A.2}$$

The Hermitian transpose is the complex conjugate of the transpose and is used when one or more elements in the vector are complex numbers. It is defined as:

$$\boldsymbol{x}^{\mathbf{H}} = [\, x_1^* \;\; x_2^* \;\; \cdots \;\; x_n^* \,] \tag{A.3}$$

where the asterisk denotes the complex conjugate. Thus the squared magnitude of a complex vector is obtained by multiplying it by its Hermitian transpose, which is why you see $\boldsymbol{x}.\boldsymbol{x}^{\mathrm{H}}$ in many equations.

A.3 MATRICES

A matrix may be considered as a grouping of a number of vectors of with the same number of elements. A square matrix is one for which the number of vectors is equal to the number of elements in each vector. Thus a matrix can be used to represent a system of equations in a number of unknowns. For a square matrix representation, the number of equations is equal to the number of unknown variables. A matrix may be written as:

$$\boldsymbol{A} = \begin{bmatrix} a_{11} & a_{12} & \cdots & a_{1n} \\ a_{21} & a_{22} & \cdots & a_{2n} \\ \vdots & \vdots & \vdots & \vdots \\ a_{m1} & a_{m2} & \cdots & a_{mn} \end{bmatrix} \tag{A.4}$$

The Hermitian transpose of this matrix is:

$$\boldsymbol{A}^{\mathbf{H}} = \begin{bmatrix} a_{11}^{*} & a_{21}^{*} & \cdots & a_{m1}^{*} \\ a_{12}^{*} & a_{22}^{*} & \cdots & a_{m2}^{*} \\ \vdots & \vdots & \vdots & \vdots \\ a_{1n}^{*} & a_{2n}^{*} & \cdots & a_{mn}^{*} \end{bmatrix} \tag{A.5}$$

A unit matrix is defined as one for which all elements on the diagonal are equal to one. Another important quantity is the matrix inverse, $\mathbf{A}^{-1}$ defined as $\mathbf{A}\,\mathbf{A}^{-1}=\mathbf{I}$. A typical matrix equation is written as:

$$\boldsymbol{A}\boldsymbol{x}=\boldsymbol{y} \tag{A.6}$$

where $\boldsymbol{A}$ is a matrix and x and y are vectors. If the elements of the vector, $\boldsymbol{x}$, are unknown ($x_1 x_2 x_3 \ldots. x_n$) and the quantities in the matrix, $\boldsymbol{A}$, and vector, $\boldsymbol{y}$, are real or complex numbers, the solution of this system of equations is the vector, $\boldsymbol{x}$, given by:

$$\boldsymbol{x}=\boldsymbol{A}^{-1}\,\boldsymbol{y} \tag{A.7}$$

The quantity, $\boldsymbol{A}^{-1}$, is called the inverse of matrix, $\boldsymbol{A}$, and means for its calculation are discussed in detail in books of applied mathematics. If the number of equations is equal to the number of unknowns in the vector, $\boldsymbol{x}$, (that is, the matrix, $\boldsymbol{A}$, is square), then there is a unique solution for every element in the vector, $\boldsymbol{x}$. However, if there are more equations than there are elements in $\boldsymbol{x}$, the matrix, $\boldsymbol{A}$, will no longer be square and there will be no unique solutions for the elements of $\boldsymbol{x}$. However, a pseudo-inverse of $\boldsymbol{A}$ can still be found and thus solutions for the elements of $\boldsymbol{x}$ can be found based on a least squares fit. The solution for $\boldsymbol{x}$ is then:

$$\boldsymbol{x}=(\boldsymbol{A}^{\mathrm{T}}\boldsymbol{A})^{-1}\boldsymbol{A}^{\mathrm{T}}\boldsymbol{y} \tag{A.8}$$

The quantity, $(\boldsymbol{A}^{\mathrm{T}}\boldsymbol{A})^{-1}$ is symmetric, so its inverse can be found in the usual way. The quantity, $(\boldsymbol{A}^{\mathrm{T}}\boldsymbol{A})^{-1}\boldsymbol{A}^{\mathrm{T}}$, is referred to as the generalised or pseudo-inverse. The matrix properties just discussed will be useful in the discussion of quadratic optimisation to follow.

A.4 QUADRATIC OPTIMISATION

Quadratic optimisation is the process whereby the optimum control source strengths are determined for the minimisation of the noise at a number of error sensor locations.

The control source strengths so found can then be used to evaluate the cost function (typically the sum of the squared sound pressure at each error sensor). When the number of control sources and error sensors are identical, it is possible to find control signals that will produce zero sound pressure at each error sensor for each frequency considered. However, when the number of error sensors exceeds the number of control sources, the optimal solution is calculated using the pseudo-inverse of a matrix as discussed in the previous section with the usual result of non-zero sound pressure at all of the error sensors. Note that an adaptive controller will not necessarily arrive at the same solutions as they are not unique. One way of forcing a controller to a unique solution is to use effort weighting (leakage) to include minimising the control source output in the system of equations.

Once the optimal control source outputs have been calculated, the sound pressure at any location in the sound field can be calculated, thus allowing the evaluation of quantities such as total radiated sound power and total interior potential energy for an enclosure.

Let the sound pressure at e error sensors be given by:

$$\boldsymbol{p}_p^{\mathbf{T}} = [\, p_{p1}\ p_{p2}\ \cdots\ p_{pe}\,] \tag{A.9}$$

At the same e locations, the sound pressure due to one control source is then:

$$\boldsymbol{p}_s^{\mathbf{T}} = [\, p_{s1}\ p_{s2}\ \cdots\ p_{se}\,] \tag{A.10}$$

If there are c control sources, then the vector of control source strengths may be written as:

$$\boldsymbol{q}_s^{\mathbf{T}} = [\, q_{s1}\ q_{s2}\ \cdots\ q_{se}\,] \tag{A.11}$$

We now define the acoustic transfer impedance, $\boldsymbol{Z}$, as the matrix of transfer functions between all control sources and all error sensors.

$$\boldsymbol{Z} = \begin{bmatrix} z_{11} & z_{12} & \cdots & z_{1c} \\ z_{21} & z_{22} & \cdots & z_{2c} \\ \vdots & \vdots & \vdots & \vdots \\ z_{e1} & z_{e2} & \cdots & z_{ec} \end{bmatrix} \tag{A.12}$$

The elements of the transfer impedance matrix in the above equation are measured by introducing a signal into each control source in turn and measuring the response at each error sensor with the primary source turned off. Thus,

$$\boldsymbol{p}_s = \boldsymbol{Z}\boldsymbol{q}_s \tag{A.13}$$

The total sound pressure at the error sensor locations may be represented as:

$$\boldsymbol{p}_t = \boldsymbol{p}_p + \boldsymbol{Z}\boldsymbol{q}_s \tag{A.14}$$

The cost function, J_p to be minimised is:

$$J_p = \sum_{i=1}^{e} |p_i|^2 = \mathbf{p}_t^{\mathrm{H}}\mathbf{p}_t = (\mathbf{p}_p + \mathbf{Z}\mathbf{q}_s)^{\mathrm{H}}(\mathbf{p}_p + \mathbf{Z}\mathbf{q}_s) \tag{A.15}$$

Expanding Equation (A.15) gives:

$$J_p = \mathbf{p}_p^{\mathrm{H}}\mathbf{p}_p + \mathbf{p}_p^{\mathrm{H}}\mathbf{Z}\mathbf{q}_s + \mathbf{q}_s^{\mathrm{H}}\mathbf{Z}^{\mathrm{H}}\mathbf{p}_p + \mathbf{q}_s^{H}\mathbf{Z}^{\mathrm{H}}\mathbf{Z}\mathbf{q}_s \tag{A.16}$$

which can be represented in quadratic form as:

$$J_p = \mathbf{q}_s^{\mathrm{H}}\mathbf{A}\mathbf{q}_s + \mathbf{q}_s^{\mathrm{H}}\mathbf{b} + \mathbf{b}^{\mathrm{H}}\mathbf{q}_s + c \tag{A.17}$$

The optimal set of control sources that will minimise J_p are:

$$\mathbf{q}_s(opt) = -\mathbf{A}^{-1}\mathbf{b} = (\mathbf{Z}^{\mathrm{H}}\mathbf{Z})^{-1}\mathbf{Z}^{\mathrm{H}}\mathbf{p}_p \tag{A.18}$$

and the optimal value of the cost function is:

$$J_o = c - \mathbf{b}^{\mathrm{H}}\mathbf{A}^{-1}\mathbf{b} = (\mathbf{p}_p^{\mathrm{H}}\mathbf{p}) - (\mathbf{p}_p^{\mathrm{H}}\mathbf{Z})(\mathbf{Z}^{\mathrm{H}}\mathbf{Z})^{-1}(\mathbf{Z}^{\mathrm{H}}\mathbf{p}_p) \tag{A.19}$$

The cost function noise reduction in dB is then:

$$NR = 20\log_{10}\left[\frac{\mathbf{p}_p^{\mathrm{H}}\mathbf{p}}{J_o}\right] \tag{A.20}$$

In an experimental situation, all of the elements in the transfer function matrix, $\mathbf{Z}$, can be measured for each frequency of interest using the transfer measurement option on a spectrum analyser. The primary noise at the error sensors can also be measured to provide $\mathbf{p}_p$. These measurements can then be used with Equation (A.19) to determine the minimum achievable value of the cost function for an ideal controller. To simulate realistic controller conditions, it is possible to add errors to the transfer function estimates when the optimum control source values are being calculated and use the actual transfer function estimates for calculating the cost function.

It is possible to use optimal set of control sources to calculate the sound pressure at locations other than the error sensors, so that the effectiveness of the control strategy on global quantities such as sound power or interior potential energy can be determined.

APPENDIX B

ADDITIONAL INFORMATION

B.1 CURRENT RESEARCH

A number of papers covering recent research may be found in the proceedings of Active '97 (Budapest, Hungary, 1997), Active '99 (Ft Lauderdale, USA, 1999), the 5th International Congress on Sound and Vibration, (Adelaide, South Australia, 1997), the 6th International Congress on Sound and Vibration (Copenhagen, Denmark, 1999) the 7th International Congress on Sound and Vibration (Garmisch, Germany, 2000) and Internoise 2000 (Nice, France). Future congresses in the same series as the two above (annually for the congresses of the International Institute of Acoustics and Vibration and the Institute of Noise Control Engineering series and every two years for the "Active" series) are likely to continue to have a significant number of papers on active noise control.

B.2 USEFUL WEB-SITES FOR MORE INFORMATION B.

2.1 General information

1. http://users.erols.com/ruckman/ancfaq/ancfaq1.htm
   Contains detailed information on the fundamental principles underlying active noise control and a list of educational institutions where it is taught. Also contains information about companies with commercial active noise control products.

2. http://www.Non.com/news.answers/active-noise-control-faq.html
   Early version of the site in 5 above. Some of the internet addresses provided for suppliers of hardware are out of date.

3. http://www.mecheng.adelaide.edu.au/anvc/home.shtml
   Contains details of current research and links to many other relevant sites.

4. http://www.iiav.org
   International Institute of Acoustics and Vibration. Contains information on conferences and how to obtain the proceedings mentioned above.

5. http://users.aol.com/inceusa/ince.html
   Institute of Noise Control Engineering. Contains information on conferences and how to obtain the proceedings mentioned above.

6. http://www.ecgcorp.com/velav
   General information on acoustics and vibration with a section devoted to active noise control.

B.2.2 Commercial Products and Demonstrations

1. http://www.causal.on.net
   Contains detailed manuals on active control and commercially available active noise control systems.

2. http://www.lordcorp.com/nvx/NVX_Home.html
   Contains flight test data for active noise control systems in aircraft.

3. http://www.arborsci.com/sound.htm
   Contains details of an educational kit for demonstrating active noise control.

4. http://www.Mailbag.com/users/dgsnx_mr/MAIN1.htm
   Expensive controller product descriptions.

5. http://www.elliottaviation.com//smshom.html
   Contains flight test data for active noise control in some mid-size aircraft.

6. http://www.nct-active.com/
   Contains details of headset products and communications noise cancellers.

7. http://www.technofirst.com/tfus.htm
   Contains details of duct silencer and headset products

8. http://www.signalsystemscorp.com/smanc.html
   Contains details of multi-channel controller products.

B.2.3 Research Organisations and Universities

9. http://leoleo.mme.tcd.ie/Groups/SAV/asanca.html
   Information on aircraft noise control.

10. http://www.mecheng.adelaide.edu.au/anvc/home.shtml
    Contains details of current research and links to a multitude of other relevant sites.

11. http://www.val.me.vt.edu/
    Contains details of current research, links to relevant sites and an active noise control demonstrator.

INDEX